NOTE TO USERS

This reproduction is the best copy available.

UMI®

University of Alberta

Characterization of PDEδ in *Caenorhabditis elegans* and *Danio rerio*

by

Jessica Jane Smith   Ⓒ

A thesis submitted to the Faculty of Graduate Studies and Research in partial fulfillment
of the requirements for the degree of Doctor of Philosophy

in

Molecular Biology and Genetics

Department of Biological Sciences

Edmonton, Alberta

Spring 2004

Canadä

Abstract

UNC-119 is involved in nervous system development in *C. elegans* where it is required for several processes including cell body placement, fasciculation, and axon branching. The only identifiable homologue of UNC-119 is PDL-1 (phosphodiesterase 6 delta). Both *unc-119* and *pdl-1* are expressed throughout the nervous system in *C. elegans*, and both have highly conserved mammalian homologues (UNC119 and PDEδ respectively) which are enriched in the retina. The conservation of these proteins suggests that they play an important role in development or function of the nervous system.

Biochemical analysis of mammalian PDEδ (rod cGMP phosphodiesterase 6 delta) suggests that this protein binds and solubilizes a number of prenylated proteins, including several members of the Ras superfamily. The biological role of PDEδ is unclear and prior to this study no PDEδ mutations were known. This thesis describes the identification and characterization of a PDEδ knockout in *C. elegans*. Despite the strong conservation of PDEδ, *pdl-1* knockout worms do not appear to have a phenotype. Double mutant analysis shows that this cannot be explained by redundancy between *pdl-1* and *unc-119*.

A yeast 2-hybrid screen was used to identify potential PDL-1 interactors in *C. elegans*. Five proteins were identified, four of which have a prenylation signal. In addition, directed 2-hybrid analysis was used to show a weak interaction between PDL-1 and EVL-20. EVL-20 is the *C. elegans* homologue of Arl2, a small GTP-binding protein which has been shown to be stabilized in its active form by PDEδ. These 2-hybrid results suggest that the function of PDEδ is conserved between mammals and *C. elegans*.

Preliminary analysis of PDEδ in the zebrafish *Danio rerio* shows that the PDEδ transcript and protein are maternally provided and expressed in embryos up to at least 100 hours post-fertilization. *In situ* hybridization shows that PDEδ transcript is expressed ubiquitously in embryos. Attempts to produce a phenocopy of PDEδ loss of function using morpholino antisense oligonucleotides were unsuccessful. It remains to be seen whether PDEδ loss-of-function can produce a phenotype in any species.

I would like to dedicate this work to

the memory of my grandfather

Gordon Smith

Acknowledgements

I would like to thank all of the members of the Pilgrim lab. This was not an easy project and their support and humour have made a world of difference. First I would like to thank Dave Pilgrim for allowing me the freedom to become an independent scientist. I would also like to thank Shawna Maguire, Heather Lemon, Angela Manning, Wayne Materi, Kathy Bueble, Paul Stothard, and Bryan Crawford for taking the time to help me learn techniques and for many thoughtful discussions. Further thanks go to Morris Maduro, Dave Hansen, Wanyuan Ao, Serene Wohlgemuth, D'Arcy Page, Tamara Checkland, Chantal Denholm, Torah Kachur, Laura Horlick, Carlos Egydio de Carvalho, Janette Berg, Kent Borgstrom, and Crissy St. Germaine for many lively conversations.

I would also like to extend my appreciation to my committee members Mike Walter and Shelagh Campbell as well as my candidacy examining committee members John Bell, Ross Hodgetts, and Kathy Magor. I feared firing squads and instead met smiles.

I would like to commend Jack Scott and Rakesh Bhatnagar for their calm and patient teaching of confocal microscopy and I would like to thank Gary Ritzel for his interest and good ideas. A debt of gratitude also goes out to a number of labs for sharing worms and reagents. I would particularly like to thank Don Moerman and the *C. elegans* Knockout Consortium, Bob Barstead, Andy Fire, Theresa Stiernagle, Min Han, Joseph Beavo, Bernie Lemire, and Rick Kahn.

More personally, I would to thank the BioSci moving team for their strength and patience during my nomadic period. Finally, I would like to thank my friends and family for their unflagging faith and encouragement.

Table of Contents

List of Tables

List of Figures

List of Symbols, Nomenclature, & Abbreviations

ARF	adenosine ribosylation factor
Arl	adenosine ribosylation factor like
Cdc	cell division cycle
ce	*Caenorhabditis elegans*
cGMP	cyclic guanine nucleotide monophosphate
CNS	central nervous system
dr	*Danio rerio*
EST	expressed sequence tag
evl	everted vulva
FAK	focal adhesion kinase
Fyn	FYN oncogene related to SRC, FGR, YES
Gal4AD	Gal4 activation domain
Gal4BD	Gal4 DNA binding domain
GAP	GTPase activator
GARP	glycoprotein A repetitions predominant
GDI	guanine dissociation inhibitor
GEF	guanine nucleotide exchange factor
GFP	green fluorescent protein
GST	glutathione S transferase
Hck	hemopoietic cell kinase
HRP	horseradish peroxidase

hs	*Homo sapiens*
IgG	immunoglobulin G
IL	interleukin
KLH	keyhole limpet hemocyanin
PCR	polymerase chain reaction
PDE	rod cGMP phosphodiesterase
PDEδ	delta subunit of rod cGMP phosphodiesterase
pdl	phosphodiesterase 6 delta
Rab	Ras related GTP binding protein
RACE	rapid amplification of cDNA ends
Ral	Ras related GTP binding protein
Rap	Ras related GTP binding protein
Ras	transforming gene of sarcoma virus
Rheb	Ras homologue enriched in brain
Rho	Ras homologue
RNAi	RNA mediated interference
Rnd	Ras related GTP binding protein (<u>ro</u>u<u>nd</u>)
RP	retinitis pigmentosa
RPGR	retinitis pigmentosa GTPase regulator
RT	reverse transcriptase
SH	Src homology
Src	sarcoma virus oncogene

TK	tyrosine kinase
unc	uncoordinated
UTR	untranslated region
VFT	Vps fifty three

Introduction

Traditionally geneticists have used mutant phenotypes to identify genes involved in a particular process. With the increasing availability of genome sequence, we can frequently use homology to identify genes of interest and then target those genes directly. Both approaches have merit. Traditional genetics is a wonderful tool for identifying genes involved in a particular process, without relying on preconceived notions of the molecular players involved. On the other hand reverse genetics allows the researcher to target established pathways in different model systems, allowing comparison and refinement of existing models. This thesis describes the use of reverse genetics to try to further our understanding of the role of the *unc-119* gene family in the nematode *Caenorhabditis elegans* and the zebrafish *Danio rerio*.

1.1 *C. elegans* and *Danio rerio* as model systems

While it is relatively easy to study cell biology or biochemistry in mammalian cell culture, it is difficult and expensive to perform genetic analysis in a mammalian system. Brood sizes are small; embryos develop internally; animals are opaque, preventing direct visualization of tissues during development; and generation times tend to be quite long. These drawbacks have inspired researchers to find more amenable model systems such as *E. coli*, yeast, *Drosophila*, *C. elegans*, and *Danio rerio*.

C. elegans has found wide use as a genetic system over the last four decades. Its small size coupled with a short reproduction time and ability to self fertilize make it highly amenable to genetic research. Unlike most organisms, *C. elegans* has an invariant somatic cell lineage, which makes it possible to identify and follow individual cells throughout the life of the worm. In addition, *C. elegans* is transparent, allowing for visualization of internal tissues in living animals. Finally, *C. elegans* mutants with motility defects are generally viable making this a wonderful system in which to study muscle or nervous system defects.

Specifically our lab is interested in studying nervous system development using *C. elegans* as an experimental model. One of the genes we have chosen to study is *unc-119*.

1

As described in section 1.3, *unc-119* is expressed throughout the nervous system of *C. elegans* and *unc-119* mutants show an array of nervous system defects (Maduro and Pilgrim, 1995; Maduro, 1998; Knobel *et al.*, 2001). These defects can be visualized through the use of GFP reporter constructs and *unc-119* worms can be maintained as homozygotes despite their strong paralysis. This degree of paralysis would almost certainly be lethal in other systems, making *C. elegans* a natural choice for genetic analysis of the *unc-119* gene family.

While *C. elegans* is very good genetic system, its relative simplicity means that it cannot always act as a model for mammalian function. Although *C. elegans* has several tissue types, an adult hermaphrodite consists of only 959 somatic cells and lacks many complex structures such as a circulatory system, eyes/photoreceptors, limbs, and many organs. The simplicity of *C. elegans* makes it easy to study individual tissues but does not necessarily reflect the complex developmental and regulatory processes that are required to create a fully functional mammal. For example, UNC-119 family members have been shown to be strongly expressed in the mammalian retina (Higashide *et al.*, 1996; Florio *et al.*, 1996). Since *C. elegans* does not have a photosensory system there may be specific aspects of UNC-119 function that cannot be studied in the worm. To address this, we have expanded our research to include the study of UNC-119 family members in other systems including zebrafish.

Danio rerio is an intermediate model organism that is more complex than *C. elegans* but easier to work with than mammals. The fish is a vertebrate and hence has most of the tissues and organs found in mammals. However, the fish has a number of advantages over mammals as a model system. Zebrafish have a relatively large brood size and embryos develop very rapidly outside the mother. These embryos are small and transparent allowing for visualization of living tissues during development. Unlike *C. elegans*, zebrafish are not hermaphroditic, but it is possible to produce haploid embryos from F1 animals and these haploids can be rapidly screened for mutations which affect embryonic development. It is also possible to perform targeted knockdown of zebrafish genes through the use of *morpholino antisense oligonucleotides*.

2

Using the combined strengths of *C. elegans* and zebrafish, we hope to develop a better understanding of the function of the UNC-119 gene family than would be possible with either species alone.

1.2 Axon guidance and nervous system structure in *C. elegans*

The *C. elegans* nervous system is relatively simple consisting of only 302 neurons in the adult hermaphrodite. The placement of cell bodies, processes, and synaptic connections is largely invariant and has been mapped by White *et al.* (1986). Many neurons have cell bodies in the head of the worm, near the pharynx; a smaller cluster of cell bodies is present in the tail. The head and tail ganglia together account for approximately 65% of the nerve cell bodies in the worm. The remaining cells are distributed along the ventral nerve cord and a few cells are present along the body wall. The major fascicles in the worm are the nerve ring in the head plus the ventral and dorsal nerve cords which run along the length of the animal. Commissures project circumferentially around the worm extending from cell bodies in the ventral cord and projecting longitudinally along the dorsal nerve cord. Axons are generally unbranched and make connections through gap junctions and chemical synapses. *C. elegans* is unusual among animals in that its axons do not project into muscles to form synapses. Rather, muscles send projections known as muscle arms to the dorsal or ventral nerve cord. Diagrams of the nervous system structure of *C. elegans* are provided in Appendix I.

The structure and layout of axon processes is established through axon migration. In order to be effective, nerve cells must project axons to the appropriate locations so that they can synapse with appropriate targets. This involves both circumferential and longitudinal migration as well as fasciculation with other processes. Axons migrate using a filipodial structure known as the growth cone. During axon migration, growth cones send out processes in several directions. Depending on the availability of guidance cues and adhesion molecules, growth cones concentrate actin towards an attractive cue or away from a repulsive cue and stabilize the microtubule cytoskeleton in the appropriate direction (for review see Dickson, 2002). Through a series of filipodial projections and

3

retractions axons are able to grow forward or turn as appropriate. Once the axon reaches its destination, synapses are formed and the growth cone collapses.
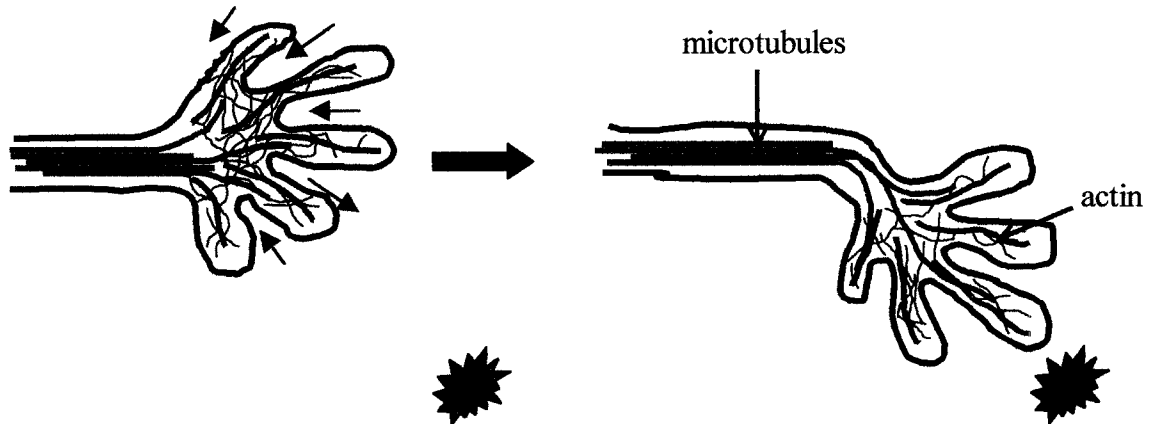
Figure 1.1 Model of growth cone migration towards an attractant. Arrows indicate stabilization or retraction of individual filopodia. The blue star represents an attractive cue.

The best characterized guidance cues in *C. elegans* are the netrin UNC-6 and its receptors UNC-5 and UNC-40. These molecules are required for circumferential guidance of axons (Hedgecock *et al.*, 1990). UNC-6 is thought to be present in a gradient originating from the ventral midline (Wadsworth *et al.*, 1996). Axons expressing UNC-5 are repelled by UNC-6 and migrate towards the dorsal side of the animal (Hamelin *et al.*, 1993). Axons expressing UNC-40 are either attracted or repelled by UNC-6 depending on the absence or presence of UNC-5 respectively (Chan *et al.*, 1996). Other guidance molecules involved in axon migration include the dorsal repulsive molecule Slit and its receptor SAX-3/Robo (Zallen *et al.*, 1998; Hao *et al.*, 2001). Basement membrane components such as nidogen and type XVIII collagen are also required for proper axon guidance (Kim and Wadsworth, 2000; Ackley *et al.*, 2001).

Sensing the environment is only the first step in axon guidance. The shape and structure of the growth cone is governed by the architecture of the actin cytoskeleton (for review see Luo, 2002). Cellular machinery acting downstream of guidance cue receptors transduces extracellular signals into cytoskeletal rearrangements. Cytoplasmic molecules known to be involved in axon guidance include the GTPases Rho, Rac, and Cdc42 (for review see Yuan *et al.*, 2003; Dickson, 2001); proteins which regulate these GTPases, such as the guanine nucleotide exchange factor UNC-73 (Steven *et al.*, 1998); UNC-

4

34/Enabled which acts downstream of SAX-3/Robo (Yu *et al.*, 2002); and the actin-binding protein UNC-115 (Lundquist *et al.*, 1998).

In summary, axons migrate using growth cones which sense guidance and adhesion cues in the extracellular environment. These cues are interpreted by downstream signalling molecules that regulate the structure of the cytoskeleton. In turn, localized stabilization of the cytoskeleton allows axons to grow in a particular direction. Once an axon reaches its target, synapses are formed and axon growth halts. Many of the molecules involved in this process have been identified and researchers are beginning to map the pathways involved. Meanwhile new molecules continue to be uncovered, particularly those that act downstream of surface receptors to control axon structure. One such molecule is UNC-119.

1.3 *unc-119* in *C. elegans*

The first *unc-119* mutant was identified in *C. elegans* by Dave Pilgrim and subsequently characterized by Morris Maduro (Maduro and Pilgrim, 1995; Maduro, 1998). Loss-of-function mutations in *unc-119* are recessive and give rise to worms which are largely paralyzed. *unc-119* animals are able to move their heads and forage, but they swim very poorly and tend to remain ventrally coiled and immobile. These animals are dumpy compared to wild-type and have a reduced brood size (50%). They have difficulty responding to environmental cues as evidenced by failure to form dauer larvae upon starvation and through the maintenance of constitutive pharyngeal pumping in the absence of food. Failure to enter dauer is likely due to an inability to sense dauer pheromone rather than an inherent inability to form dauer larvae as *unc-119* animals can enter dauer in a constitutive *daf-7* background. Finally, *unc-119* animals have a dye-filling defect in the ciliated endings of their chemosensory neurons. In wild-type worms the amphid and phasmid neurons, which are open to the environment, will take up exogenously applied dye solutions (Hedgecock *et al.*, 1985). *unc-119* animals fail to take up dye, indicating that they have structural defects in these neurons (Maduro, 1998).

Neural GFP markers expressed in *unc-119* animals show that their nervous system is highly disorganized: the ventral nerve cord is defasciculated and axonal processes show

5

aberrant branching. Consistent with the neural phenotype of *unc-119* mutants, *unc-119* reporter constructs have been shown to be expressed throughout the nervous system in *C. elegans* (Maduro and Pilgrim, 1995; Maduro, 1998).

A detailed examination of structural defects in the nervous system of *unc-119* animals was carried out by Knobel *et al.* (2001). They focused on the DD motor neurons in *unc-119(ed3)* animals. These neurons show branching defects and a failure to bifurcate along the dorsal cord. In addition, they have supernumerary commissures that project from the ventral nerve cord. Through careful analysis, Knobel *et al.* (2001) determined that the primary defect in the axons of *unc-119* animals results from a failure to suppress axon branching. Axon outgrowth proceeds more or less normally but axons send out secondary growth cones after primary outgrowth is completed. These secondary growth cones produce axon branches and extra commissures. Transient expression of UNC-119 under control of a heat shock promoter is able to suppress branching while the protein is present but branching begins once the protein degrades, again suggesting that UNC-119 prevents neurons from producing secondary processes.

In addition, Knobel *et al.* (2001) looked at cell autonomy and localization of UNC-119. They showed that UNC-119 acts cell autonomously by expressing UNC-119 in the DD motor neurons under control of the *unc-47* promoter. This expression rescued the morphology of DD neurons but failed to rescue the defects in other neurons. Immunolocalization showed that native UNC-119 is expressed in neurons. There is no apparent subcellular compartmentalization of UNC-119 although it shows enrichment in axonal processes relative to cell bodies.

UNC-119 acts cell autonomously to regulate nerve cell placement and axon structure in *C. elegans*. *unc-119* mutants show a variety of defects including axon branching, improper elongation of axons along the dorsal cord, cell body mislocalization, and defasciculation of axon processes. Axon branching is suppressed by the continued expression of UNC-119 in the nervous system. These data suggest that UNC-119 acts cytoplasmically to regulate the cytoskeleton during nerve cell migration and axon outgrowth. It also appears to prevent formation of ectopic growth cones once axon

6

outgrowth is completed. Finally, UNC-119 is required to respond to adhesion cues and allow axon fasciculation. The multi-faceted nature of UNC-119 suggests that it regulates the cell's response to a variety of guidance and adhesion cues. How this is accomplished is not yet known. UNC-119 may act as an intermediate signalling molecule or it may directly affect the actin cytoskeleton.

1.4 Conservation of UNC-119

UNC-119 is highly conserved. EST sequences that encode proteins similar to UNC-119 can be found in the genomes of diverse species such as *Chlamydomonas, Drosophila*, zebrafish, and mice (Figure 1.2). While *C. elegans* has a single copy of *unc-119*, there are at least two UNC-119 paralogues in human and zebrafish (Manning, 1999; Denholm, 2003). The presence of UNC-119 in a unicellular organism such as *Chlamydomonas* suggests that UNC-119 plays a fundamental role that is not inherently specific to the nervous system.

In addition to sequence conservation, UNC-119 shows functional conservation between *Drosophila*, human, and *C. elegans* (Maduro *et al.*, 2000). Both the *Drosophila* and human versions of UNC-119 are able to rescue *C. elegans unc-119* mutants. *In situ* hybridization against UNC-119 in *Drosophila* shows that the transcript is expressed throughout the central nervous system (CNS) and in peripheral nerves (Maduro *et al.*, 2000). The expression pattern of mammalian UNC-119 is less specific. Northern analysis shows strong expression in mouse retina with low level expression in adrenal gland, cerebellum, fibroblast, and kidney (Swanson, *et al.*, 1998). Northern analysis on human embryonic tissue shows ubiquitous expression as does *in situ* staining in mouse embryos (Denholm, 2003). *In situ* staining in zebrafish embryos also shows ubiquitous expression of the UNC-119 transcript (Manning, 1999). The expression of UNC-119 in neural tissue of worms, flies, and humans suggests that UNC-119 plays a common role in nervous system development or function. However, the expanded expression pattern of UNC-119 in fish and mammals again suggests the possibility of a more general role for this protein.

7

The fact that UNC-119 is so highly conserved among a wide array of organisms suggests that it plays an essential role in the cell. Invertebrates such as *C. elegans* and *Drosophila* show UNC-119 expression limited to the nervous system while higher organisms such as humans and zebrafish express UNC-119 in many tissues. Regardless of differences in expression pattern, the function of UNC-119 has been maintained as shown by the ability of *Drosophila* and human UNC-119 to rescue a *C. elegans* *unc-119* mutant. Therefore study of UNC-119 function in any species should help us to understand the cellular role of this protein.

```
hsUNC119     1  --------MKVKKGGGGAGTATESAPGPSGQSVAPIPQPPAESESGSESE
drUNC119b    1  --------MKVKKG------------------------------CNTT
dmUNC119     1  MSVVGKQLNPVQSSGAGAVTTSSSAAAGSSSSNSGVEANGGSGGSSGAAA
ceUNC119     1  ---------------------MKAEQQQQSIAPGSATFPSQMPRPPP
crUNC119     1  --------------------------------------------------

hsUNC119    43  PDAGPGPRPGPLQRKQPIGPEDVLGLQRITGDYLCSPEENIYKIDFVRFK
drUNC119b   11  DLGVPVTTEEELLANKTISPEDVLGLQKITENYLCSPEDNLYNIDFTRFK
dmUNC119    51  AGAGASGDAKRPAESSSVTPDLVLHLTKITDDYLCSANANVFEIDFTRFK
ceUNC119    27  VTEQAITTEAELLAKNQITPNDVLALPGITQGFLCSPSANVYNIEFTKFQ
crUNC119     1  -------------MAQITPLVVLSYTKPASGYLCPLNANTFGIFFLKFE

hsUNC119    93  IRDMDSGTVLFEIKKPPVSERLP---------------INRRDLDPNAGR
drUNC119b   61  IRDMETGTVLFEITKPPSTDRG--------------DKRDVDPNAGR
dmUNC119   101  IRDLESGAVLFEIAKPPSEQYPEGLSSDETMLAAAEKLSLDDTADPNAGR
ceUNC119    77  IRDLDTEHVLFEIAKPENETEEN----------------LQAQAESAR
crUNC119    37  IKEYDTNTVVYQVAREPDSEPLP--------------EVLDPEIEDMIR

hsUNC119   128  FVRYQFTPAFLRLRQVGATVEFTVGDKPVNNFRMIERHYFRNQLLKSFDF
drUNC119b   94  FVRYQFTPAFLRLRQVGATVEFTVGDIPINNFRMIERHYFREQLLKSFDF
dmUNC119   151  YVRYQFTPAFLNLKTVGATVEFTVGSQPLNNFRMIERHFFRDRLLKTFDF
ceUNC119   109  YVRYRFAPNFLKLKTVGATVEFKVGDVPITHFRMIERHFFKDRLLKCFDF
crUNC119    72  SVKYTFPASFLKFKTVRTLLEFCVGPQPVSNLRMIERHFFKDKLVRTYDF

hsUNC119   178  HFGFCIPSSKNTCEHIYDFPPPLSEELISKMIRHPYETQSDSFYFVDDRLV
drUNC119b  144  EFGFCIPSSKNTCEHIYEFPPPLSEDLIREMILHPYETQSDSFYFVDNKLV
dmUNC119   201  EFGFCFPFSKNTVEHIYKFPNLPPDLVAKMISSPYETRSDSFYFVGNRLV
ceUNC119   159  EFGFCMPNSRNNCEHIYKFPQLSQQLMDDMINNPNETRSDSFYFVENKLV
crUNC119   122  EFGFCIPNSTNSWEAIYDVPEYPAGVINDYVTSPWAHKSDSFYFVDNKLI

hsUNC119   228  MHNKADYSYSGTP--
drUNC119b  194  MHNKADYSYSGGP--
dmUNC119   251  MHNKADYAYDGGNIV
ceUNC119   209  MHNKADYSYDA----
crUNC119   172  MHNKAFYQYVQD---
```

Figure 1.2   Comparison of UNC-119 protein among a variety of species. In order from top to bottom; human UNC119, *Danio rerio* Unc119b, *Drosophila melanogaster* UNC-119, *C. elegans* UNC-119, and *Chlamydomonas reinhardtii* UNC-119. Black shading indicates identity while grey shading indicates similarity. At least 80% of sequences must match for shading to apply.

8

1.5 UNC-119 function in mammals

As discussed in the previous section the UNC-119 transcript has been shown to be widely expressed in mammals. However hsUNC-119 was first identified as a retinally enriched transcript (Higashide *et al.*, 1996) and subsequent study of mammalian UNC-119 has largely focused on the retina.

The distribution of UNC-119 transcript has been studied by *in situ* hybridization in mouse and rat retina. Both show localization of UNC-119 transcript to photoreceptors (Swanson, *et al.*, 1998; Higashide *et al.*, 1996). Immunostaining for UNC-119 protein in human and rat retina shows localization to the photoreceptor outer segments with weaker staining in inner segments (Higashide *et al.*, 1998). Electron microscopy shows that the UNC-119 staining is localized to the photoreceptor synapse.

The role of UNC-119 in the retina is not well understood. It has been suggested that UNC-119 may be localized to the membrane or synaptic vesicles of the ribbon synapse (Higashide *et al.*, 1998) where it could play a role in vesicle trafficking. A heterozygous truncation in UNC-119 has been correlated with retinal dystrophy in one patient (Kobayashi *et al.*, 2000) and overexpression of this truncated form of UNC-119 under control of the rhodopsin promoter leads to retinal degeneration in a mouse model. This shows that overexpression of a mutant form of UNC-119 can interfere with retinal function. Whether this occurs through interrupted vesicle transport remains to be determined.

In vitro studies have provided some insight as to the potential function(s) of UNC-119. Yeast 2-hybrid and coimmunoprecipitation have been used to demonstrate interaction between UNC-119 and three members of the Arl (ADP ribosylation factor-like) family: Arl1, Arl2 and Arl3 (Van Valkenburgh *et al.*, 2001; Kobayashi *et al.*, 2003). The Arl proteins are small GTP-binding proteins which are defined by their similarity to the ADP-ribosylation factor (ARF) family of GTP-binding proteins. While the ARF proteins are regulators of vesicle traffic (for review see Chavrier and Goud, 1999) the Arl proteins play a variety of roles.

9

Arl1 has been primarily studied in yeast where it has been shown to be involved with vesicle transport. *Arl1Δ* yeast show membrane traffic defects including a decrease in protein secretion (Rosenwald *et al.*, 2002). Arl1p has been shown to interact with components of the GARP/VFT complex which is thought to tether endocytic vesicles to the Golgi (Panic *et al.*, 2003). In addition, Arl1 has been shown to be localized to the Golgi in mammalian cells (Lowe *et al.*, 1996; Lu *et al.*, 2001). Overexpression of the dominant active Arl1(Q71L) in cultured CHO cells leads to expansion and disorganization of the Golgi while expression of the dominant negative Arl1(T31N) causes the Golgi to disassemble, suggesting that Arl1 helps to control Golgi structure (Lu *et al.*, 2001). Finally, a mutation in the *Drosophila* homologue of Arl1, *arflike*, results in zygotic lethality (Tamkun *et al.*, 1991). These data suggest that Arl1 plays an important role in the regulation of the Golgi complex and membrane traffic in a variety of species.

Arl2 has been shown to be involved in cytoskeletal dynamics. A mutation in the *C. elegans* homologue of Arl2, *evl-20*, leads to a variety of cytokinetic and morphogenetic defects resulting from disorganization of the microtubule cytoskeleton (Antoshechkin and Han, 2002). In addition, studies in mammalian cell culture show that Arl2 regulates the interaction of tubulin-specific chaperone cofactor D with tubulin (Bhamidipati *et al.*, 2000). Specifically, Arl2 in its GDP bound state interacts with cofactor D and prevents cofactor D overexpression from destroying microtubules. Finally, the fission yeast homologue of Arl2, Alp41, is an essential gene proposed to be involved in microtubule biogenesis (Radcliffe *et al.*, 2000). A deletion mutant of alp41 is able to be rescued by overexpression of cofactor D (alp1). These data strongly suggest a conserved role for Arl2 in the regulation of microtubules, possibly through interaction with cofactor D.

Finally, Arl3 has been studied in the human retina where it colocalizes with microtubules (Grayson *et al.*, 2002). Arl3 is expressed throughout the retina but enriched in the connecting cilium of photoreceptors. In addition, Arl3 copurifies with microtubules in HeLa cells suggesting that it is generally associated with the cytoskeleton. Arl3 has also been shown to interact with the retinitis pigmentosa protein RP2. This protein has functional overlap with the tubulin-specific chaperone cofactor C (Bartolini *et al.*, 2002). Cofactor C and D act together as a GTPase activator (GAP) for β-tubulin and its GTP

10

hydrolysis allows for the assembly and release of native tubulin heterodimers (Tian *et al.*, 1999). Like cofactor C, RP2 can stimulate tubulin GTPase activity in concert with cofactor D. Therefore Arl3 appears to be involved in the regulation of microtubule dynamics through interaction with tubulin assembly factors.

In addition to interacting with Arl family members, hsUNC-119 has been shown to interact with the interleukin 5 receptor IL5-Rα and to activate Lyn, its downstream effector (Cen *et al.*, 2003). Lyn activation by UNC-119 results in increased eosinophil survival. The interaction between UNC-119 and Lyn is mediated through the SH2 and SH3 binding motifs present in UNC-119. Finally, UNC-119 has been shown to interact with two other Src tyrosine kinase (SrcTK) family members, Hck and Fyn. These data implicate UNC-119 as a regulator of intracellular signalling.

1.6 The role of *C. elegans* UNC-119

Given the available evidence, it seems that hsUNC-119 plays a role in cell signalling. In *C. elegans*, UNC-119 suppresses axon branching. This may occur through stabilization of the microtubule cytoskeleton, perhaps through interaction with Arl family members. For example, UNC-119 may be involved in intracellular signalling to prevent cells from responding to neurotrophic guidance cues once their axons have reached their target.

It is important to remember that axon branching is not the only *unc-119* defect. *unc-119* animals show severe fasciculation defects in the ventral nerve cord and their axon processes often fail to extend along the dorsal nerve cord. In addition, *unc-119* animals show cell body displacement of the DA/DB motor neurons along the ventral cord (Wayne Materi, personal communication). These observations combine to suggest a role for UNC-119 during nervous system development. It is possible that UNC-119 modulates the response of cells to guidance and adhesion cues. Nerve cells must be able to interpret and respond to growth cues and, equally importantly, stop responding to cues once they have completed outgrowth. It is feasible that UNC-119 is involved in the downstream signalling for both processes. UNC-119 may be used to interpret extracellular signals from axon guidance cues (akin to its interaction with IL-5Rα and Src tyrosine kinases)

11

and relay those signals to microtubule assembly cofactors, resulting in appropriate regulation of the microtubule cytoskeleton.

Other members of the lab are testing these hypotheses about the function of UNC-119 in C. elegans. They are attempting to identify protein partners of UNC-119 through yeast 2-hybrid and co-purification. This should allow us to determine whether UNC-119 interacts with surface receptors and/or microtubule assembly factors. If UNC-119 is a signalling molecule, we should be able to identify proteins that act upstream and downstream of UNC-119. Given the pleiotropic nature of unc-119 mutations, it is likely that many factors influence UNC-119 activity. Once these are identified, we can begin to use genetic and biochemical approaches to refine our understanding of UNC-119 function.

A way to indirectly study the function of UNC-119 is to investigate related proteins that might have similar function. In C. elegans, there is only one protein that shares significant sequence similarity with UNC-119, the predicted protein C27H5.1. Combined study of UNC-119 and C27H5.1 should allow for understanding of the UNC-119 gene family as a whole and allow us to determine whether there is functional overlap between these two proteins. If so, then study of C27H5.1 function would lead to further insight about the function of UNC-119. A sequence comparison of UNC-119 and C27H5.1 is shown in Figure 1.3.

```
UNC-119     1   M K A E Q Q Q Q S I A P G S A T F P S Q M P R P P P V T E Q A I T T E A E L L A K N Q I T P N D V L
C27H5.1     1   - - - - - - - - - - - - - - - - - - - - - - - - - - - - - - - - - - - - - - - - - - - - - - - -

UNC-119    51   A L P G I T Q G F L C S P S A N V Y N I E F T K F Q I R D L D T E H V L F E I A K P E N E T E E N L
C27H5.1     1   - - - - - - M A T T A T R H Q D S K L S E K A E S I L A G F K L N W M N L R D A E T G K V L W Q S T

UNC-119   101   Q A Q A E S A R Y V R Y R F A P N F L K L K T V G A T V E F K V G D V P I T H F R M I E R H F F K D
C27H5.1    45   E D M A D P K R E H K A H V P K N L L K C R T V S R E I N F T S - S V K I E K F R L E Q R V Y L K G

UNC-119   151   R L L K C F D F E F G F C M P N S R N N C E H I Y E F P Q L S Q Q L M D D M I N N P N E T R S D S F
C27H5.1    94   T I I E E W Y F D F G F V I P D S T N T W Q N M I E A A P E S Q M F P P S V L S G - - N V V V E T L

UNC-119   201   Y F V E N K L V M H N K A D Y S Y D A
C27H5.1   142   F Y D G D L L V S T S R V R L Y Y D -
```

Figure 1.3   Comparison of C27H5.1 and UNC-119 proteins in C. elegans. Black shading indicates identity while grey shading indicates similarity.

.

12

1.7 Why study C27H5.1?

When I began my thesis project, little was known about the molecular function of UNC-119. Preliminary phenotypic analysis had revealed that *unc-119* mutant animals have axon guidance and branching defects (Maduro, 1998), but the cause of these defects was not yet known. As C27H5.1 is the only recognizable homologue of *unc-119* in *C. elegans* we thought that we might be able to shed light on the function of *unc-119* by studying this gene as well. The belief that C27H5.1 might function similarly to *unc-119* was strengthened by the observation that a C27H5.1 promoter::GFP fusion shows expression throughout the nervous system. In addition both UNC-119 and C27H5.1 have highly conserved mammalian homologues which are retinally expressed (Higashide *et al.*, 1996; Florio *et al.*, 1996). These similarities led us to speculate that UNC-119 and C27H5.1 play similar roles and that C27H5.1 might also influence axon guidance in *C. elegans*.

This reasoning became the foundation for my Ph.D. project. The potential importance of this work was augmented by the fact that C27H5.1 is extremely well conserved throughout metazoans. C27H5.1 and its mammalian homologue, the delta subunit of rod cGMP phosphodiesterase (PDEδ), share 70% identity and 85% similarity at the amino acid level. The conservation of C27H5.1 suggests that this protein has an important role that would be worthy of investigation. BLAST searches of various genomic and EST databases have confirmed conservation of C27H5.1/PDEδ throughout a wide variety of metazoans (Figure 1.4). In light of this conservation, C27H5.1 was officially named *pdl-1* (phosphodiesterase 6 delta) and shall be referred to as such throughout the remainder of this work.

```
Human          1   ----------M S A K D E R A R E I L R G F K L N W M N L R D A E T G K I L W Q G T E D L S V P
Cow            1   ----------M S A K D E R A R E I L R G F K L N W M N L R D A E T G K I L W Q G T E D L S V P
Dog            1   ----------M S A K D E R A R E I L R G F K L N W M N L R D A E T G K I L W Q G T E D L S V P
Chicken        1   ----------M S A T D E R A K E I L R G F K L N W M N L R D A E T G K I L W Q G T E D L S V P
Xenopus        1   ----------M S Q D E R A K Q I L K G F K L N W M N L R D A E T G K I L W Q G T E D L S F P
Trout          1   ---M S D S D I M S S T E D R A K E I L K G F K L N W M N L R D A E T G K I L W Q G T E D L S L P
zebrafish      1   ----------M S S D E D R A K E I L K G F K L N W M N L R D A E T G K V L W Q G T E D L S L P
R_pipiens      1   -----------M S S N E R A K K I M D G F K L N S M I L R D G E T G K T L W Q G A E D L S F P
C_intestinalis 1   -------M A S E A N H P E Q V D K I L D G F K L N W M N L R D A S G K V L W Q G D S D L S K P
C_elegans      1   M A T T A T R H Q D S K L S E K A E S I L A G F K L N W M N L R D A E T G K V L W Q S T E D M A D P
H_roretzi      1   --------------M Q D K S A Q I M E G F T L N W M N L R D A G T G K I P W Q G S D D L S R P
Drosophila     1   --------M G S D D Q S A G D R I Q K G F Q I N I M I L R D A D G K I I W Q E N K D F S A P
A_gambiae      1   --------M G T D D L G K G E K I L N G F Q I N M M I L R D A D G K I I W Q E N K D F S C P


Human          42  G V E H E A K V P K K I L K C K A V S R E I N F S S T E Q M E K F R L Q K V Y F K G Q C L E E W T
Cow            42  G V E H E A K V P K K I L K C K A V S R E I N F S S A E Q M E K F R L Q K V Y F K G Q C L E E W T
Dog            42  G V E H E A K V P K K I L K C K A V S R E I N F S S A E Q M E K F R L Q K V Y F K G Q C L E E W T
Chicken        42  G V E H E A K V P K K I L K C K A V S R E I N F S S A E Q M E K F R L Q K V Y F K G Q C L E E W T
Xenopus        41  G V E H E A K V P K K I L K C K A V S R E I N F S S A E Q M E K F R L Q K V Y F K G Q C L E E W T
Trout          48  G V E H E A K V P K K I L K C K A V S R E I N F S S S E K L E K F I L Q K V F F K G Q C L E E W T
zebrafish      42  G V E H E A K V P K K I L K C K A V S R E I N F S S V E K L E K F R L Q K V F F K G Q C L E E W T
R_pipiens      41  G V E H E A K V P K K I L K C K S V S R E I N F A E E E M E N F R L Q K V Y F K G Q C L E E W S
C_intestinalis 45  G F E H E A K V P K K I L K C K A V S R E I N F S S L E V M E K F R L Q R V L F K G K C L E E W T
C_elegans      51  K R E H K A K V P K N L L K C K T V S R E I N F S S V K I E K F R L Q K V Y L K G T I I E E W Y
H_roretzi      39  G Q E H E A K V P K K I L K C K A V S R E I N F S S K K S M K K F R L Q K V I F Q G R V L E E W Y
Drosophila     43  D Q E H E A K V P V K I L D M K A V S R E I N F T I E S M E N F R L Q K V L F K G R I M E E W T
A_gambiae      43  D V E H E A K V P V K I L S L K A V S R E I N F G T V E A M E N F R L D Q K V L F K G R I M E E W T


Human          92  F E F G F V I P N S T N T W Q S L I E A A P E S Q M M P A S V L T G N V I I E T K F F D D D L L V S
Cow            92  F E F G F V I P N S T N T W Q S L I E A A P E S Q M M P A S V L T G N V I I E T K F F D D D L L V S
Dog            92  F E F G F V I P N S T N T W Q S L I E A A P E S Q M M P A S V L T G N V I I E T K F F D D D L L V S
Chicken        92  F E F G F V I P N S T N T W Q S L I E A A P E S Q M M S A N V L T G N V I I E T K F I D D D L L V S
Xenopus        91  F E F G F V I P N S M N T W Q S L I E A A P E S Q M M P A N V L T G N V V I E T K F F D D D L L V S
Trout          98  F E F G F V I P N S T N T W Q S L I E A A P E S Q M M P A N V L T G N V V I E T K F F D D D L H V S
zebrafish      92  F E F G F V I P N S T N T W Q S L I E A A P E S Q M M P A N V L T G N V V I E T K F F D D D L H V S
R_pipiens      91  F E F G F V M P N S V N T W Q S M I E A A P E S Q M M P A N V L T G N V I I E T K F F D A D L L V S
C_intestinalis 95  F E F G F V I P D S T N T W Q S V I E A A P A S Q M M P A S V L S G N V V I E T Q F F D D D V L V S
C_elegans      101 F D F G F V I P D S T N T W Q N M I E A A P E S Q M F P P S V L S G N V V V E T L F F D G D L L V S
H_roretzi      89  F Q F G F V I P D S T N T W Q S T I E A A P Q G Q M M P A H V L S G N V V I E T N F F D E D A L V S
Drosophila     93  F E M G F V G A N T T N T W Q S T I E A A P E S Q M M P A K V L N G N V T I Q T S F F D N K T L I T
A_gambiae      93  F E M G W V S P N T T N T W Q S T I E A A P E S Q M M P A K V L N G N V T I E T S F F D G D T L I S


Human          142 T S R V R L F Y V
Cow            142 T S R V R L F Y V
Dog            142 T S R V R L F Y V
Chicken        142 T S R V R L F Y V
Xenopus        141 T S R V R L F Y V
Trout          148 T S R V R L F Y V
zebrafish      142 T S R V R L F Y V
R_pipiens      141 T S R V R L F Y V
C_intestinalis 145 T S R V R I I Y V
C_elegans      151 T S R V R L I Y D
H_roretzi      139 Q S R V R V F Y V
Drosophila     143 K S V V R L I Y I
A_gambiae      143 K S V V R L I Y I
```

Figure 1.4   Conservation of PDEδ protein among metazoans. In order from top to bottom: *Homo sapiens, Bos taurus, Canis familiaris, Gallus gallus, Xenopus laevis, Oncorhynchus mykiss, Danio rerio, Rana pipiens, Ciona intestinalis, Caenorhabditis elegans, Halocynthia roretzi, Drosophila melanogaster, Anopheles gambiae*. Black shading indicates identity while grey shading indicates similarity.

1.8 PDEδ and the retina

Mammalian UNC-119 and PDEδ show high levels of expression in the retina (as well as lower levels of expression in other tissues) while *unc-119* and *pdl-1* show pan-neural expression in *C. elegans*. As well, both UNC-119 and PDL-1 show high degrees of conservation with their mammalian homologues (57% and 70% identity respectively).

14

These observations led us to speculate that this protein family might play a unique role in the nervous system of *C. elegans* and a corresponding role in vertebrate photoreceptors. While UNC-119 has been implicated in the regulation of cytoskeletal dynamics, PDEδ has been shown to influence phototransduction.

1.8.1 Phototransduction

Phototransduction refers to the complex regulatory cascade that allows photoreceptors to respond to light (Figure 1.5). When light hits a photoreceptor, it causes a conformational change in the chromophore-associated protein rhodopsin. In turn, rhodopsin activates the G-protein transducin. The GTP bound α subunit of transducin detaches from the $\beta\gamma$ subunits and activates phosphodiesterase (PDE) by displacing its inhibitory γ subunits. The newly active PDE then hydrolyzes the secondary messenger cGMP. cGMP binds to ion channels in the membrane, causing them to be kept open. Once PDE is activated it converts cGMP to GMP and the ion channels are closed leading to hyperpolarization of the cell. While the ion channels are closed, calcium is extruded from the cell causing a drop in internal calcium concentration. This loss of calcium stimulates guanylate cyclase activity, thereby replenishing cGMP levels. As well, the alpha subunit of transducin undergoes GTP-hydrolysis to return its GDP bound state. Once transducin is inactivated, the inhibitory PDEγ subunits reassociate with phosphodiesterase and cGMP hydrolysis stops. All of these adaptations allow cGMP levels to rise, causing the ion channels to open and the cell to depolarize once again (Yarfitz and Hurley, 1994).

15
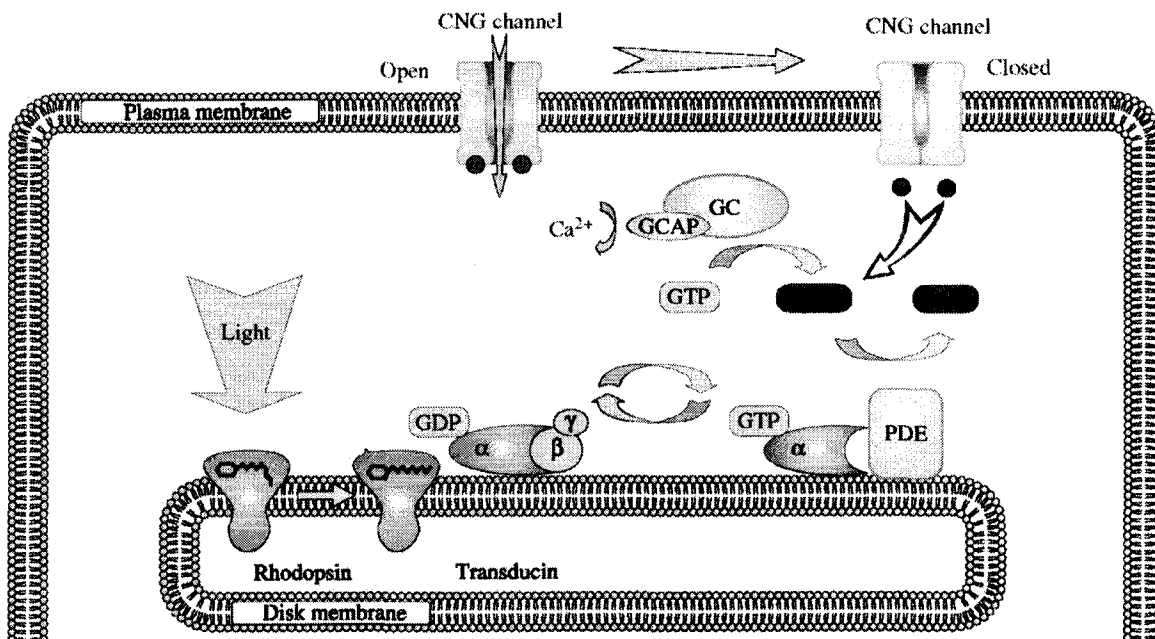
Figure 1.5 Vertebrate phototransduction. This figure illustrates the visual transduction cascade in vertebrate photoreceptors. PDE = phosphodiesterase, GC = guanylate cyclase, CNG channel = cyclic nucleotide gated channel. Figure from Kramer and Molokanova (2001).

1.8.2 PDEδ and Phosphodiesterase

PDEδ was first identified through co-immunoprecipitation with rod cGMP phosphodiesterase (PDE) and was accordingly termed the delta subunit (Gillespie *et al.*, 1989). Specifically, PDEδ is associated with the soluble fraction of PDE. It has been shown that PDEδ is able to bind to and solubilize PDE from the membrane, perhaps by binding the isoprenylated carboxyl termini of the catalytic α and β subunits (Florio *et al.*, 1996). Further investigation showed that the carboxyl peptides of PDEα and β must be prenylated and methylated for PDEδ binding to occur (Cook *et al.*, 2000). This suggests a potential regulatory mechanism whereby PDEδ binding could be controlled through the methylation state of PDE.

1.8.2.1 Prenylation

Many proteins become membrane associated through lipid modification. Prenylation is one form of lipid modification where a cysteine residue near the carboxyl terminus is

16

covalently linked to a farnesyl (15-carbon) or geranylgeranyl (20-carbon) isoprenyl lipid moiety. The most common target sequence for prenylation is the carboxyl terminal CAAX motif where C is cysteine, A represents an aliphatic amino acid, and X represents any amino acid. The isoprenyl group is covalently linked to the cysteine residue by a prenyl transferase. After lipid transfer, the AAX peptide is removed by a prenylation dependent endopeptidase making the prenylated cysteine the carboxyl terminal amino acid. The protein can then be methylated to further increase its membrane association (Zhang and Casey, 1996). Unlike transmembrane proteins, which are permanently membrane-bound, prenylated proteins can be transiently associated with the membrane depending on their prenylation state and the presence or absence of accessory proteins. For example, the small GTPase Cdc42 is associated with the membrane through its prenyl group but is solubilized through binding with RhoGDI (Leonard et al., 1992).

In addition to regulating membrane association, prenylation can be required for protein-protein interactions as shown for the PDEδ interaction with PDE (Cook et al., 2000). Inhibition of prenylation in mammalian cells leads to disassembly of the actin cytoskeleton indicating that prenylation is necessary for proper cell function (Fenton et al., 1992). Many proteins are prenylated including transducin (Lai et al., 1990), yeast mating factor (Anderegg et al., 1988), nuclear lamin B (Farnesworth et al., 1989), and many members of the Ras superfamily of small GTPases (for review see Zhang and Casey, 1996).

Although PDEδ binds to the catalytic subunits of PDE, this binding does not appear to affect its catalytic activity (Florio et al., 1996). However, binding by PDEδ does affect the overall rate of phototransduction (Cook et al., 2001). In the presence of PDEδ, the rate of cGMP hydrolysis by PDE is reduced. The presence of PDEδ also slows photoreceptors' return to the "off" state after light exposure. This suggests that PDEδ can play a role in the modulation of phototransduction. The precise mechanism behind this modulation is not clear although it has been postulated that PDEδ may slow phototransduction by removing PDE from contact with membrane-bound transducin. Moving PDE away from transducin could impede the interaction between the α subunit

17

of transducin with the inhibitory PDEγ subunits, thereby reducing the rate of PDE activation and consequently slowing the overall rate of cGMP hydrolysis.

The final effect of PDEδ binding to PDE is on the non-catalytic cGMP binding sites of the PDEαβ dimer. In addition to the catalytic cGMP binding sites that hydrolyze cGMP during phototransduction, PDEαβ has two non-catalytic cGMP binding sites. Non-activated, membrane bound PDE (αβγ$_2$) exchanges cGMP at one non-catalytic site while the second site is non-exchangeable (Mou *et al.*, 1999). Conversely, non-activated soluble PDE (αβγ$_2$δ) exchanges cGMP at both sites. While the effect of cGMP binding to the non-catalytic sites is unclear, it has been proposed that the cGMP bound state of the non-catalytic subunits may influence the binding affinity of the inhibitory γ subunits. If so, binding by PDEδ could indirectly stabilize or destabilize γ binding to PDE and thereby modulate photoreceptors' sensitivity to light.

1.8.3 PDEδ and RPGR

Rod cGMP phosphodiesterase is not the only retinal protein to have been shown to interact with PDEδ. PDEδ interacts with retinitis pigmentosa GTPase regulator (RPGR) as shown by yeast 2-hybrid and *in vitro* assays (Linari *et al.*, 1999). Mutations in RPGR are associated with retinal dystrophy, although the function of the RPGR protein is unknown. Recent work on RPGR has shown that the protein is localized to the connecting cilium in photoreceptors (Hong *et al.*, 2000; Hong *et al.*, 2001), tethered there through its interaction with RPGR interacting protein (RPGRIP) (Zhao *et al.*, 2003). The connecting cilium of a photoreceptor links the nucleus-containing inner segment to the photosensitive outer segment. Proteins must be transported through the connecting cilium to reach the outer segment and the regulated movement of signal transduction proteins through the connecting cilium appears to play a part in rod photoadaptation (McGinnis *et al.*, 2002). Mice lacking RPGR show a lack of polarized opsin distribution to the outer segment of cones, suggesting that RPGR is necessary for directed transport of opsin from the inner to outer segments (Hong *et al.*, 2000). Supporting this hypothesis, a yeast 2-hybrid screen with the RCC-homologous domain of RPGR identified several isoforms of the RPGR interacting protein RPGRIP1 (Roepman *et al.*, 2000). These

18

RPGRIP1 isoforms share sequence similarity with proteins involved in vesicle transport. Finally, RPGR is localized to the Golgi in mice (Yan *et al.*, 1998). Thus, while RPGR has not been directly shown to affect vesicle transport, there is mounting evidence that this protein is required for vesicle transport from the inner to outer segments of photoreceptors.

PDEδ has been shown to interact with two retinal proteins, PDE and RPGR, both of which play very different roles. PDE is involved in phototransduction while RPGR is likely involved in vesicle transport. The disparate roles of these two proteins suggest a regulatory role for PDEδ in the retina. It has already been shown that overexpression of PDEδ leads to a decrease in the rate of phototransduction coupled with a slowing of return to the "off" state (Cook *et al.*, 2001). This could occur through solubilization of PDE as previously discussed. However, the emerging evidence suggesting a role for RPGR in vesicle transport suggests that PDEδ may also influence vesicle transport in photoreceptors. Vesicle transport is required to move membrane-bound proteins such as rhodopsin and transducin to the outer segment. Interaction with RPGR could provide a second way for PDEδ to influence phototransduction.

1.9 PDEδ beyond the retina

While PDEδ expression is strong in the retina, northern blot analysis shows the presence of transcript in a variety of mammalian tissues including brain, spleen, adrenal gland, lung, peripheral blood, ovary, testis, liver, heart, placenta, skeletal muscle, and kidney (Florio *et al.*, 1996; Lorenz *et al.*, 1998; Marzesco *et al.*, 1998; Wang *et al.*, 1999). This ubiquitous expression suggests a general role for PDEδ outside the retina. Biochemical studies have identified a number of proteins which interact with PDEδ, most of which are not retina-specific. These proteins are discussed below.

1.9.1 PDEδ and Rab13

PDEδ has been shown to interact with Rab13, Arl family members, and a number of Ras family GTPases. The first of these to be reported was the interaction with Rab13, a small

19

GTPase which has a prenylation signal at its carboxyl terminus. PDEδ has been shown to bind to prenylated Rab13 and cause it to dissociate from the membrane (Marzesco *et al.*, 1998; Marzesco *et al.*, 2001). Rab 13 has been shown to localize to vesicles in fibroblasts and tight junctions in epithelial cells (Zahraoui *et al.*, 1994) while in mouse blastocysts Rab13 localization corresponds to the beginning of tight junction assembly (Sheth *et al.*, 2000).

Further work has shown that Rab13 is required for proper assembly of tight junctions in cell culture (Marzesco *et al.*, 2002). Specifically, expression of a constitutively GTP-bound form of Rab13 [Rab13(Q67L)] leads to disorganized tight junctions which are unable to act as barriers for nonionic molecules. Conversely, expression of an inactive form of Rab13 [Rab13(T22N)] reduces diffusion of tracer molecules relative to wild-type but does not visibly disrupt tight junction structure. Disruption of tight junction assembly by expression of Rab13(Q67L) is believed to occur through interrupted distribution of the tight junction protein claudin1. The authors suggest that GTP-bound Rab13 is required for the recruitment of claudin1 to the epithelial tight junction, whereas Rab13 inactivation may be required for claudin1 incorporation. The effect, if any, that the interaction between PDEδ and Rab13 may have on tight junction assembly is unknown.

1.9.2 PDEδ and the Arl Protein Family

The Arl (ARF-like) proteins are defined by their similarity to ADP-ribosylation factors (ARFs). ARF proteins have a well demonstrated role in vesicle transport and other cellular processes (for review see Sprang, 2002; Chavrier and Goud, 1999). The Arl proteins share sequence similarity with the ARFs but lack certain features of ARF activity (Kahn *et al.*, 1991). These differences have led to Arl proteins being placed in a different subfamily than the ARF proteins, despite their sequence similarity. PDEδ has been shown to interact with three Arl proteins: Arl1, Arl2, and Arl3 (Linari *et al.*, 1999; Renault *et al.*, 2001; Van Valkenburgh *et al.* 2001; Hanzal-Bayer *et al.*, 2002). The proposed functions of these three proteins were discussed in detail in section 1.3. Briefly, they appear to be involved in cytoskeletal dynamics and vesicle transport.

20

PDEδ was first shown to interact with Arl3 by yeast 2-hybrid (Linari *et al.*, 1999). This interaction is specific to the GTP-bound form of Arl3. Both wild-type and constitutively GTP bound forms of Arl3 [Arl3(Q71L)] interact with PDEδ in the yeast 2-hybrid system, while a constitutively GDP bound form of Arl3 [Arl3(T31N)] fails to do so. This study went on to show that PDEδ coimmunoprecipitates with Arl3(Q71L) in kidney cell culture. Finally it was shown that PDEδ stabilizes Arl3 in its GTP bound form. As mentioned previously, Arl3 has been implicated in the control of cytoskeletal dynamics. PDEδ may regulate the activity of Arl3 thereby influencing cytoskeletal stability and rearrangement.

The PDEδ interaction with Arl2 is the best characterized of all the Arl interactions. Again, PDEδ binds preferentially to Arl2 in its GTP-bound state (Van Valkenburgh *et al.*, 2001). Recently, the structure of PDEδ in association with Arl2-GTP has been resolved by X-ray crystallography (Renault *et al.*, 2001; Hanzal-Bayer *et al.*, 2002). The crystal structure reveals that PDEδ has a similar organization to Rho guanine dissociation inhibitor (RhoGDI), despite an absence of sequence similarity between these two proteins (Figure 1.6).

RhoGDI interacts with prenylated Rho GTPases, solubilizing them from membranes and inhibiting GDP/GTP exchange by preventing dissociation of GDP from the nucleotide binding pocket (Fukomoto *et al.*, 1990; Isomura *et al.*, 1991). Like RhoGDI, PDEδ has a hydrophobic pocket which could accommodate a lipid moiety (Hanzal-Bayer *et al.*, 2002) (Figure 1.7). As Arl2 is not prenylated, this hydrophobic pocket is not involved in the interaction between these two proteins. However, it is likely involved in the interaction between PDEδ and prenylated proteins such as PDE and Rab13.

21
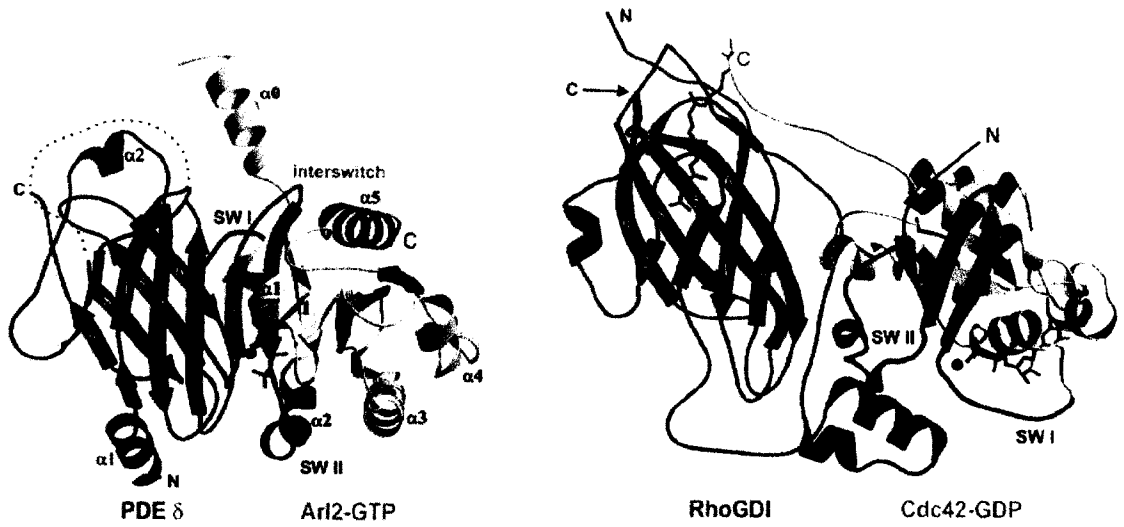
Figure 1.6 Comparison of crystal structure between PDEδ/Arl2 complex and RhoGDI/Cdc42-GDP complex. Cdc42 interacts with RhoGDI through its carboxyl lipid modification (prenylation). As shown Arl2 is not prenylated and interacts with PDEδ through amino acid interactions. Both RhoGDI and PDEδ have a similar β sandwich structure. Figure modified from Hanzal-Bayer (2002).
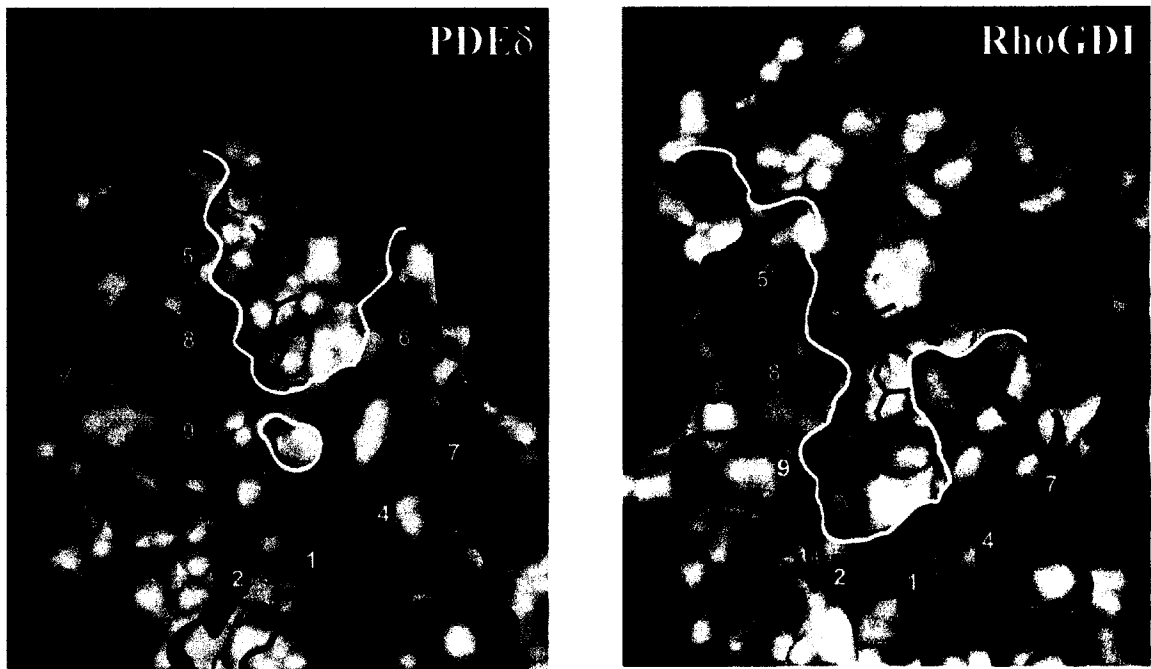
Figure 1.7 Comparison of RhoGDI lipid binding pocket with the putative lipid binding pocket in PDEδ. Comparison of the crystal structures of RhoGDI and PDEδ reveals that PDEδ has a putative lipid binding pocket similar to that of RhoGDI. A small conformational shift would be required to open the PDEδ pocket. The hydrophobic pocket is outlined in white while the proposed location of a farnesyl group is drawn in red. Figure modified from Hanzal-Bayer (2002).

Arl2 has been shown to play a role in the regulation of cytoskeletal dynamics in *C. elegans*, humans, and yeast (Antoshechkin and Han, 2002; Bhamidipati *et al.*, 2000; Radcliffe *et al.*, 2000). It has also been shown that PDEδ stabilizes Arl2 in its GTP-bound form although it is not clear whether PDEδ is able to activate Arl2. It is therefore possible that PDEδ binding acts to prolong signalling by Arl2 although it may or may not initiate the signalling process. PDEδ may serve to bring prenylated proteins, such as Rab13 and others described in the following section, into close proximity with Arl2. Since Arl2 interacts with tubulin cofactors it is conceivable that Arl2, in conjunction with PDEδ, localizes certain prenylated proteins to microtubules.

Finally, PDEδ has been shown to interact with Arl1 by yeast 2-hybrid (Van Valkenburgh *et al.*, 2001). Again, this interaction is specific to the GTP bound form of Arl1. Unlike Arl2 and Arl3, Arl1 is believed to play a role in vesicle trafficking. Arl1 localizes to the Golgi and regulates Golgi structure in mammalian cells (discussed in section 1.5). PDEδ binds to Arl1 in its active GTP-bound form and may promote Arl1 activity.

1.9.3 PDEδ and Ras Family Members

Recently, PDEδ has been shown to interact with several members of the Ras superfamily of small GTPases. Specifically, yeast 2-hybrid assays have been used to show interaction with H-Ras, Rheb, Rho6, Gα$_{i1}$, Rap1A, Rap2B, RhoA, RhoB, and Rnd1 (Hanzal-Bayer *et al.*, 2002; Nancy *et al.*, 2002). These interactions do not depend on the nucleotide state of the GTPase, as PDEδ interacts equally well with GTP and GDP bound H-Ras, Rap2B, Rap1A, RhoA, and Rnd1 (Nancy *et al.*, 2002). The PDEδ interactions are specific to certain Ras family members as PDEδ fails to interact with proteins such as RalB and Rab6. These interactions are likely to be physiologically relevant as PDEδ expression is able to solubilize H-Ras, N-Ras, and K-Ras in HeLa cells. This suggests that PDEδ has the same solubilizing effect on Ras proteins as it does on Rab13 and PDE.

Ras family proteins are involved in regulation of a wide variety of cellular processes including cell division, cytoskeletal dynamics, vesicle transport, differentiation, and gene expression (for review see Takai *et al.*, 2001). These proteins act as molecular switches

23

by alternating between an inactive GDP-bound state and an active GTP-bound state. Most of these proteins have an intrinsic GTPase activity which can be enhanced or decreased by interaction with regulatory proteins. Guanine nucleotide exchange factors (GEFs) promote the switch from GDP to GTP, while GTPase activating proteins (GAPs) promote GTP hydrolysis. Guanine nucleotide dissociation inhibitors (GDIs) prevent GDP-GTP exchange. These interacting proteins respond to cellular signalling to control the activity of Ras family GTPases.

It is not entirely clear where PDEδ fits into this regulatory network. It seems clear that PDEδ solubilizes these proteins through interaction with their prenylated carboxyl termini. However, binding of PDEδ occurs regardless of whether the proteins are in their GDP or GTP bound state (Nancy *et al.*, 2002), suggesting that PDEδ does not affect nucleotide binding or hydrolysis. One proposal is that PDEδ is required for transport of newly synthesized proteins through the cytosol. Alternatively, PDEδ might regulate Ras family protein activity by moving these proteins in and out of the membrane, thereby removing them from proximity with other membrane-bound signalling molecules. If PDEδ does release Ras proteins from membranes, this must occur transiently or at low level as there have been no reports of a cytosolic pool of Ras protein.

1.10 PDEδ summary

Interaction studies are continually uncovering new binding partners for PDEδ. In most cases, these interactions appear to rely on PDEδ binding to the prenylated carboxyl termini of its partners. Proteins which interact with PDEδ have been implicated in a wide variety of cellular processes including phototransduction, vesicle transport, differentiation, division, and cytoskeletal regulation. PDEδ does not appear to directly affect the activity of its partners either through controlling their nucleotide binding state (with the exception of the Arl proteins) or by influencing their catalytic activity. Most of these interactions have been identified through directed studies and it is unknown how many other protein partners have yet to be identified. Despite this wealth of interaction data, we do not know the biological role of PDEδ. For a summary of PDEδ interactions see Table 1.1.

24

Protein	Prenylation signal?	Interaction with PDEδ identified by	Solubilized by PDEδ?	Effect of PDEδ on protein function/activity
Arl1	no	yeast 2-hybrid[1]	n/d	likely stabilizes Arl1 in its GTP-bound form
Arl2	no	affinity co-purification[2]	n/d	likely stabilizes Arl2 in its GTP-bound form
Arl3	no	yeast 2-hybrid[3] co-immunoprecipitation[3]	n/d	stabilizes Arl3 in its GTP-bound form
Gα$_{i1}$	yes	yeast 2-hybrid[4]	n/d	n/d
H-Ras	yes	yeast 2-hybrid[4,5] co-immunoprecipitation[5]	yes	n/d
PDE	yes	co-immunoprecipitation[6]	yes	allows cGMP exchange at both non-catalytic cGMP binding sites
Rab13	yes	yeast 2-hybrid[7] affinity co-purification[7]	yes	n/d
Rap1A	yes	yeast 2-hybrid[5]	yes	n/d
Rap2B	yes	yeast 2-hybrid[5]	yes	n/d
Rheb	yes	yeast 2-hybrid[4]	n/d	n/d
Rho6	yes	yeast 2-hybrid[4,5]	n/d	n/d
RhoA	yes	yeast 2-hybrid[5]	n/d	n/d
RhoB	yes	yeast 2-hybrid[5]	n/d	n/d
RPGR	yes	yeast 2-hybrid[8] affinity co-purification[8]	n/d	n/d

Table 1.1 Summary of proteins which have been shown to interact with mammalian PDEδ.
n/d = no data available. [1]Van Valkenburgh et al., 2001; [2]Renault et al., 2001; [3]Linari et al., 1999a; [4]Hanzal-Bayer et al., 2002; [5]Nancy et al., 2002; [6]Gillespie et al., 1989; [7]Marzesco et al., 1998; [8]Linari et al., 1999.

PDEδ may be required for transport of prenylated guanine nucleotide binding proteins. However, that doesn't address the effect of PDEδ on the Arl proteins. These are not prenylated and their interaction with PDEδ occurs through a different mechanism. More importantly PDEδ affects the nucleotide binding state of the Arl proteins, suggesting that it may regulate their function. PDEδ may act as a downstream effector for the Arl proteins, maintaining them in their activated state and acting as a bridge between activated Arls and various Ras family members. Alternatively, the interactions of PDEδ with its various protein partners may independent of one another and PDEδ may play multiple regulatory or transport roles within the cell.

While it is possible to speculate that PDEδ may play a regulatory role in the cell, it is difficult to imagine what effect it has on the development or function of an organism. This thesis describes my efforts to determine the effect of a PDL-1/PDEδ loss of function in the nematode *Caenorhabditis elegans* and the zebrafish *Danio rerio*. Before I started

25

this work, there were no PDEδ mutations known in any species. I hoped that genetic analysis of *pdl-1* would help us to understand the function of PDL-1/PDEδ *in vivo*.

1.11 Investigating the role of PDL-1/PDEδ

At the beginning of this study, I set out to identify and then characterize the effects of a *pdl-1* loss-of-function mutation. I expected a *pdl-1* mutant to have a clear phenotype based on the strong conservation of the PDL-1 protein. Specifically I predicted that a *pdl-1* mutant would be sterile; lethal; or uncoordinated, as is the case for *unc-119*. I attempted to create a *pdl-1* loss of function through mutagenesis and RNA interference (RNAi). Mutagenesis was carried out concurrently in our lab and by the *C. elegans* Genome Knockout Consortium. I screened for a mutation in *pdl-1* by PCR deletion screening, F1 screening for a visible phenotype in worms hemizygous for *pdl-1*, and pre-complementation screening for lethal alleles. I also used RNAi to try to phenocopy a *pdl-1* loss of function. Eventually, the Genome Knockout Consortium found a deletion in *pdl-1* and I moved on to phenotypic characterization of the deletion mutant.

In addition to carrying out phenotypic characterization, I wanted to determine the expression pattern of *pdl-1* and identify its protein partners. Through the use of *pdl-1*::GFP reporter constructs, I was able to confirm that *pdl-1* is expressed throughout the nervous system. I also raised polyclonal antisera against the PDL-1 protein. I had intended to use these antisera to look at its subcellular localization but immunostaining was unsuccessful. Finally, I used a yeast 2-hybrid screen to try to identify *C. elegans* proteins that interact with PDL-1. I had hoped that the yeast 2-hybrid screen would identify similar protein partners to those found in mammalian systems as well as to identify new protein partners that might be specific to *C. elegans*.

In the final year of my Ph.D. program, I decided to study PDEδ in the zebrafish *Danio rerio*. As discussed in the previous sections, mammalian PDEδ has been studied extensively *in vitro* and many protein interactions have been identified. Unfortunately, the function of PDEδ and the significance of these interactions *in vivo* is still a mystery. I

26

had hoped to shed some light on the matter through the study of PDEδ in a vertebrate model organism.

Since there is genomic sequence available for zebrafish PDEδ, I was able to clone the cDNA and perform 3'RACE. I performed *in situ* hybridization to determine the PDEδ expression pattern. In addition, I carried out immunostaining on zebrafish embryos using the polyclonal antibody raised against *C. elegans* PDL-1. The antibody showed cross-reactivity with zebrafish PDEδ on a western blot, suggesting that it could be used for embryo staining. Finally, I used antisense morpholino oligonucleotides to inhibit translation and/or splicing of the PDEδ transcript. This technique allows for knockdown phenocopy in early zebrafish embryos. Since the *C. elegans pdl-1* mutant appears to be wild-type, I wanted to see if knockdown in a more complex organism would have a phenotypic effect.

Until this study, there were no known mutations in PDEδ in any species. I set out to find such a mutation in the hopes that genetic analysis would help to provide some context for the biochemical work which has been carried out in mammals.

1.12 Specific objectives of this work

1.   Identify and characterize the *pdl-1* loss of function phenotype in *C. elegans*.

2.   Confirm nervous system expression of *pdl-1* using GFP reporter constructs.

3.   Raise antibodies against PDL-1.

4.   Identify proteins that interact with PDL-1 using the yeast 2-hybrid system.

5.   Clone zebrafish PDEδ and characterize its expression.

6.   Determine the zebrafish PDEδ knockdown phenotype in the early embryo.

27

Materials and Methods

A list of strains and genotypes is provided in Appendix II. Primer sequences are provided in Appendix III.

Part 1: *C. elegans*

2.1 *C. elegans* culture conditions

Unless otherwise noted, nematodes were grown at 20°C on NGM agar plates seeded with *E. coli* strain OP50 (Brenner, 1974).

2.2 Making *pdl-1*::GFP constructs

The promoter region of *pdl-1* was cloned into an expression vector by Michelle Patterson (nee Chambers). She used PCR with primers A1066 and A1065 to amplify a 5408 bp product from N2 genomic DNA. This includes 4929 bases of upstream sequence as well as exon 1 and part of exon 2. The PCR product was digested with XhoI and BamH1 then cloned into pBluescriptSK⁻ (Stratagene). To make the transcriptional GFP fusion, the promoter sequence was subcloned into Fire lab expression vector pPD95.79 as a BamHI/SalI fragment (Information about the Fire Lab Expression Vector Kit is available at ftp://ftp.wormbase.org/pub/elegans_vector/FireLabVectors/).

Translational *pdl-1*::GFP fusion constructs were made by subcloning either *pdl-1* cDNA (pJS33) or genomic DNA (pJS100) behind the *pdl-1* promoter in pBluescript. Full length *pdl-1* cDNA was subcloned behind the *pdl-1* promoter as an SstI fragment. Genomic *pdl-1* sequence was PCR amplified from N2 genomic DNA using C27JSF2 and C27JSR2. This PCR product was first cloned into pGEM-T (Amersham) and then subcloned behind the *pdl-1* promoter as an SstI fragment. For both the cDNA and genomic constructs, GFP coding sequence was subcloned into the coding region of *pdl-1* immediately after the start codon. This was accomplished by subcloning GFP as an Msc1 fragment from the Fire lab exon insertion vector pPD119.16.

28

All GFP constructs were co-injected with the dominant transformation marker pRF4 (*rol-6(su1006)*) into the gonad of N2 worms to produce transgenic lines (Mello *et al.*, 1991). The transcriptional *pdl-1*::GFP fusion was integrated into the genome with UV irradiation while the translational *PDL-1*::GFP fusions have been maintained as extrachromosomal arrays.

2.3 5' and 3' RACE to clone full-length *pdl-1* cDNA

To produce cDNA, total RNA from mixed stage worms was reverse transcribed using the Gibco 3'RACE adapter primer and Superscript II RT (Invitrogen). For 3' RACE, the cDNA was primed using the Gibco adapter primer. For 5' RACE, the cDNA was primed using MMA17. Subsequent PCR amplification was performed using nested primer sets. The 3' RACE product was subjected to 40 rounds of amplification with C273RACE1 and UAP (Gibco) followed by subsequent amplification with C273RACE2 and UAP. The 5' RACE product was amplified using MMA18 and LVSL1 followed by subsequent amplification with C275RACE2 and LVSL1.

The RACE products were cloned into pGEM-T (Amersham) and confirmed by sequencing. Full-length *pdl-1* cDNA was produced by subcloning the MluI/SalI fragment from the 3' RACE product in pGEM-T (pJS4) into MluI/SalI digested 5' RACE product in pGEM-T (pJS3).

2.4 Northern analysis of *pdl-1* transcript

Total RNA was isolated from mixed stage N2 worms as follows. Worms were grown on plates and collected in M9 buffer. 1 ml of Trizol (Gibco) was added to 250 μl of packed worms. The worms were vortexed for 1 minute, allowed to sit at room temperature for 5 minutes, then spun at top speed in a 4°C microfuge for 10 minutes to pellet cell debris. I added 200 μl chloroform to the supernatant, vortexed for 15 seconds, and let sit at room temperature for 2 minutes. The tube was the spun at 14,000 rpm in a 4°C microfuge for 15 minutes. The RNA was precipitated from the aqueous phase by adding 600 μl isopropanol. After 10 minutes at room temperature the tubes were spun at top speed in a 4°C microfuge for 15 minutes. The pellet was washed in 100 μl 75% EtOH in DEPC

29

treated H$_2$O, spun at 7500 rpm for 5 minutes at 4°C, and briefly air dried. RNA was finally resuspended in 150 µl DEPC treated water.

1-15 µg of RNA were size separated on a 1.5% agarose formaldehyde gel and transferred to Genescreen Plus nylon membrane (NEN Life Science Products) in 10x SSC using capillary transfer. The resulting blot was crosslinked in a UV Stratalinker and prehybridized in Hybrisol (Intergen).

A *pdl-1* probe was prepared by gel purifying an MscI/NcoI fragment of *pdl-1* cDNA using the Sephaglas BandPrep Kit (Amersham). Approximately 75 ng of template was radiolabelled with [32]P dCTP using the T7 Quickprime Kit (Pharmacia) as per the manufacturer's instructions. Hybridization was performed overnight at 65°C. Washes were performed at 65°C as follows: 2x SSC - 15 min.; 2x SSC - 15 min; 2x SSC, 0.1% SDS – 30 min.; and 0.1x SSC, 0.1% SDS – 10 minutes. The blot was exposed to film at –80°C for 17 days.

2.5 Deletion library construction

The PCR deletion library was constructed as follows. Ten plates of worms were grown until there was an abundance of eggs and gravid adults. These were treated with 100% bleach to remove adults and larvae thereby producing a synchronous population of embryos. The embryos were plated onto 12 streaked plates and allowed to develop to L4/early adult. The worms were then mutagenized at room temperature for 4 hours in a solution of 1 mM EMS in M9 buffer, transferred to fresh plates (500 worms/plate), and allowed to lay eggs. After two days, the F1 larvae were transferred to new plates (approximately 500 worms per plate on 576 plates). The worms were allowed to reproduce until all available *E. coli* had been consumed and all embryos had hatched. This gave rise to a population of predominantly F2 animals, with some F3 animals present.

Once the plates cleared, worms were collected from each plate in 1.5 ml of M9 buffer and divided into three aliquots. Two of the aliquots were cryogenically frozen while the third was used for DNA preparation. To prepare DNA, worms were suspended in 100 µl

30

worm lysis buffer [50mM KCl, 10mM Tris-HCl pH8.3, 2.5 mM $MgCl_2$, 0.45% Tween-20, 0.45% NP-40, 0.01% gelatin, 200µg/ml proteinase K] and frozen at -80°C for 20 minutes. They were then incubated at 65°C for four hours with occasional mixing, followed by 20 minutes at 95°C. Finally the DNA samples were diluted by adding an equal volume of ddH_2O.

The DNA was then pooled in an arrayed fashion. Pools of DNA from 8 or 12 plates of worms were made by combining 50µl of DNA from each preparation (Figure 2.1). Genuine deletions should be detected in two pools, and can be used to address the deletion to a single plate of worms.

	1	2	3	4	5	6	7	8	9	10	11	12	
A	O	O	O	O	O	O	O	O	O	O	O	O	→ pool A
B	O	O	O	O	O	O	O	O	O	O	O	O	→ pool B
C	O	O	O	O	O	O	O	O	O	O	O	O	→ pool C
D	O	O	O	O	O	O	O	O	O	O	O	O	→ pool D
E	O	O	O	O	O	O	O	O	O	O	O	O	→ pool E
F	O	O	O	O	O	O	O	O	O	O	O	O	→ pool F
G	O	O	O	O	O	O	O	O	O	O	O	O	→ pool G
H	O	O	O	O	O	O	O	O	O	O	O	O	→ pool H
	↓	↓	↓	↓	↓	↓	↓	↓	↓	↓	↓	↓	
	pool 1	pool 2	pool 3	pool 4	pool 5	pool 6	pool 7	pool 8	pool 9	pool 10	pool 11	pool 12	
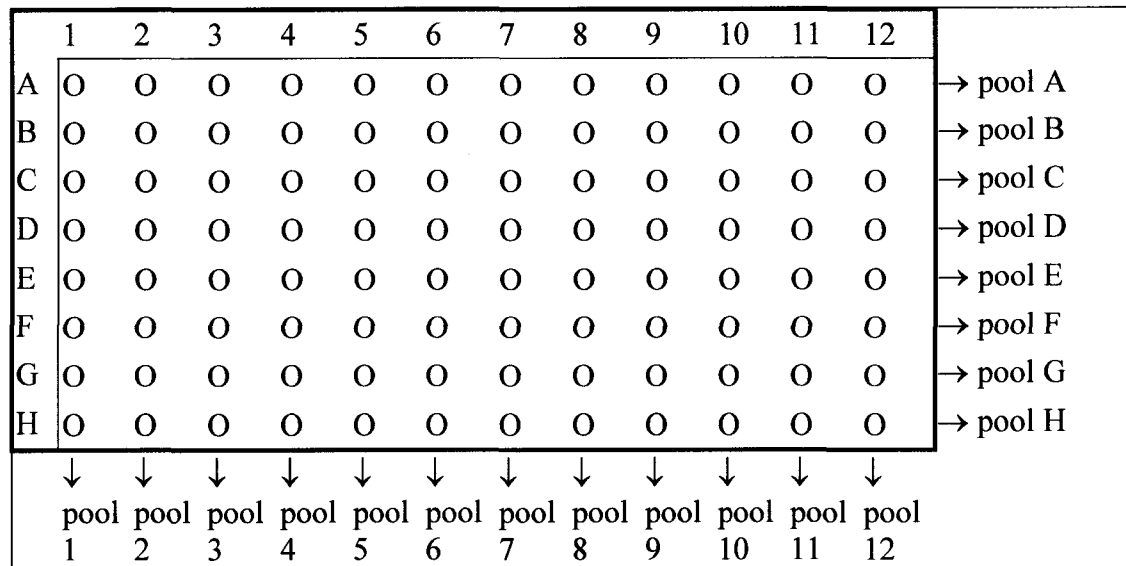
Figure 2.1   Deletion library DNA pooling. For example a deletion band detected in pool B and pool 8 can be attributed to plate B8. A deletion band that appears in only one pool or unrelated pools (e.g. pool 5 and pool 8) is a spurious result.

2.6 Deletion library screening

Pooled DNA from four 96-well plates was screened for deletions in *pdl-1* using nested PCR. All reactions were 25 µl, with 5 µl of template for round 1 and 2 µl of template for the nested reaction. The round 1 primers were C27JSF1 and C27JSR1. The nested primers were C27JSF2 and C27JSR2. The reaction mix consisted of: 0.2 mM dNTPs, 10

31

pmol each primer, 30 mM Tricine (pH 8.4), 2 mM $MgCl_2$, 5 mM β-mercaptoethanol, 0.01% gelatin, 0.1 % polidocanol, and 0.5 μl Taq DNA polymerase. The reaction conditions were 1x [94°C – 1 min., 58°C – 30 sec., 72°C – 45 sec.], 39x [94°C – 30 sec., 58°C – 30 sec., 72°C – 45 sec.] and PCR was performed in an MJ Research PTC-100 thermal cycler.

2.7 RNA interference

Double stranded RNA was produced by amplifying *pdl-1* cDNA from pJS30 using the primers "T7 big" and "SP6 becomes T7". The PCR product was electrophoresed on an agarose gel and purified using the Sephaglas BandPrep Kit (Amersham). The purified PCR product was then used as the template for *in vitro* transcription using the Ambion T7 Megascript kit as per the manufacturer's instructions. The resulting double stranded RNA was injected into N2 worms undiluted or at a dilution of 10^{-1} in DEPC treated H_2O.

Feeding RNAi constructs were prepared by cloning cDNAs of interest into the Fire Lab vector L4440. This vector contains a multiple cloning site flanked by two T7 transcription start sites, allowing for expression of dsRNA in *E. coli*, which are then fed to *C. elegans* (Kamath *et al.*, 2000). Feeding RNAi constructs were transformed into HT115 *E. coli* and individual colonies were inoculated into LB-Amp medium and grown overnight. In the morning, 400 μl of each overnight culture was used to inoculate 10 ml of LB-Amp and the cells were allowed to grow for 2.5 hours at 37°C. Cultures were induced by adding 10 μl of 1M IPTG and allowed to grow another 4 hours. After induction, cells were concentrated to a volume of 3 ml and plated on NGM + 1mM IPTG plates in approximately 250 μl aliquots. Single L4/young adult N2 animals were transferred onto each plate and allowed to feed for 24 hours. After this time, the adults were removed and the progeny were observed over the next few days to determine whether they exhibited a visible phenotype.

2.8 Finding a deficiency that removes *pdl-1*

Before performing an F1 screen for potential *pdl-1* alleles, it was necessary to determine whether any of the available deficiencies in chromosome II remove *pdl-1*. Four

32

candidate deficiencies were found using the information available in Wormbase (www.wormbase.org): mnDf97, mcDf1, mnDf88, and mnDf105 (see Figure 3.8). All four are sizeable deletions which remove at least one essential gene. The relevant strains were ordered from the *C. elegans* Genome Center and PCR on dead embryos (i.e. those homozygous for the deficiencies) was used to test for presence or absence of the *pdl-1* locus.

For PCR, individual dead embryos were picked into 2.5 μl of lysis buffer (20mg/ml chitinase, 50 mM NaCl, 70 mM KCl, 2.5 mM $MgCl_2$, 2.5 mM $CaCl_2$), frozen at -80°C for 15 minutes, incubated at 60°C for 1 hour, and then incubated at 95°C for 15 minutes. The single embryo lysates were used as templates for PCR with a mix of four primers: C273RACE2, A1066, ED3L, and ED3U. C273RACE2/A1066 amplify *pdl-1* while ED3L/ED3U amplify *unc-119* (on chromosome III) and serve as an internal PCR control.

2.9 F1 screen for uncoordinated mutants

This screen was performed using the strain ML335 [*dpy-2(e489)* mcDf1 *unc-4(e120)*/mnC1 *dpy-10(e128)* *unc-52(e444)* II]. Three 6 cm plates of ML335 animals were bleached to synchronize a large population of embryos. These were grown until the population consisted primarily of L4 larvae and young adults. These animals were mutagenized for four hours in 0.5 mM ENU (in M9 buffer) and then plated on 6 cm plates at a density of approximately 10 worms/plate. Worms were grown at room temperature and allowed to produce the F1 generation. The F1 worms were screened for locomotory defects and mutants were singled onto freshly streaked worm plates to confirm transmission of the phenotype into the F2. Of the 182 F1 animals singled, 29 transmitted an uncoordinated phenotype.

2.10 Precomplementation screen

To prepare for this screen, ML335 animals were injected with a 100ng/μL solution of pJS17 (genomic *pdl-1*) and pSU006 ($P_{F25B3.3}$::GFP). Transgenic progeny were identified by GFP fluorescence and a stably transmitting line was established. Worms were mutagenized as described in section 2.8 and plated at a density of approximately 25

33

worms/plate. Wild-type F1 worms expressing GFP were singled onto freshly streaked 6 cm plates and allowed to lay eggs. These plates were screened for lethality associated with GFP loss. In any case where there was 98-100% transmission of the transgenic array, the plates were maintained and screened again in the F3 generation. Approximately 1400 plates were screened and no lethal alleles were recovered.

2.11 Outcrossing and confirming the *pdl-1(gk157)* deletion

When I received the homozygous *pdl-1(gk157)* deletion strain VC282 from the *C. elegans* Genome Knockout Consortium, there were a number of males present. *C. elegans* is a hermaphrodite species and males occur spontaneously at low frequency (Wood, 1988). It is common to have an increased frequency of males in the first few generations after mutagenesis (personal observation). I used the *pdl-1* males to begin outcrossing with DP295 [mIn1 *dpy-10(e128)* mIs14 II] homozygotes. The worms were outcrossed four times by repeatedly picking wild-type male progeny and crossing to mIn1[dpy-10(e128) mIs14] hermaphrodites. After the last outcross, hermaphrodite progeny were allowed to self-fertilize and *pdl-1* homozygotes were re-established by selecting for absence of the balancer.

To confirm that the *pdl-1* line was homozygous for the *pdl-1* deletion, I isolated DNA from a recently cleared plate of worms. Worms were washed in M9, resuspended in a final volume of 100 μL M9, and frozen at −80 °C for 15 minutes. After removing the worms from the freezer, I added 100 μL of 2x lysis buffer (100mM KCl, 20mM Tris-HCl pH 8.3, 5mM $MgCl_2$, 0.02% gelatin, 0.9% Tween-20, 0.9% NP-40, 200 μg/ml proteinase K) and incubated the worms at 65 °C for 2 hours. After lysis, I boiled the worms for 15 minutes and added 200 μL of H_2O. I then used 2 μL of this crude DNA preparation as a template for PCR with C27JSF11 and C275RACE1 (primers that flank the *pdl-1* deletion). N2 genomic DNA was used as a positive control.

Finally, I performed Southern analysis to ensure that there are no duplications of the *pdl-1* locus in the *pdl-1(gk157)* deletion animals. DNA was isolated from eight plates each of N2 and *pdl-1* animals grown on 10 cm rich agarose plates (50mM NaCl, 0.75% peptone,

34

1.5% agarose, 1 mM $CaCl_2$, 1mM $MgSO_4$, 25 mM KH_2PO_4, 5 µg/ml cholesterol) seeded with OP50 *E. coli*. The worms were grown until the plates had almost cleared and the worms formed a visible wave across the plate. At this point, the worms were washed off the plates with H_2O and washed twice with 15 ml ddH_2O to remove any bacteria. Finally, the worms were transferred to 1.5 ml microfuge tubes with no more than 200 µL packed worms per tube. The worms were resuspended in 500 µl lysis buffer (100 mM Tris-HCl pH 8.5, 100 mM NaCl, 50 mM EDTA, 1% SDS, 1% β-mercaptoethanol, 100 µg/ml proteinase K) and frozen at −80°C for 30 minutes. They were then incubated at 60°C, adding an additional 5 µL proteinase K (100 mg/ml) to each tube every hour for the first three hours. The lysis was allowed to continue overnight. The next day the lysates were extracted twice with 700 µl phenol:chloroform:isoamyl alcohol (25:24:1) and once with chloroform:isoamyl alcohol (24:1). After the final extraction, the DNA was precipitated by adding 1.2 ml 95% EtOH and spooled onto a glass rod. The spool was washed in 70% EtOH, dried briefly and resuspended overnight in 700 µL TE. The DNA was then treated with 2.8 µL of RNAase A (10 mg/ml) and digested at 37 °C for one hour. This was followed by a second round of phenol:chloroform extraction as described above.

To make the Southern blot, 2 µg of N2 and *pdl-1*(gk157) DNA were digested with 20 units of the following enzymes: BglII, EcoR1, and HindIII (Invitrogen). The digests were run on a 0.8% agarose gel in TAE buffer. Once electrophoresis was complete, the gel was exposed for 1 minute on a UV transilluminator to nick the DNA. The gel was then soaked 2 x 15 minutes in several gel volumes denaturing buffer (0.5 M NaOH, 1.5 M NaCl) followed by 2 x 30 minutes in several gel volumes neutralizing buffer (1M Tris, 1.5 M NaCl). After neutralization, the DNA was transferred to Genescreen Plus nylon membrane in 20x SSPE using capillary transfer. The resulting blot was crosslinked in a UV Stratalinker and prehybridized overnight at 65°C in hybridization solution (6x SSPE, 5x Denhardt's, 0.5% SDS, 0.1 mg/ml salmon sperm DNA).

The probe was prepared by PCR amplifying genomic *pdl-1* sequence with the primers MMA17 and C27JSF1. The PCR product was gel purified using the Sephaglas BandPrep

35

Kit (Amersham) and used as template for radiolabelling. Approximately 75 ng of template was labelled with ^{32}P dCTP using random hexamer priming with Klenow polymerase. The probe was diluted to 10^6 counts/ml and hybridization was performed overnight at 65°C. The blot was washed 3 x 30 minutes with 0.2x SSPE, 0.5% SDS at 65°C and exposed to film for 24 hours at –80°C.

2.12 Phenotypic characterization of *pdl-1(gk157)*

All worms were grown on NGM agar seeded with OP50 *E. coli* at room temperature unless otherwise noted. General observations (movement, mating, touch response, etc.) were made using a dissecting microscope with transmitted illumination.

2.12.1 Sensory System Tests

The dye filling assay was performed by soaking worms in a 0.4 mg/ml solution of FITC in M9 buffer. Worms were left to soak for 2-3 hours before being removed to seeded worm plates and allowed to feed for 1 hour to remove ingested FITC from their intestine. Worms were then observed using fluorescence microscopy and scored for the presence/absence of FITC in their amphid and phasmid neurons.

pdl-1 worms were tested for chemotactic ability in three ways. First they were tested for response to the volatile compounds isoamyl alcohol (10^{-1} in 95% ethanol) and butanol (10^{-2} in 95% ethanol). Chemotaxis plates were prepared as described in Ward (1973). Well fed worms were washed 3x with 1.5 ml S-basal buffer (Sulston and Hodgkin, 1988) followed by one wash in 1.5 ml ddH$_2$O. Immediately before use, plates were prepared by aliquoting 1 μl of attractant plus 1 μl of 1M sodium azide onto a spot near the edge of the plate and 1 μl of diluent plus 1 μl of 1M sodium azide on the opposite side of the plate as diagrammed in Figure 2.2. The worms were then plated in a small volume of water (5-10 μl) at the center of the plate and allowed to migrate for 1 hour. After migration, the number of worms within a 1cm radius of each spot (attractant/diluent) was counted and the chemotaxis index calculated.

36
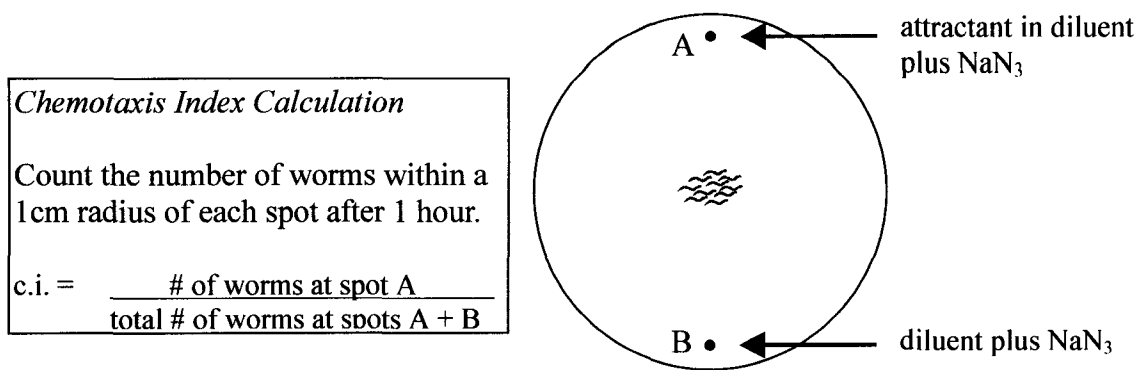
Figure 2.2   Volatile compound chemotaxis assay setup.

Second, worms were tested for response to the water soluble attractant ammonium acetate. In this case, 10 cm plates were poured with 20 ml of CTX agar which either contained or lacked 75 mM ammonium acetate (Wicks *et al.*, 2000). Immediately before use, the agar was cut into quarters and assembled into quadrant plates as diagrammed in Figure 2.3. The gaps between the quadrants were sealed with a small volume of CTX agar lacking ammonium acetate and briefly allowed to solidify. Well-fed worms were washed as described above and plated onto each of the two quadrants containing ammonium acetate. Worms were allowed to migrate for 45 minutes and then the number of worms in each quadrant was counted.
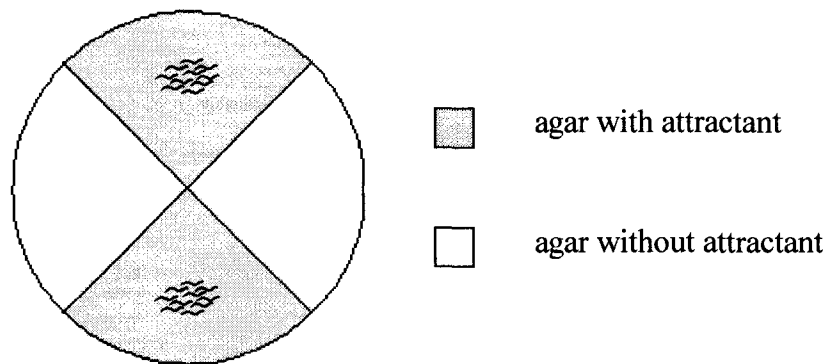
Figure 2.3   Water soluble attractant assay plate.

Finally *pdl-1* worms were tested for response to the water soluble repellants CuSO$_4$ (150 mM) and SDS (2%) as described in Wicks *et al.* (2000). Briefly, worms are separated from a volatile attractant by a line of chemorepellant on the plate. The plate setup is diagrammed in Figure 2.4. Normal worms will be attracted to the volatile compound

37

(10^{-1} isoamyl alcohol) but will not cross the aversive substance barrier within one hour of plating. The water soluble aversion index is calculated by dividing the number of worms that have crossed the barrier by the total number of worms plated.
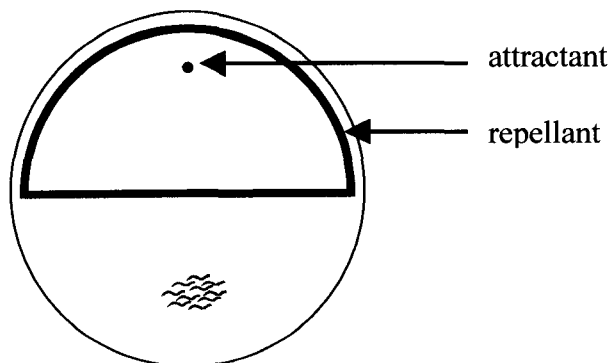
Figure 2.4   Water soluble aversion assay plate.

2.12.2 Structural Analysis of Nervous System

To look at the nervous system in *pdl-1* animals, three integrated GFP markers were used: F25B3.3::GFP, P*daf-7*::GFP, and P*unc-129*::GFP. F25B3.3 is a pan-neural marker which was prepared and characterized in our lab, P*daf-7*::GFP marks the two ASI neurons in the head (Ren *et al.*, 1996), and P*unc-129*::GFP marks the DA/DB motor neurons (Colavita *et al.*, 1998). All three markers were crossed into a *pdl-1* background and these worms were observed by fluorescence microscopy. Images were acquired by confocal microscopy.

2.12.3 Levamisole Sensitivity Test

In this test, a 200 µl drop of 25 mM levamisole is placed onto an NGM agar plate. Worms are then picked into the drop and observed for 30 seconds to see if they hypercontract in response to the drug.

2.13 Yeast 2-hybrid screen

This screen was performed using the yeast 2-hybrid library RB1 (a gift from Bob Barstead). The bait plasmid was constructed by cloning full-length *pdl-1* cDNA into the 2-hybrid vector pGBD-C1 as a BamHI/PstI fragment (construct = pJS15). The bait

38

plasmid was transformed into PJ69-4A yeast (James *et al.*, 1996) and this strain was used for screening. To screen the library, yeast carrying the bait plasmid were grown in SC-TRP overnight and then diluted to 5 x 10^6 cells/ml in YAPD. They were grown for approximately two cell doublings in YAPD before being used for transformation.

After growth in YAPD, cells were washed in sterile water followed by 100 mM lithium acetate. After being washed, the cells were resuspended to a final concentration of 2 x 10^9 cells/ml in 100 mM lithium acetate and divided into 50 µl aliquots. To each aliquot was added: 240 µl 50% PEG, 55 µl 1M LiAc, 5 µl salmon sperm DNA (10mg/ml), 27 µl water, and 3 µl RB1 library (0.447 mg/ml). Cells were resuspended by running the tubes over a rack and then incubated at 30°C for 30 minutes followed by 40 minutes heat shock at 42°C. After heat shock, the cells were pelleted briefly, resuspended in 400 µl water, and plated onto 15 cm SC-TRP-LEU-HIS-ADE plates. A 20 µl aliquot was reserved from several of the transformation mixes and plated onto SC-TRP-LEU to determine the transformation efficiency.

After transformation, the quadruple knockout plates were allowed to grow at 30°C for a total of 21 days. As yeast colonies became visible they were streaked onto SC-TRP-LEU plates for maintenance. In total approximately 70,000 clones were screened and 66 potential positives were identified.

Prey plasmids were isolated by growing the yeast in SC-LEU liquid medium overnight followed by growth on SC-LEU plates. Eight colonies from each plate were patched onto SC-TRP-LEU. Those that failed to grow were assumed to have lost the bait plasmid. Prey plasmids were isolated by phenol:chloroform extraction and transformed into competent *E. coli*. Finally, plasmids were isolated from *E. coli* and digested with XhoI to confirm the presence of an insert.

After the prey plasmids were isolated, they were transformed back into yeast carrying the *pdl-1* bait plasmid and tested again for growth on quadruple knockout medium. Those that failed to reconstruct were withdrawn from further study. The remaining plasmids were sequenced with the primer Gal4AD to determine identity, frame, and orientation.

39

Prey that were in-frame with the Gal4 activation domain were tested for interaction with the unrelated baits Rad7 and Snf1. This was done by co-transforming the prey and bait into PJ69-4A yeast and assaying for growth on SC-TRP-LEU-HIS-ADE medium.

2.14 Yeast 2-hybrid domain analysis

To test which regions of PDL-1 are required for interaction with the various prey, I made a number of bait constructs containing different regions of *pdl-1*. This was done by PCR amplification with a variety of *pdl-1* and vector specific primers using pJS15 as template. In all cases, the *pdl-1* specific primers were designed to add a BamH1 (5' end) or Pst1 (3' end) site to allow digestion of the PCR product and subsequent cloning into the 2-hybrid bait plasmid pGBD-C1. Table 2.1 outlines the primers used and the regions of PDL-1 that are included in each construct.

Construct	Primer Pair	PDL-1 amino acids included
pJS43	C27DOMF1/TermseqCD	51-159
pJS44	C27DOMF2/TermseqCD	77-159
pJS45	C27DOMF4/TermseqCD	126-159
pJS46	C27DOMR1/Gal4BD	1-48
pJS47	C27DOMR4/Gal4BD	1-97
pJS48	C27DOMR3/Gal4BD	1-128
pJS49	C27DOMF5/C27DOMR4	51-97
pJS50	C27DOMF5/C27DOMR3	51-128
pJS51	C27DOMR2/C27DOMR3	77-128

Table 2.1 Primers used to construct yeast 2-hybrid PDL-1 domain constructs. (See Appendix III for sequences.)

After cloning, the constructs were sequenced to confirm the absence of PCR induced mutations. The domain constructs were then transformed into yeast containing positive prey plasmids. The transformations were allowed to grow on SC-TRP-LEU and then patched onto SC-TRP-LEU-HIS-ADE to assay for growth under selective conditions. Those that grew were scored as positive interactions.

40

2.15 Constructing GFP reporters for the yeast 2-hybrid positives

To determine the expression pattern of the positives identified in my yeast 2-hybrid screen, I produced transcriptional GFP fusions for all five genes. Promoter sequences were approximated using the sequence data from the 2-hybrid clones along with gene predictions available in the *C. elegans* database (available at www.wormbase.org). In cases where there was an upstream gene within 5 kbp, primers were designed to amplify the region between the 3' end of the upstream locus and the start codon of the gene of interest. When there was no proximal upstream locus primers were designed to amplify roughly 5-6 kb of sequence upstream of the start (Table 2.2). In all cases, GFP was fused in-frame to the coding region in exon 2.

Gene	Primers Used	Product Size
C02F5.7	C02PROMF1/C02PROMR1	2851
C49G7.3	C49PROMF1/C49PROMR1	2031
W05B5.1a	W05PROMF1/W05PROMR1	5101
Y55F3AM.9	Y55PROMF1/Y55PROMR1	6032
Y113G7A.3	Y113PROMF1/Y113PROMR1	4707

Table 2.2   Primers used to amplify yeast 2-hybrid prey promoters. (See Appendix III for sequences.)

For all five promoters, PCR was performed using N2 genomic DNA as template. The C49G7.3 promoter PCR product was digested with HindIII and SalI and then cloned directly into the Fire lab GFP vector pPD95.77. All other PCR products were first cloned into pGEM-T (Amersham) then subcloned into GFP vectors. The promoter for C02F5.7 was cloned into pPD95.77 as a HindIII/SalI fragment, W05B5.1a was cloned into pPD95.77 as a BamHI/PstI fragment, Y55F3AM.9 was cloned into pPD95.75 as a MscI/PstI fragment, and Y113G7A.3 was cloned into pPD95.77 as a BamHI/SalI fragment.

Once the GFP constructs were made, they were transformed into wild-type *C. elegans* by germ-line microinjection. Injection mixes consisted of approximately 75 ng/µl GFP plasmid mixed with 75 ng/µl pRF4 as a cotransformation marker. N2 worms were

41

injected and screened for rolling progeny, indicative of the presence of pRF4. They were then examined by fluorescence microscopy to confirm GFP expression. Images were collected using either a SPOT camera (Diagnostic Instruments) on a compound microscope or confocal microscopy.

2.16 RNAi against yeast 2-hybrid positives

Portions of the prey cDNAs were subcloned from the pACT vector into the Fire lab vector L4440 as XhoI fragments. In instances where more than one fragment was liberated by XhoI, the largest fragment was selected for subcloning. The smallest fragment used was approximately 400 bp (C02F5.7) while the largest was approximately 1.5 kbp (W05B5.1a).

For feeding RNAi, constructs of C02F5.7, C49G7.3, Y55F3AM.9, and Y113G7A.3 cDNA in L4440 were transformed into HT115 bacteria. Induction and plating was carried out as described in section 2.6. One L4/young adult N2 animal was transferred onto each plate and allowed to lay eggs for 24 hours. In total 12 plates were set up for each construct. After 24 hours, the adult animals were removed and the progeny were examined for signs of a phenotype over the next few days.

I also tried RNAi by injection of dsRNA for C02F5.7, C49G7.3, W05B5.1a, and Y55F3AM.9. In this case, I used the "T7 big" primer to amplify the various cDNAs cloned into L4440. This results in cDNA with a T7 sequence on either end. The PCR products were gel purified using the Sephaglas BandPrep Kit (Amersham) and used as template for *in vitro* transcription with the Ambion T7 Megascript kit as per the manufacturer's instructions. The resulting double stranded RNA was injected into *mg366* worms (a mutant with enhanced RNAi sensitivity- a gift from Gary Ruvkun's lab) either undiluted or at a 10^{-1} dilution in DEPC treated H_2O.

2.17 Confirming yeast 2-hybrid interactions by vector swapping

The five yeast 2-hybrid prey identified in the screen with PDL-1 were subcloned out of the prey plasmid pACT into the Gal4 DNA binding domain plasmid pGBD-C2. C02F5.7, W05B5.1a, Y55F3AM.9, and Y113G7A.3 were all cloned non-directionally as

42

BglII fragments. C49G7.3 was subcloned as a XhoI fragment into SalI digested pGBD-C2 due to the presence of an internal BglII site in the insert. Conversely, *pdl-1* was subcloned into the Gal4 activating domain plasmid pGAD-C1 as a BamHI/PstI fragment. I also subcloned human PDEδ into pGAD-C1 as a BamHI/PstI fragment (from pJS42).

2.18 Arl2 directed yeast 2-hybrid

In order to test UNC-119 and PDEδ for interaction with Arl2, I cloned *C. elegans* and human UNC-119 into the Gal4 activating domain plasmid pGAD-C1. *C. elegans unc-119* was subcloned from pUBP-2 (Wayne Materi) as a SmaI/BglII fragment while human UNC-119 was subcloned from pHBP1 (Wayne Materi) as an EcoRI/BglII fragment. I also subcloned zebrafish PDEδ into pGAD-C1. This was accomplished by amplifying zebrafish PDEδ cDNA from pJS114 using "zfdelta real F3" and SP6 as primers. The PCR product was digested with BamHI/PstI and cloned into pGAD-C1.

Using these constructs along with the human PDEδ and *pdl-1* Gal4 AD constructs made previously, I was able to test for interaction with human Arl2, human Arl2(Q70L) and *C. elegans* EVL-20(Q70L), all which were fused to the Gal4 DNA binding domain. These constructs were received as generous gifts; Arl2 and Arl2(Q70L) from Richard Kahn and EVL-20(Q70L) from Min Han.

To test for interaction between the Arl2 and PDEδ, constructs were co-transformed into PJ69-4A yeast and plated onto SC-TRP-LEU medium to select for transformants. Two colonies from each transformation were then tested for growth on SC-TRP-LEU-HIS-ADE medium. Growth on this medium indicates interaction between the bait and prey proteins. As well, individual colonies from each plate were patched onto SC-TRP-LEU and tested for expression of the LacZ reporter using a β-galactosidase assay.

For the β-galactosidase assay, patched yeast were lifted onto a circle of #1 Whatman filter paper. The filter was treated with three rounds of freeze-thaw with liquid nitrogen and then placed, yeast side up, onto another two rounds of filter paper saturated in Z-buffer (100mM sodium phosphate pH 7.0, 10 mM KCl, 1 mM MgSO$_4$, 1% Xgal). The

43

reaction was allowed to take place in the dark at 30°C. Filters were inspected at 15 minutes, 30 minutes, and 3 hours to record which patches of yeast had turned blue.

2.19 Antibody production

Polyclonal antibodies were raised against PDL-1 peptides and full-length PDL-1 protein. For the peptide antibodies, two synthetic peptides were ordered from Research Genetics. Peptides were designed to contain approximately 60% hydrophilic amino acids in hopes that such a peptide would be exposed on the surface of the nascent protein. The peptide RHQDSKLSEKAEC (C27R7E18) was chosen from the divergent amino terminus of PDL-1 while KIEKFRLEQRVYLKC (C27K79K92) was chosen from the middle of PDL-1. C27K79K92 was chosen because polyclonal antibodies have been successfully raised against the analogous peptide in human PDEδ (Florio *et al.*, 1996). Both peptides were synthesized with a cysteine added to their carboxyl terminus to allow directed coupling to the carrier protein keyhole limpet hemocyanin (KLH).

For coupling, 100 µl of a 25 mg/ml solution of m-Maleimidobenzoyl-N-hydroxysuccinimide ester (MBS) was added to 1 ml of 10mg/ml KLH in PBS with constant stirring. This mixture was stirred at room temperature for 30 minutes, then divided in half and concentrated in Millipore Ultrafree-MC 10,000 NWML filter units. Each filter was washed once with 400 µl PBS to remove any excess MBS. After washing the protein was removed from the spin columns and resuspended to a final volume of 1 ml in PBS. The resulting solutions were placed into small glass vials with a stir bar.

Peptide C27K79K92 was dissolved to a final concentration of 1 mg/ml in PBS while peptide C27R7E18 was dissolved to a final concentration of 1 mg/ml in water as it was insoluble in PBS. The peptides were then added to the KLH at a 400X molar excess (780 µl for C27K79K92 and 610 µl for C27R7E18) and the pH of the two solutions was adjusted to approximately 7.0-7.5 using 0.25M HCl. The mixtures were then allowed to stir for 3 hours at room temperature. After coupling, the proteins were dialyzed into four 2.5 L changes of PBS. After dialysis, each conjugate was diluted in PBS to a final concentration of 5 ml (approximately 1 mg/ml) and stored at –20°C.

44

Two rabbits were injected for each peptide. Rabbits 9B6 and 9B8 were injected with C27K79K92 and rabbits 9B1 and 9B3 were injected with C27R7E18. In all cases, rabbits were injected with 750 μg of immunogen in Freund's adjuvant (Sigma). The first injection was done in Freund's complete adjuvant while all subsequent boosts were done in Freund's incomplete adjuvant. Rabbits were injected seven times at 3-4 week intervals before exsanguination. Exsanguination was delayed due to the fact that two of the rabbits (9B1 and 9B3) became pregnant during the immunization regime and were allowed to carry their kits to term. After exsanguination, the serum was aliquoted and stored at -80°C.

For the holoprotein antibody, PDL-1 was bacterially expressed behind a His$_6$ tag. Briefly, *pdl-1* cDNA was cloned into pRSETA (Invitrogen) as a BamHI/PstI fragment. This construct (pJS14) was transformed into BL21(DE3 pLysS) *E. coli* (Stratagene) to allow IPTG induction of expression. Cells were grown at 37°C in 500ml flasks of SOB to an OD$_{600}$ of approximately 0.5 and induced by adding 600 μl of 1M IPTG. After induction, the cells were grown another 4.75 hours before being pelleted and frozen at -80°C.

For purification, cells were resuspended in 20 ml guanidine lysis buffer (6 M guanidine HCl, 0.5 M NaCl, 50 mM Tris-HCl, pH 7.8) and lysed with a tissue homogenizer. The lysate was then spun for 15 minutes at 10,000 rpm in a refrigerated centrifuge to pellet insoluble debris. The supernatant was added to 4 ml of Probond resin (Invitrogen) which has been prepared by washing with 10 ml binding buffer (8 M urea, 0.5M NaCl, 50 mM Tris-HCl, pH 7.8). The resulting slurry was rocked gently for 10 minutes at room temperature then washed 1x10 minutes with 10ml binding buffer, 2x10 minutes with wash buffer (8 M urea, 0.5 M NaCl, 50 mM Tris-HCl, 40 mM imidazole, pH 7.8), followed by another 1x30 minutes with wash buffer. After washing, the beads were transferred to a column and eluted with increasing concentrations of imidazole (10 ml of wash buffer with 150, 300, 450, or 600 mM imidazole). The eluates from elutions 2-4 were combined and dialyzed into several changes of PBST at 4°C. Most of the protein came out of solution during dialysis. The insoluble protein was collected by filtering the

45

protein slurry through a 0.2 micron filter. The moist protein was scraped off the filter (~670 mg) and frozen at -20°C for later use.

For inoculation, the insoluble protein was suspended in PBS at a concentration of approximately 1.3 mg/ml. Each injection contained approximately 0.66 mg of damp protein suspended in Freund's adjuvant (complete for the first injection and incomplete for the boosts). Two rabbits, 9AG1 and 9AG4, were injected with insoluble His_6:PDL-1 on a monthly basis. 9AG1 was injected three times before she suffered an injury and had to be put down. 9AG4 was injected four times before exsanguination. Again, the sera were aliquoted and stored at -80°C.

2.20 Testing antisera for reactivity against PDL-1

Peptide antisera were tested for reactivity against 1 µg of their corresponding KLH conjugated peptides on a dot blot. Briefly, 1 µl of a 1 mg/ml solution of conjugated peptide was spotted onto nitrocellulose and allowed to dry. The membrane was blocked with 5% skim milk powder in PBST then probed with a 1/500 dilution of immune serum. Detection was carried out using 1/2500 anti-rabbit HRP conjugated secondary antibody (Amersham) and ECL Plus Western Blotting Detection Reagents (Amersham) as per the manufacturer's instructions. The immunosera were also tested for reactivity against cell lysate prepared from *E. coli* expressing His_6::PDL-1. Cells from 1 ml of culture were lysed by boiling in 200 µl sample buffer (125 mM Tris, 20% glycerol, 2% SDS, 2% β-mercaptoethanol, 0.001% bromphenol blue, pH 6.8) and run on a 15% SDS polyacrylamide gel. The protein was then electroblotted to nitrocellulose and immunodetection was performed as described for the dot blots.

Holoprotein antisera were tested for reactivity against recombinant GST::PDL-1 either as crude *E. coli* lysate or as purified protein. In either case, the protein was run on either a 12% or 15% SDS polyacrylamide gel and blotted onto nitrocellulose. Immunodetection was carried out as described above except that the anti-rabbit HRP conjugated secondary was used at a dilution of 1/5000 and the detection reagent was Supersignal West Pico Chemiluminescent Substrate (Pierce) again used as per the manufacturer's instructions.

46

All antisera were tested for immunoreactivity against N2 lysate. Worms were lysed in one of three ways. Most commonly, a recently cleared plate of worms was collected and boiled in 100 µl of sample buffer. The lysate was spun at top speed in a microfuge for one minute to remove cell debris and then loaded immediately onto a gel. Secondly, worms were suspended at a concentration of 1 mg/ml in worm buffer (50 mM ethanolamine, 5 mM DTT, 2 mM EDTA, 1 mM PMSF), microwaved at high power for 25 seconds, and boiled for 5 minutes after adding an equal volume 2x sample buffer. Samples were run through a 26 gauge needle and pelleted at top speed for 3 minutes in a microfuge to remove cell debris. Finally, worms were diluted 1/5 in PBS with complete protease inhibitor cocktail (Roche) and French pressed four times at 1500 psi. After lysis, the worms were centrifuged for 15 minutes at 10,000 rpm to pellet insoluble material. The soluble and insoluble fractions were mixed with sample buffer and boiled for 5 minutes before use. All three lysis techniques gave similar yields and results on Western blots with PDL-1 antisera.

2.21 Antibody purification

Antiserum from rabbit 9AG4 showed the highest titer and reactivity against recombinant PDL-1 protein so this serum was selected for purification by affinity chromatography. Recombinant GST::PDL-1 protein was purified from 2 L of BL21(DE3 pLysS) *E. coli* (Stratagene) carrying the plasmid pJS25. Cultures were grown in 2xYT medium and induced with 1 mM IPTG for 3 hours at 37°C. After induction, cells were collected by centrifugation at 10,000 rpm for 15 minutes and stored at -20°C overnight.

The next morning, the cells were resuspended to a total volume of 80 ml in PBS and French pressed four times at 1500 psi. After lysis, Triton X-100 was added to a final concentration of 1% and the lysates were allowed to sit on ice for 30 minutes with occasional mixing. The lysates were then centrifuged at 10,000 rpm for 15 minutes in a refrigerated centrifuge to pellet insoluble debris. The protein was purified from the supernatant by batch binding to 2 ml of Glutathione Sepharose 4B resin (Amersham) for 30 minutes at room temperature. After binding the beads were washed three times with 20 ml PBS. Finally, protein was eluted three times in 2 ml elution buffer (50mM Tris-

47

HCl pH 8.0, 10 mM glutathione). Eluates were combined and dialyzed into 10 L coupling buffer (0.1 M sodium bicarbonate, 0.5 M NaCl, pH 8.3).

To make the affinity column, 2.5 ml of purified GST::PDL-1 (0.5 mg/ml) was diluted to a final volume of 14 ml in coupling buffer. Earlier attempts at coupling with more highly concentrated protein were unsuccessful as the protein came out of solution on contact with the beads. To prevent this, a dilute solution of GST::PDL-1 (roughly 90 μg/ml) was used for coupling to 0.33 g of CNBr Activated Sepharose Fast Flow (Amersham) prepared according to the manufacturer's instructions. Coupling was allowed to proceed for 4 hours at room temperature with gentle rocking. After coupling, the beads were washed ten times alternating between 7 ml coupling buffer and 7 ml wash buffer (0.1 M sodium acetate, 0.5 M NaCl, pH 4.0). This was followed by five washes with 5 ml coupling buffer and finally two washes with 5 ml PBS.

The antibody was purified by incubating 2 ml of serum from rabbit 9AG4 (diluted with 4 ml PBS) with the GST::PDL-1 conjugated Sepharose. Binding was allowed to proceed overnight at 4°C with gentle rocking. After binding, the beads were washed three times with 10 ml PBS at room temperature. Antibody was eluted from the column in five 1 ml fractions of glycine elution buffer (0.1 M glycine, pH 2.4). Immediately upon collection, fractions were neutralized by adding 30 μl of 3 M Tris (pH 8.8) and 20 μl of 5 M NaCl. Western blotting was used to test the purified antibody for reactivity against GST::PDL-1. Since there was residual activity in the serum that had been bound to the column, purification was repeated to collect the remaining anti-PDL-1 antibody from the serum. After purification all 10 elutions were pooled and concentrated to a final volume of approximately 500 μl in an Ultrafree 15 Centrifugal Filter Device with a 10,000 MW cutoff (Millipore). The antibody was then stored at 4°C.

Part 2: *Danio rerio*

2.22 Zebrafish culture conditions

Adult fish and embryos were grown at 28°C using standard culture conditions (Westerfield, 2000).

48

2.23 Identifying zebrafish PDEδ

BLAST searches were performed against zebrafish genomic and EST sequence using the NCBI BLAST server at www.ncbi.nlm.nih.gov/genome/seq/DrBlast.html. Genomic sequence was originally identified in the WGS traces database but was later found in the HTGS database.

Gene prediction was performed using the "gene finding with similarity" program at www.softberry.com/berry.phtml. This program combines FGENESH with protein comparison, allowing you to enter a homologous protein to help refine the FGENESH output. Since PDEδ is so well conserved, I was able to use this gene finding approach to rapidly identify the exon-intron boundaries in the zebrafish genomic sequence.

2.24 3'RACE and cloning PDEδ cDNA

Total RNA was prepared from 72 hpf embryos (AB strain). Approximately 75 embryos were collected and washed twice in water. Embryos were suspended in a small amount of Trizol (Gibco) and ground with a small plastic pestle. After grinding, Trizol was added to a final volume of 1 ml and the tube was allowed to sit at room temperature for 5 minutes before being spun at top speed in a 4°C microfuge for 10 minutes. 200 μl of chloroform was added to the supernatant and the mixture was vortexed for 15 seconds then left to sit at room temperature for 2 minutes. The tube was then spun at top speed in a 4°C microfuge for 15 minutes. The RNA was precipitated from the aqueous phase by adding 600 μl isopropanol. After 10 minutes at room temperature, the tubes were spun at top speed in a 4°C microfuge for 15 minutes. The pellet was washed in 100 μl 75% EtOH in DEPC treated H_2O, spun at 7500 rpm for 5 minutes at 4°C, and briefly air dried.

Approximately 2.5 μg of the total RNA was used as a template for reverse transcription with Superscript II Reverse Transcriptase (Invitrogen). The reaction was primed with 10 pmol adapter primer (Gibco) and carried out as instructed by Invitrogen. I used 1 μl of the first strand synthesis as template for PCR with primers that anneal just outside the PDEδ open reading frame, "zfdelta real F2" and "zfdelta real R2". The PCR product was

49

gel purified using the Sephaglas BandPrep Kit (Amersham) and cloned into pGEM-T (Amersham). Four independent clones were then sequenced with the T7 primer.

3' RACE was performed using PCR with "zfdelta real F2" and universal adapter primer (UAP, Gibco) followed by a nested reaction with "zfdelta real F1" and UAP. Each round of PCR used 1 µl of template (72 hpf first strand cDNA for the first reaction) and 30 cycles of amplification. To reduce PCR induced mutations PCR was performed using a 25:1 mixture of Taq and Pfu polymerases. The band from the nested reaction was gel purified and cloned into pGEM-T (Amersham).

Finally, a fragment of genomic PDEδ was amplified by PCR with the primers "zfdelta real F1" and zfdelta real R1". The template for this reaction was genomic DNA prepared from a wild-type fish purchased at a pet store. Again, the PCR product was gel purified and cloned into pGEM-T. All clones were confirmed by sequencing with T7 and/or SP6.

2.25 Low stringency Southern

Genomic DNA was prepared from a single wild-type female zebrafish purchased from a pet store. The fish was dissected to remove any scale material, then frozen and ground in liquid nitrogen. The ground tissue was resuspended in 1300 µl lysis buffer (100 mM Tris pH 8.0, 100 mM NaCl, 50 mM EDTA, 1% SDS, 1% β-mercaptoethanol, 100 µg/ml proteinase K) and digested overnight at 60°C. The DNA was then purified by phenol-chloroform extraction and ethanol precipitated. After precipitation, the DNA was resuspended in 500 µl TE and treated with 2 µl RNAase A (25 mg/ml) at 37°C for 1.5 hours. The RNAase A was removed by phenol-chloroform extraction and the DNA was once again ethanol precipitated. Finally, the DNA was dissolved in 300 µl TE.

To make the Southern blot, I digested 2 µg of DNA with 20 units of the following enzymes: BglII, EcoRI, HindIII, NotI, PvuII, and SstI (Invitrogen). The digests were run on a 0.7% agarose gel in TAE buffer (40 mM Tris, 65 mM glacial acetic acid, 1 mM EDTA). Once electrophoresis was complete, the gel was exposed for 1 minute on a UV transilluminator to nick the DNA. The gel was then soaked 2 x 15 minutes in several gel volumes of denaturing buffer (0.5 M NaOH, 1.5 M NaCl) followed by 2 x 30 minutes in

50

several gel volumes of neutralizing buffer (1M Tris, 1.5 M NaCl). After neutralization, the DNA was transferred to Genescreen Plus nylon membrane (NEN Life Science Products) in 20x SSPE using capillary transfer. The resulting blot was crosslinked in a UV Stratalinker and prehybridized for five hours at 65°C in hybridization solution [6x SSPE, 0.5% SDS, 0.1 mg/ml salmon sperm DNA, 5x Denhardt's (0.1% Ficoll, 0.1% polyvinylpyrrolidone, 0.1% bovine serum albumin) (Denhardt, 1966)].

The probe was prepared using an SstI/PstI fragment of zebrafish PDEδ cDNA digested from pJS111. This was gel purified using the Sephaglas Bandprep Kit (Amersham). Approximately 75 ng of template was radiolabelled with ^{32}P dCTP using random hexamer priming with Klenow polymerase. The probe was diluted to 10^6 counts/ml and hybridization was performed overnight at 65°C. The blot was washed 1 x 30 minutes with 1x SSPE, 0.1% SDS at room temperature, followed by 2 x 30 minutes at 37°C. The blot was then exposed to film for 10 days at -50°C.

2.26 Northern analysis of PDEδ expression

Total RNA was isolated from approximately 25 wild-type zebrafish oocytes and embryos of the following stages: 4, 9, 13, 17, 22, 31, 48, 60, 72, 96 hpf. As well, RNA was collected from a single adult female. RNA was isolated by collecting and flash freezing fish in liquid nitrogen. The frozen fish tissue was suspended in 1 ml of RNAzol (Tel-Test) and ground with a small plastic pestle before adding 100 μl chloroform. After the addition of chloroform, samples were incubated on ice for 15 minutes and then centrifuged at 14,000 rpm in a 4°C microfuge for 30 minutes. RNA was precipitated by adding an equal volume of isopropanol to the aqueous layer and incubating overnight at -20°C. The next morning, the samples were centrifuged at 14,000 rpm in a 4°C microfuge for 30 minutes and the resulting pellet was washed with 70% ethanol in DEPC treated water. Samples were centrifuged for another 15 minutes, then allowed to air dry briefly before resuspending in 50 μl of diethylpolycarbonate (DEPC)-treated water.

To make the northern blot, 10 μl of RNA from each stage was run on a 1.2% agarose formaldehyde gel with MOPS running buffer [20 mM morpholinopropanesulfonic acid

51

(MOPS) pH 7.0, 1 mM EDTA, 5 mM sodium acetate, 3% formaldehyde]. The DNA was then transferred to Genescreen Plus nylon membrane (NEN Life Science Products) in 10x SSC. The resulting blot was crosslinked in a UV Stratalinker and prehybridized overnight at 65°C in Church Buffer (7% SDS, 0.5 M sodium phosphate pH 7.2, 1mM EDTA, 0.1 mg/ml yeast tRNA, 1% BSA) (Church and Gilbert, 1984).

The probe was prepared as described for the low stringency Southern and diluted to 10^6 counts/ml in Church Buffer. Hybridization was performed overnight at 65°C. The blot was then washed at 65°C as follows: 2 x 15 minutes in 2x SSC; 30 minutes in 2x SSC, 0.1% SDS; and 10 minutes in 0.1x SSC, 0.1% SDS. The blot was then exposed to film for 14 days at -50°C.

2.27 Developmental RT-PCR

RNA was prepared from pet-store fish oocytes and embryos (6, 12, 18, 24, 72, and 100 hpf) as described in section 2.24. This RNA was used as template for reverse transcription with Superscript II reverse transcriptase (Invitrogen) primed with adapter primer (Gibco). Roughly 1.5 μg of each RNA was used as template and the reaction was carried out as instructed by Invitrogen. I used 0.5 μl of each first strand synthesis as template for PCR with the primers "zfdelta real F2" and "zfdelta real R2".

2.28 Developmental western

Protein lysate was prepared from pet-store zebrafish embryos by placing embryos into an equal volume of SDS-PAGE gel loading buffer. The embryos were ground with a plastic pestle and boiled for 5 minutes. Finally, the lysates were centrifuged at top speed in a microfuge for 2 minutes to pellet any debris. Lysates were run on a 15% SDS polyacrylamide gel at 10 μl per lane and transferred to nitrocellulose by electroblotting. The blot was blocked with 5% skim milk powder in PBST and probed with a 1/250 dilution of purified 9AG4 antibody (raised against *C. elegans* PDL-1 protein). The secondary antibody was a 1/5000 dilution of HRP conjugated anti-rabbit (Amersham). Detection was carried out using Supersignal West Pico Chemiluminescent Substrate (Pierce) and the blot was exposed to film overnight.

52

2.29 *In situ* hybridization

I prepared an *in situ* probe against PDEδ using the 3' UTR sequence. The 3' UTR sequence was subcloned from pJS116 into pBluescript as a KpnI/SstII fragment. It was then amplified by PCR with the primers T3 and "T7 big". The PCR product was gel purified and used as template for *in vitro* transcription.

Transcription was carried out using the T3 and T7 Megascript kits (Ambion). The T3 reaction gives rise to an antisense probe while the T7 reaction gives rise to the sense control probe. Approximately 330 ng of DNA was used as template for each reaction. The reaction mix was set up according to the manufacturer's instructions except the nucleotide mix was changed to include 75 mM each of CTP, ATP, and GTP; 48.75 mM UTP; and 26.25 mM DIG labelled UTP. Transcription was allowed to proceed for 4 hours at 37°C. Finally, the RNA was precipitated by LiCl precipitation, resuspended in 50 μl DEPC treated water containing 1 μl RNase Out (Invitrogen), and stored at -80°C.

In preparation for *in situ* staining, embryos were collected and grown in embryo medium (Westerfield, 2000). Once they reached the desired stage, they were manually dechorionated and placed briefly on ice before being fixed overnight at 4°C in 4% paraformaldehyde in PBST. After fixation, embryos were washed several times in PBST and then dehydrated successively with 25% methanol in PBST, 50% methanol in PBST, and 100% methanol in PBST. Embryos were then frozen at -20°C for at least 16 hours. After freezing, embryos were rehydrated in a series of 50% methanol in PBST, 25% methanol in PBST, and PBST.

Embryos were permeabilized by digestion with 2 μg/ml proteinase K in PBST (0.1 M sodium phosphate, 0.1 M sodium chloride, 0.1 % Tween-20, pH 7.5). Proteinase K digestion was carried out at room temperature for various amounts of time depending on the age of the embryo. 24 hpf embryos were digested for 2 minutes, 36 hpf embryos for 5 minutes, 48 hpf embryos for 20 minutes, and 78 hpf embryos for 35 minutes. After digestion, embryos were fixed for 20 minutes at room temperature with 4%

53

paraformaldehyde in PBST. After fixation, embryos were washed several times in PBST to remove the paraformaldehyde.

The embryos were then placed in preheated hybridization solution (50% formamide, 5x SSC, 500 µg/ml yeast tRNA, 0.1% Tween-20, 50 µg/ml heparin, pH 6.0) at 70°C and prehybridized for two hours. After prehybridization, the probes were added to a final dilution of 1/200 and hybridization was allowed to proceed overnight at 70°C. In the morning, the fish were washed for five minutes with each of the following solutions at 70°C: wash buffer (50% formamide, 1x SSC, 0.1% Tween-20), 2:1 wash buffer:2x SSCT, 1:1 wash buffer:2x SSCT, 1:2 wash buffer:2x SSCT, and finally 2x SSCT alone. After the 2x SSCT wash, embryos were washed another 2 x 30 minutes in 0.2x SSCT.

After the final 0.2x SSCT wash, the embryos were placed at room temperature and rinsed once with PBST. They were then placed in blocking solution (40 mg/ml BSA and 5% goat serum in PBST) for at least 2 hours at room temperature or overnight at 4°C. After blocking, embryos were placed in 1/10,000 Anti-Digoxigenin-AP Fab fragments (Roche) diluted in blocking solution and incubated overnight at 4°C. Finally, embryos were washed 4 x 25 minutes in PBST at room temperature, followed by a five minute wash in 0.05% Tween-20.

Detection was carried out by washing the embryos 3 x 15 minutes in NTMT (100 mM NaCl, 50 mM $MgCl_2$, 100 mM Tris pH 9.5, 0.05% Tween-20) and then adding 20 µl/ml NBT/BCIP Stock Solution (Roche) diluted in NTMT. Staining was carried out in the dark at room temperature. Embryos were monitored as the staining progressed and staining was stopped at a desired level by removing the staining solution and replacing it with 0.05% Tween-20. Staining duration ranged from 30 minutes for the UNC-45 control probe up to overnight for the PDEδ probes. After staining, embryos were placed overnight in methanol with 0.01% Tween-20 to remove non-specific background. Finally, embryos were mounted in glycerol and photographed using a SPOT camera (Diagnostic Instruments) mounted on a Leica dissecting microscope.

54

2.30 Immunostaining

For immunostaining, zebrafish embryos were grown to a desired stage in embryo rearing medium at 28°C. They were then placed briefly on ice and fixed either overnight at 4°C in 4% paraformaldehyde or for two hours at room temperature in 2% trichloroacetic acid (TCA). Both fixatives were diluted in PBST. After fixation, the embryos were washed with several changes of PBST and permeabilized with Triton X-100 diluted in 5% BSA or 5% donkey serum solution in PBST. A 0.4% solution of Triton X-100 was used to permeablize embryos younger than 48 hpf while a 4% Triton X-100 solution was used for embryos 48 hpf or older. In all cases, permeabilization was carried out for 30 minutes at room temperature.

2.30.1 DAB Staining

After permeabilization, embryos were blocked for two hours at room temperature in 5% BSA, 0.1% Triton X-100 in PBS. After blocking, PDL-1 antibody (purified from rabbit 9AG4) was added to a dilution of 1/50 and anti-FAK (Santa Cruz Biotechnology) was added to a dilution of 1/250 in blocking solution. Embryos were incubated with primary antibody overnight at 4°C. In the morning, embryos were washed 4 x 25 minutes with PBS + 0.1% Triton X-100 then transferred to a 1/300 dilution of Anti-Rabbit IgG HRP (Amersham). The secondary antibody incubation was allowed to proceed for 4 hours at room temperature, then embryos were washed 4 x 25 minutes with PBS + 0.1 % Triton X-100. After the washes, embryos were placed in DAB staining solution (0.5% DAB, 1% DMSO in PBS) and allowed to sit for 15 minutes at room temperature. Staining was initiated by adding 2.5 μl of 3% hydrogen peroxide per 1 ml of staining solution. Staining was allowed to proceed for 10-30 minutes at room temperature, then stopped by washing the embryos repeatedly in PBST.

2.30.2 Immunofluorescence

Staining was carried out as described in section 2.30.1 with a few modifications. Washes were performed in PBST, blocking was performed using 10% donkey serum, and the

55

secondary antibody was Alexa Fluor 488 (Molecular Probes) diluted 1/2500 in blocking solution. UV fluorescence microscopy was used to look for staining in these fish.

2.31 Morpholino injections

Three morpholino antisense oligonucleotides were designed and ordered from GeneTools (Philomath, OR). The first, "zfdelta real ATG" (5' TCGTCCGAAGACATCTTTTT CCTTG 3') was designed against the start site of PDEδ. The second, "zfdelta ex2don" (5' AACCACAAACCTTCATGTTCTACCC 3'), was designed against the exon 2 splice donor. The third, "zfdelta" (5' GACGTTGTCATTTATTTGATTTTCG 3') was designed against the start site of a purported zebrafish PDEδ EST present in the zebrafish EST database (see section 3.8 for a discussion of this EST). Since this sequence does not appear to be present in the zebrafish genome and this morpholino does not appear to have any specific phenotypic effect in zebrafish embryos, it has been used as a negative control for morpholino toxicity and injection effects.

For injection, morpholinos were diluted to a final concentration of 1-5 mg/ml in water with 0.1% phenol red as a tracer. Morpholinos were injected using glass needles drawn from 1 mm capillary tubes. Zebrafish embryos used for injection had completed 3 or fewer cell divisions and morpholinos were injected into the yolk at an approximate volume of 2-5 nl per injection. The injection setup is diagrammed in Figure 2.5. After injection, embryos were collected in embryo medium and grown on a slide warmer at 28°C. Development was monitored over the next 24-48 hours to determine whether the fish showed any morphological or developmental defects.

56

needle powered by
nitrogen tank

glass slide

10 cm petri
dish lid

embryos in a small volume
of embryo medium
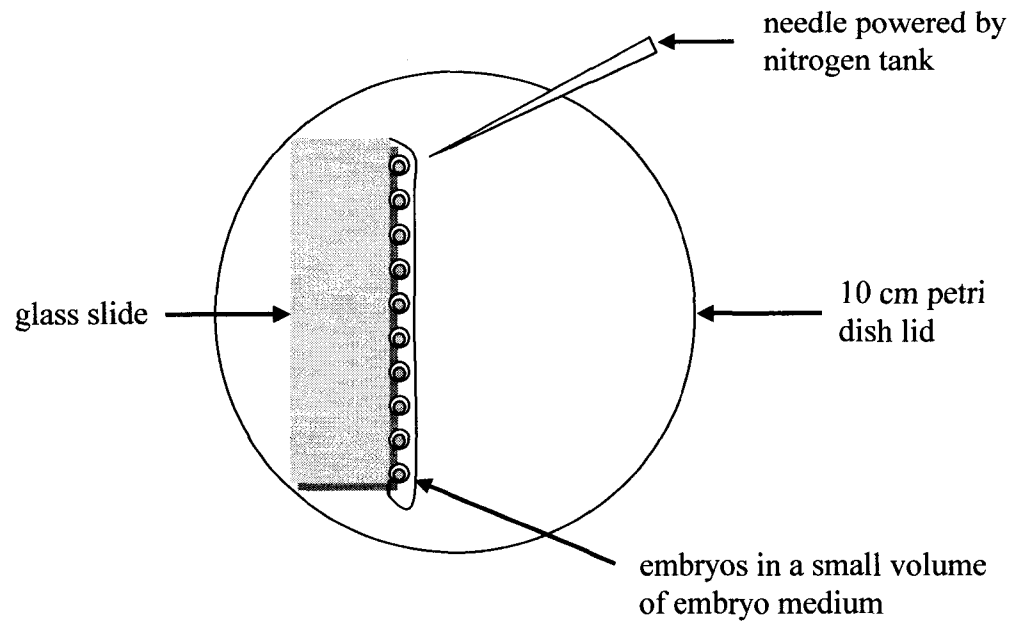
Figure 2.5   Zebrafish embryo injection set-up.

2.32 Confirming efficacy of splice donor morpholino

In order to determine whether the splice donor directed morpholino (zfdelta ex2don) was having an effect, RNA was isolated from embryos 24 hours after injection. RNA isolation was performed as described in section 2.24, using 20 embryos from each round of injection. Since there were fewer embryos used to produce RNA, all of the volumes were halved. After purification, the RNA pellets were dissolved in 40 μl DEPC treated water. 2 μg of RNA was used as template for reverse transcription with adapter primer (Gibco) and Superscript II reverse transcriptase (Invitrogen). PCR was performed on 1 μl of each first strand synthesis using "zfdelta real F2" and "zfdelta real R2" as primers. The expected product size for correctly spliced transcript is 501 bp while a transcript containing intron 2 is expected to give a product of 732 bp.

57

Results

Part 1: *C. elegans*

3.1 Expression pattern of *pdl-1*

A transcriptional fusion in which GFP is expressed under control of the *pdl-1* upstream region shows expression throughout the nervous system of the worm beginning early in embryogenesis and maintained through adulthood (Figures 3.1 - 3.3). In addition to nervous system expression, hermaphrodites show expression in vulval muscles and variable expression in pharyngeal muscles (Figure 3.2). Translational fusions using the same promoter driving either genomic DNA or cDNA fused in-frame with GFP show expression only in the nervous system (Figure 3.3). These constructs show fluorescence throughout neural cell bodies and processes, suggesting that PDL-1 is cytoplasmic. As transgenes are present at high copy number, it is difficult to ascertain whether there is any regional localization of the protein within the cytoplasm.
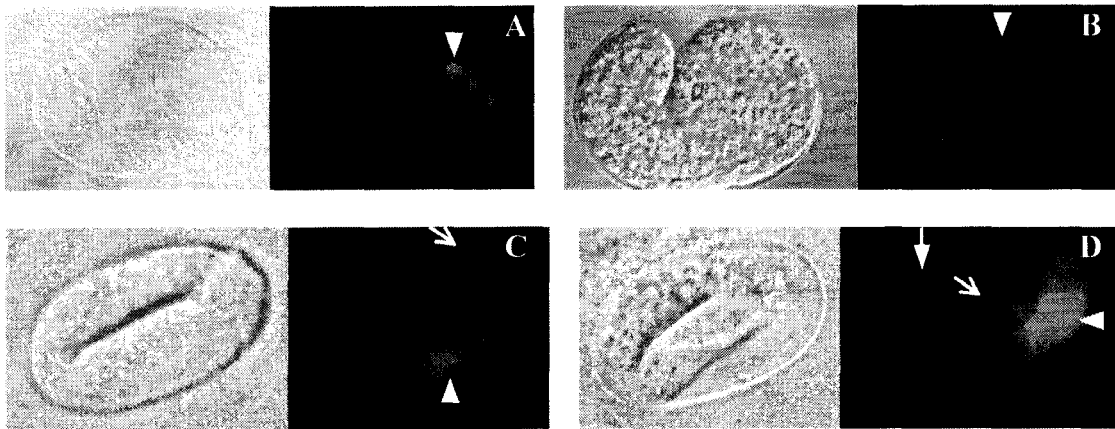
Figure 3.1   Embryonic expression of P*pdl-1*::GFP in strain DP265 (edIs128). Each panel depicts an embryo of a different developmental stage: (A) an early embryo prior to morphogenesis (B) a 1.5-fold embryo (C) a 2-fold embryo (D) a 3-fold embryo. GFP is most visible at the anterior of the animal, consistent with expression in neurons of the developing nerve ring (arrowheads). It is also possible to distinguish the tail ganglia in the 2-fold and 3-fold embryo (open arrows) as well as the ventral cord in the 3-fold embryo (closed arrow).

58
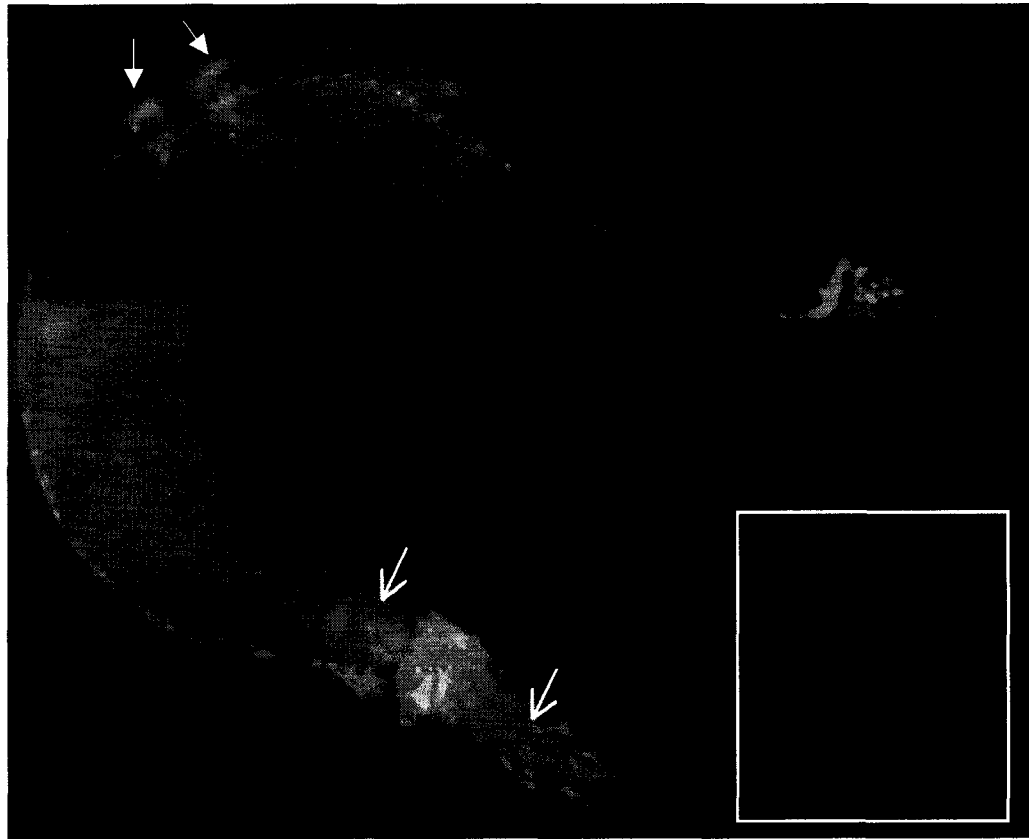
Figure 3.2   Expression of transcriptional *pdl-1*::GFP fusion in an adult hermaphrodite (strain DP265). The anterior of the worm is positioned at the bottom of the picture. The visible process bundle is the ventral nerve cord. Open arrows indicate pharyngeal muscle while the closed arrow indicates vulval muscle. The inset shows the vulval muscle expression in a second animal from a ventral perspective.

Figure 3.3 Expression of a translational *pdl-1*::GFP fusion in an adult hermaphrodite (strain DP290 (edEx134)). Fluorescence is visible in axon processes including the ventral nerve cord as well as nerve cell bodies. The head and tail are shown at high magnification and reduced exposure to allow better resolution of processes and cell bodies. Arrows indicate axon processes (the large process is the ventral nerve cord). The worm is oriented with the anterior to the left.

Ideally, I would like to have determined the subcellular localization of PDL-1 through immunostaining. I have raised antibodies against PDL-1 (described in section 3.7) but have been unable to use them successfully for immunostaining.

3.2 Studying the *pdl-1* transcript

pdl-1 was first identified by a BLAST search of the *C. elegans* genomic database with UNC-119. The only significant BLAST hit (P<0.1) was the predicted gene C27H5.1 (P=2.9x10^{-6}), which has since been renamed *pdl-1* to reflect its similarity to the rod cGMP phosphodiesterase delta subunit. As this was a predicted gene with no supporting EST data I wanted to confirm its expression and determine the boundaries of the transcript. I used RT-PCR to confirm expression of *pdl-1* and cloned the full-length transcript using 3' and 5' RACE. The 5' RACE reaction was facilitated by the presence of an SL1 splice leader at the 5' end of the transcript. The SL1 splice leader is a 22 base leader sequence which is *trans*-spliced onto the 5' end of many *C. elegans* transcripts. The complete *pdl-1* transcript consists of a 46 base 5'UTR (including the SL1 sequence), a 480 base coding region and a 130 base 3'UTR for a total of 656 bp (Figure 3.4). The coding sequence agrees with that predicted by the *C. elegans* genome database.

<u>ggtttaattacccaagtttgag</u>tcttcagagagtagagctccagtcATGGCCACTACCGCTACTCGTCATC
AAGATTCTAAATTGAGCGAAAAGGCAGAGAGCATTCTGGCTGGCTTCAAGCT
CAACTGGATGAACTTGCGTGATGCAGAAACTGGAAAAGTTCTCTGGCAGAGC
ACAGAAGACATGGCTGACCCAAAAAGGGAACACAAAGCACACGTGCCAAAG
AATCTTCTAAAATGTCGTACGGTGTCTCGTGAGATCAACTTCACTTCATCAGT
CAAAATCGAAAAATTTCGACTCGAGCAACGCGTTTATTTGAAGGGAACCATC
ATTGAAGAGTGGTATTTCGATTTTGGATTTGTCATTCCTGATTCAACAAACAC
GTGGCAAAATATGATTGAGGCAGCTCCAGAATCACAAATGTTCCCACCATCT
GTACTCAGCGGAAACGTCGTCGTCGAGACTTTATTCTATGATGGAGATCTTCT
TGTAAGCACGTCTCGAGTCCGTCTTTATTACGACTAAtacatatacattcatatccatttttccctt
ctaatccttccctgtttctccatggatctctcttttttaattcctaaaacaatacatacctaattttaatattcaatttcagaatgaaaatcttc
aacggaaaaaaaaaaaaaaaaaaaaaaaaa

Figure 3.4   *pdl-1* cDNA sequence. The coding region is in upper case and the untranslated regions are in lower case. The underlined region denotes the SL1 splice leader sequence.

61

```
Genomic segment: II:7183751..7185085
                7184k                                      7185k
C27H5.1
pdl-1
```
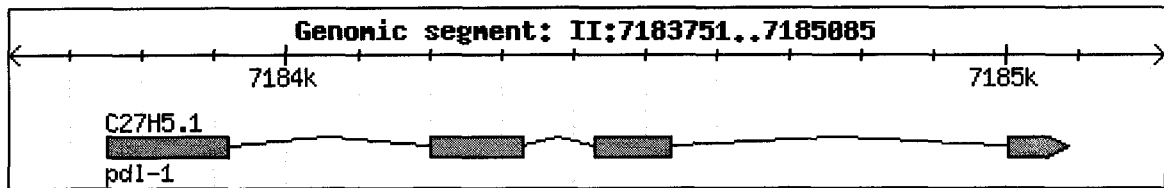
Figure 3.5   Genomic organization of *pdl-1*. The scale bar along the top of the figure indicates the nucleotide position of *pdl-1* on chromosome II. Shaded boxes indicate positions of exons. (Figure modified from www.wormbase.org).

Next I wanted to determine how many transcripts exist for *pdl-1*. To do this, I performed northern analysis using mixed stage *C. elegans* RNA. Consistent with the RACE results, the northern blot showed a single transcript of approximately 600 bases (Figure 3.6).
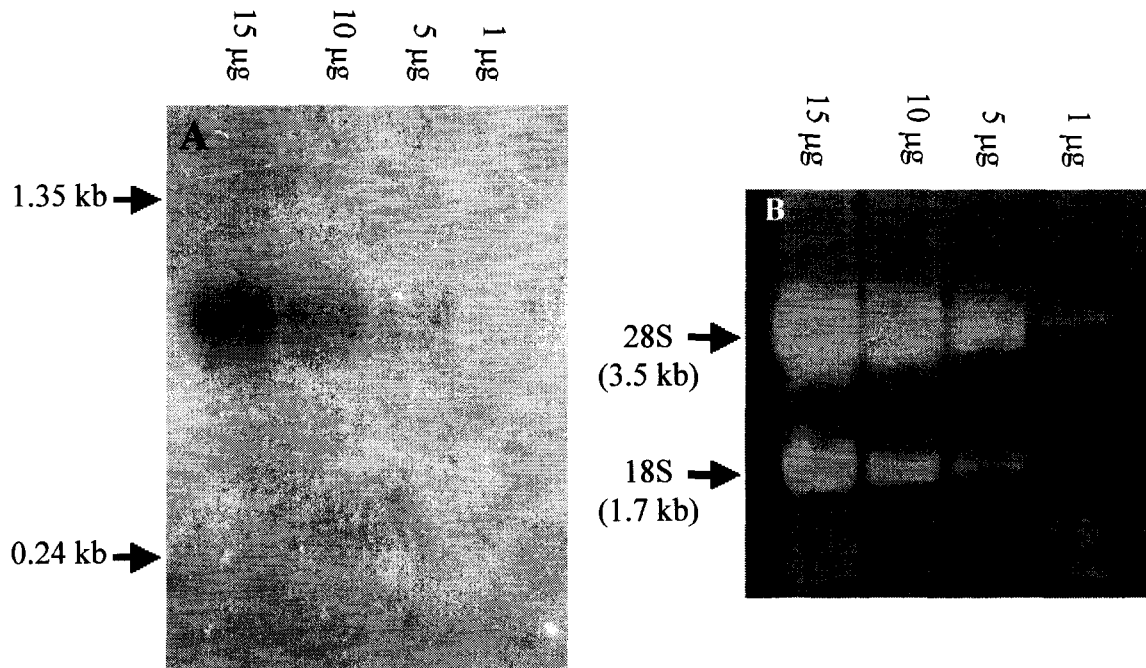
Figure 3.6   *pdl-1* northern analysis. The gel was loaded with varying amounts of mixed stage N2 total RNA as indicated. (a) Autoradiogram after 17 days exposure. (b) Ribosomal RNA bands as visualized by ethidium bromide staining prior to transfer. Both the autoradiogram and the ethidium stained gel are shown at the same magnification.

62

3.3 Attempted characterization of *pdl-1* loss of function

3.3.1 Deletion Screening

Although there has been significant biochemical analysis of the mammalian homologue of *pdl-1*, PDEδ, its function is unknown. This gene is highly conserved throughout metazoans, suggesting that it plays an important role. However, there are no known mutations in any of the PDEδ orthologues. I wanted to determine the phenotype of a *pdl-1* loss of function mutation in the genetically amenable nematode, *C. elegans*. I was particularly interested in the effect that a *pdl-1* mutation might have on the development, function, or maintenance of the nervous system.

Originally I set out to identify a deletion in *pdl-1* by PCR deletion screening. In short, this involves mutagenizing a large population of worms and subdividing the progeny into pools. The pools are then divided, with a fraction being frozen for later recovery and the remainder being used to create DNA. The DNA pools are screened by PCR to look for deletions in the gene of interest. Once a deletion is identified, worms are put through several rounds of sibling selection to isolate a homozygous or heterozygous population.

I created and screened a deletion library but did not uncover any deletions in *pdl-1*. Dave Pilgrim screened another library in Joel Rothman's lab at UC Santa Barbara. He identified two populations of worms that showed deletion bands for *pdl-1*. Unfortunately neither deletion was able to be recovered by sibling selection. In November 1998, I submitted a request for a *pdl-1* deletion to the *C. elegans* Genome Knockout Consortium in Vancouver, BC. I stopped deletion screening shortly afterward and moved on to other approaches.

3.3.2 RNAi

One approach that can be used to determine a gene's knockout phenotype is double stranded RNA interference (RNAi). This technique was first described in *C. elegans* by Fire *et al.* (1998) and has become widely used for reverse genetics. Upon learning of this new technique, I injected worms with dsRNA for *pdl-1*. Unfortunately, their progeny did

not exhibit any observable phenotype. I used *nmy-2* dsRNA as a control and it caused embryonic lethality as expected (Guo and Kemphues, 1996).

There are two possible reasons why *pdl-1* RNAi does not produce a phenotype. Either a *pdl-1* knockout has no clear phenotype or RNAi is ineffective at targeting *pdl-1*. To address this latter point, I made double stranded RNA (dsRNA) for GFP and injected it into N2 animals expressing either *unc-45*::GFP (expressed in body wall, pharyngeal, and vulval muscles) (Venolia *et al.*, 1999) or *pdl-1*::GFP. There was a clear reduction of fluorescence in the *unc-45*::GFP animals (Figure 3.7) while the fluorescence in *pdl-1*::GFP expressing animals was unaffected (data not shown). This suggests that the lack of phenotype could be due to a failure of RNAi to effectively target *pdl-1*.
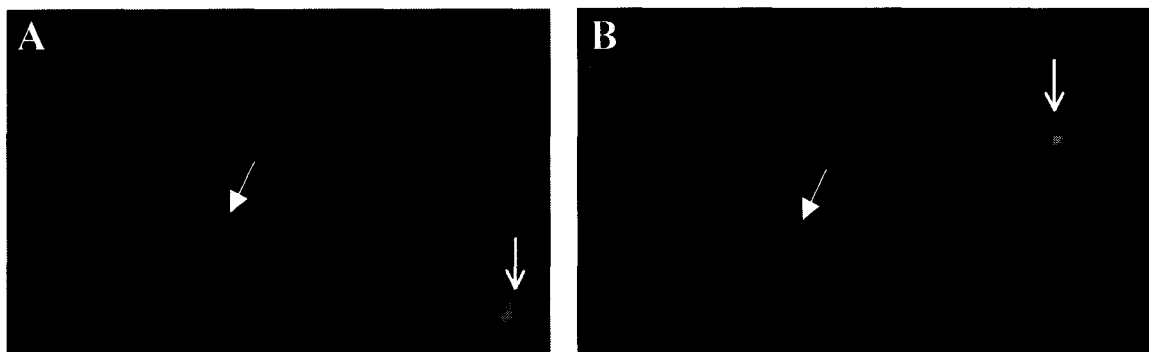
Figure 3.7　　RNAi against GFP. (a) *unc-45*::GFP worm (b) *unc-45*::GFP worm subjected to RNAi against GFP as visualized by fluorescence microscopy. Exposure was the same for both animals. Visible structures include the terminal pharyngeal bulb (open arrow) and body wall muscles (closed arrow). The anterior of the worm is to the right in both images.

While this was initially puzzling, recent studies have observed that the *C. elegans* nervous system is refractory to RNAi (Kamath *et al.*, 2000; Timmons *et al.*, 2001). This is supported by our own observation that RNAi against *unc-119* does not produce an uncoordinated phenotype in N2 animals. Fortunately, RNAi sensitive strains have recently become available to help address this problem. One of these is *rrf-3*, which carries a deletion in one of the RNA-dependent RNA polymerases. This strain shows generally enhanced sensitivity to RNAi, including RNAi in the nervous system (Simmer *et al.*, 2002). As well, Scott Kennedy in Gary Ruvkun's lab at Harvard performed a screen for worms sensitized to RNAi in the nervous system. These mutations have not

64

yet been identified, but the Ruvkun lab was kind enough to share two of these strains (*mg366* and *mg367*).

With RNAi sensitive strains in hand, I revisited RNAi against *pdl-1*, using *unc-119* as a positive control. Plating worms on bacteria expressing dsRNA for the gene of interest failed to produce an observable phenotype for either *pdl-1* or *unc-119* in N2, *rrf-3*, *mg366*, or *mg367* worms. However, injecting *unc-119* dsRNA produced a clear uncoordination defect in *rrf-3* and *mg366* worms. Injecting *pdl-1* dsRNA did not produce an observable phenotype in any of the four strains.

3.3.3 Forward Screens

When the reverse genetic approaches of deletion screening and RNAi failed to produce a phenotype for *pdl-1*, I turned to more traditional forward genetic approaches. Based on the fact that *pdl-1* is expressed in the nervous system and highly conserved, it seemed reasonable to expect that it might have an uncoordinated or lethal phenotype. I decided to perform an F1 screen for uncoordinated animals using worms hemizygous for *pdl-1*. To do this, I required a deficiency that removes the gene.

Using information available in the *C. elegans* database I identified four candidate deficiencies that could potentially remove *pdl-1*; mnDf97, mcDf1, mnDf88, and mnDf105. A map of these deficiencies is shown in Figure 3.8. I used single embryo PCR with *pdl-1* primers to screen homozygous deficiency embryos (identified by their lethal phenotype) for the presence of *pdl-1*. Internal control primers against *unc-119* were used to determine whether the individual PCR reactions worked. Of the four deficiencies tested, only mcDf1 removes the *pdl-1* locus (Figure 3.9).

65
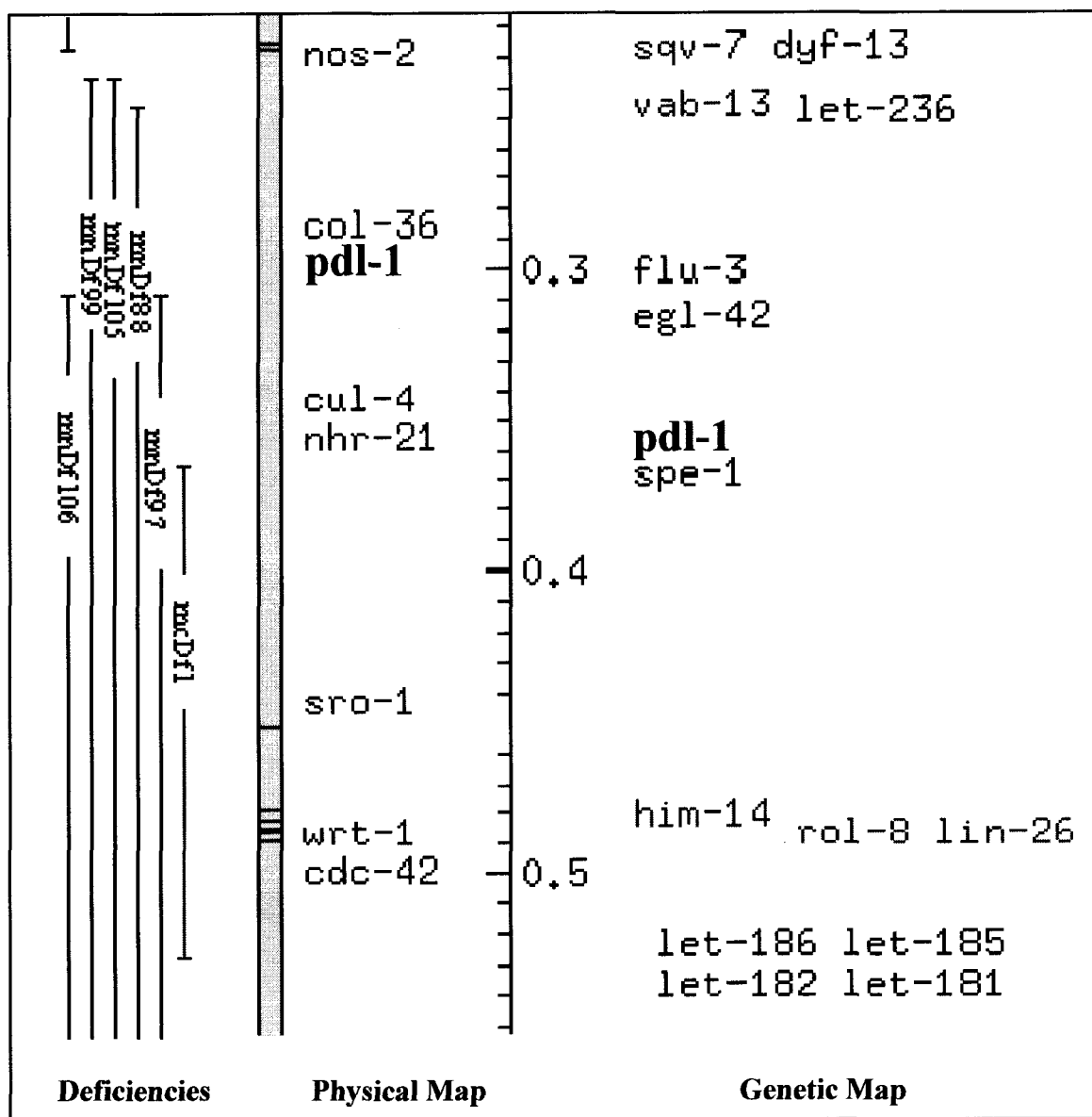
Figure 3.8   Genetic map of deficiencies on chromosome II in the region surrounding *pdl-1*. Note that the physical and genetic maps for *C. elegans* do not match exactly. The physical location of *pdl-1* and its predicted position on the genetic map are not the same. Its predicted position on the genetic map was used to select candidate deficiencies. Deficiencies were screened by PCR to determine whether or not they remove *pdl-1*. mcDf1 deletes *pdl-1* and was used in an F1 screen for uncoordinated animals. Figure adapted from www.wormbase.org.

66
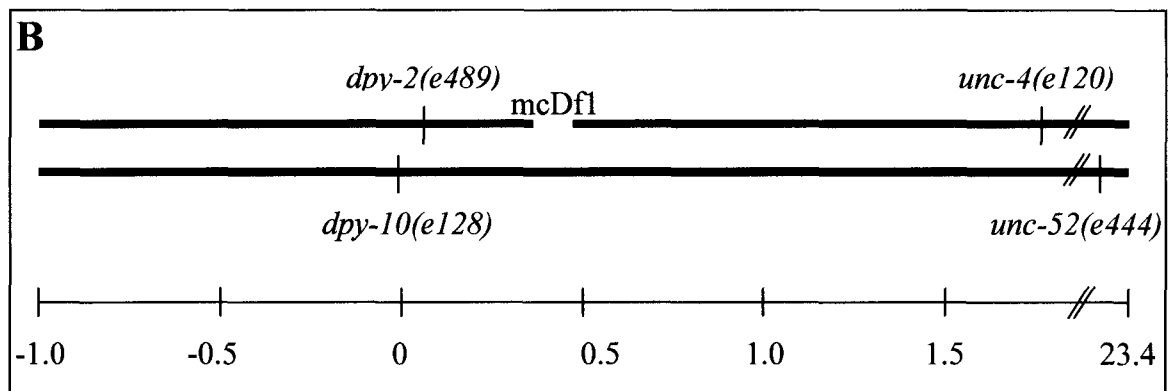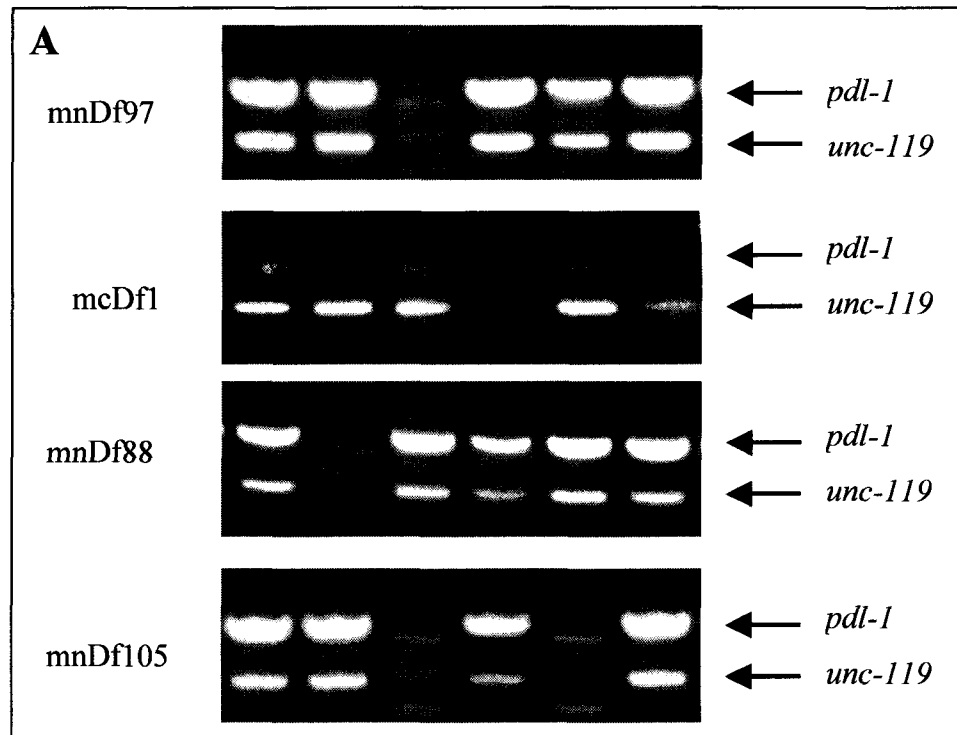
Figure 3.9 Determining whether deficiencies remove *pdl-1*. (a) Single embryo PCR on dead eggs to determine whether deficiencies remove *pdl-1*. PCR with *unc-119* primers was used as an internal PCR control. (b) Genetic map of the mcDf1 carrying strain ML335. This map includes a portion of chromosome II and shows the locations of the genetic markers present in this strain.

I used the strain ML335 [*dpy-2(e489)* mcDf1 *unc-4(e120)*/mnC1 *dpy-10(e128)* *unc-52(e444)* II] to perform an F1 screen for uncoordinated animals. As *pdl-1* is hemizygous in this strain, it should be possible to detect viable phenotypes in the F1 generation. Given the phenotype of *unc-119* and the fact that *pdl-1* is expressed in the nervous system, it seemed reasonable to suppose that a mutation in *pdl-1* could lead to an uncoordinated phenotype. I screened approximately 10^5-10^6 genomes and recovered 29

67

potential mutants. On closer investigation, I determined that I had isolated several alleles of *unc-4* and *unc-52*. I was able to test many of the suspected *unc-4* animals for complementation with the temperature sensitive mutation *unc-4(e2322ts)*. All of the worms with phenotypes similar to *unc-4* failed to complement. The suspected *unc-52* animals were much more difficult to work with as they showed poor viability and reproduction. They were classed as *unc-52* based upon their phenotype.

My next approach was to perform a pre-complementation screen for lethal alleles of *pdl-1*. This was done using a line of ML335 [*dpy-2(e489)* mcDf1 *unc-4(e120)*/mnC1 *dpy-10(e128)* *unc-52(e444)* II] worms carrying a transgenic array that includes a genomic copy of *pdl-1* along with the pan-neural GFP marker pSU006 ($P_{F25B3.3}$::GFP). Briefly, this screen relies on the ability of the transgenic array to rescue any mutations in *pdl-1*. I mutagenized the worms and then singled wild-type F1 animals expressing GFP. If the F1 animal carries a lethal mutation in *pdl-1*, all of its surviving progeny will carry the transgenic array and express GFP. If not, the F2 progeny will show variable transmission of the transgene. The transmission rate for the transgenic array in F2 animals ranged between 10% and 98%. In any case where the transmission rate was very high I maintained the plate for another generation to determine whether there was in fact 100% transmission. This was a limited screen of approximately 1400 genomes and no lethal alleles of *pdl-1* were discovered.

3.3.4 The Genome Knockout Consortium Delivers

Eventually the *C. elegans* Genome Knockout Consortium isolated a deletion in *pdl-1*. This is a 1063 bp deletion with a 40 bp insertion that removes 456 bases upstream of the start codon as well as exons 1 and 2 (Figure 3.10). Given the nature of the deletion, it should be a genetic null.

ttcagaattacaaataagttcaaataatatttttttaaaaatacattttctgtttaaacactacaatcgactatttatgtagattttctgaagaaaattttctattgcaatttc
tgcgttataagtgcccgacttactagtcatagctttatctagggaattattgaaataatatgatatttctctaaattatcacctaatcccatcctgctcaaaccacaga
accgtcgaattacgaaaagaaatatataagcagtaatatataattgtatgaatacgagttacttctcttattctcttcccttttcataaaatgtaagtgccacttataa
cacgacttcctttatgaattcaatgatctccacgtgttctttttttcataatgaccactcttcgggaacactcattttttatgctcttttccggcaatcgtcactttcgtc
aatattgactttccttgttcctaagatgaccggttcctctttcttgtgcctcggtctgtcgtcatttcctcaaaacatcactttcttcagagagtagagctccagtc
ATGGCCACTACCGCTACTCGTCATCAAGATTCTAAATTGAGCGAAAAGGCAGAGAGCAT
TCTGGCTGGCTTCAAGCTCAACTGGATGAACTTGCGTGATGCAGAAACTGGAAAAGTTC
TCTGGCAGAGCACAGAAGACATGGCTGACCCAAAAAGGGAACACAAAGgtaataagaatttcaaaaa
aagtctcggaataaaccaatcatcacaaacactatgcctggggcggtaagtaatatcgtcactgacaacacgagggaacgaacgcgagagcgtctccccc
caatgcgcgcgcacatccactgcgccattctgccacagctagcaagcaacactgagcgtgtagttaagccttcacatgtcttttaccgctggtctctaatgcaa
tgcgttttcctacaaaaatagaattgcttgaagccaacaaataaaaaactaatggattgcagCACACGTGCCAAAGAATCTTCTAA
AATGTCGTACGGTGTCTCGTGAGATCAACTTCACTTCATCAGTCAAAATCGAAAAATTTC
GACTCGAGCAACGCGTTTATTTGAAGGGAACCATCATTGAAGgtaagatagaatcactcgaatattcattatgt
tattgcacgcaatggatgaataatattggcttctggtgatgaaaactaattatgtattccgacttcagagTGGTATTTCGATTTTGGATTT
GTCATTCCTGATTCAACAAACACGTGGCAAAATATGATTGAGGCAGCTCCAGAATCACA
AATGTTCCCACCATCTGTACTCAGgtaagtaaaacaagtgcaaaagtactagatttctaagcttcaaagcttcacttcaagatacta
gaaacagaaacatgcaaaccttaatagttattaggtaaacatgaccgagtatcgtaatcaaacatttttttatatcagtcagcgttttggtaaattggcaaaaattca
aaaattgggttttgagtaatttcaaacattgctgtaggatttttaccaatacagtgtttttttataaaaattaaaaacagactttcaatatttgtactggtgaaaactgagt
aattaccgatagtttttttttttgagttttgaaacgttttagtattctttatggtatgtaattttcgtaccacaggagatgctgcacaccatcttatatataactacttaatcc
tactataaaaataacattaaattgtgttcgaggccttgacatttcgaacgattgaaaatacaatctcaatttttcagCGGAAACGTCGTCGTCG
AGACTTTATTCTATGATGGAGATCTTCTTGTAAGCACGTCTCGAGTCCGTCTTTATTACG
ACTAAtacatatacattcatatccattttttcccttctaatccttccctgtttctccatggatctctctttttttaattcctaaaacaatacatacctaattttaatattcaa
tttcagaatgaaaatcttcaacggatttatttattcatctatgtacatatgaatat

ttcagaattacaaataagttcaaataatatttttttaaaaatacattttctgtttaaacactacaatcgactatttatgtagattttctgaagaaaattttctattgcaatttc
tgcgttataagtgcccgacttactagtcatagctttatctagggaattattgaaataatatgatatttctctaaattatcacctaatcccatcctgctcaaaccacaga
accgtcgaattacgaaaagaaatatataagcagtaatatataattgtatgaatacgagttacttctcttattctcttcccttttcataaaatgtaagtgccacttataa
cacgacttcctttatgaattcaatgatctccacgtgttctttttttcataatgaccactcttcgggaacactcattttttatgctcttttccggcaatcgtcactttcgtc
aatattgactttccttgttcctaagatgaccggttcctctttcttgtgcctcggtctgtcgtcatttcctcaaaacatcactttcttcagagagtagagctccagtc
ATGGCCACTACCGCTACTCGTCATCAAGATTCTAAATTGAGCGAAAAGGCAGAGAGCAT
TCTGGCTGGCTTCAAGCTCAACTGGATGAACTTGCGTGATGCAGAAACTGGAAAAGTTC
TCTGGCAGAGCACAGAAGACATGGCTGACCCAAAAAGGGAACACAAAGgtaataagaatttcaaaaa
aagtctcggaataaaccaatcatcacaaacactatgcctggggcggtaagtaatatcgtcactgacaacacgagggaacgaacgcgagagcgtctccccc
caatgcgcgcgcacatccactgcgccattctgccacagctagcaagcaacactgagcgtgtagttaagccttcacatgtcttttaccgctggtctctaatgcaa
tgcgttttcctacaaaaatagaattgcttgaagccaacaaataaaaaactaatggattgcagCACACGTGCCAAAGAATCTTCTAA
AATGTCGTACGGTGTCTCGTGAGATCAACTTCACTTCATCAGTCAAAATCGAAAAATTTC
GACTCGAGCAACGCGTTTATTTGAAGGGAACCATCATTGAAGgtaagatagaatcactcgaatattcattatgt
tattgcacgcaatggatgaataatattggcttctggtgatgaaaactaattatgtattccgacttcagagTGGTATTTCGATTTTGGATTT
GTCATTCCTGATTCAACAAACACGTGGCAAAATATGATTGAGGCAGCTCCAGAATCACA
AATGTTCCCACCATCTGTACTCAGgtaagtaaaacaagtgcaaaagtactagatttctaagcttcaaagcttcacttcaagatacta
gaaacagaaacatgcaaaccttaatagttattaggtaaacatgaccgagtatcgtaatcaaacatttttttatatcagtcagcgttttggtaaattggcaaaaattca
aaaattgggttttgagtaatttcaaacattgctgtaggatttttaccaatacagtgtttttttataaaaattaaaaacagactttcaatatttgtactggtgaaaactgagt
aattaccgatagtttttttttttgagttttgaaacgttttagtattctttatggtatgtaattttcgtaccacaggagatgctgcacaccatcttatatataactacttaatcc
tactataaaaataacattaaattgtgttcgaggccttgacatttcgaacgattgaaaatacaatctcaatttttcagCGGAAACGTCGTCGTCG
AGACTTTATTCTATGATGGAGATCTTCTTGTAAGCACGTCTCGAGTCCGTCTTTATTACG
ACTAAtacatatacattcatatccattttttcccttctaatccttccctgtttctccatggatctctctttttttaattcctaaaacaatacatacctaattttaatattcaa
tttcagaatgaaaatcttcaacggatttatttattcatctatgtacatatgaatat

Figure 3.10 *pdl-1(gk157)* deletion. Shading indicates sequence removed by the deletion while upper case denotes exon sequence. Underlining indicates the start and stop codons of *pdl-1*.

3.4 Confirming the *pdl-1(gk157)* deletion

Before proceeding with phenotypic analysis, I wanted to ensure that the *pdl-1* mutant does not carry an extra copy of *pdl-1* in its genome. The deletion was created by UV/TMP mutagenesis and it is possible that a duplication of *pdl-1* could have been created by complex genome rearrangement as a result of chromosomal breaks caused by UV irradiation. To address this, I first performed PCR on *pdl-1* worms and confirmed that this amplifies only the deletion band (Figure 3.11). Sequencing the PCR product confirmed the deletion boundaries and insertion sequence as provided by the *C. elegans* Genome Knockout Consortium.

N2   *pdl-1*
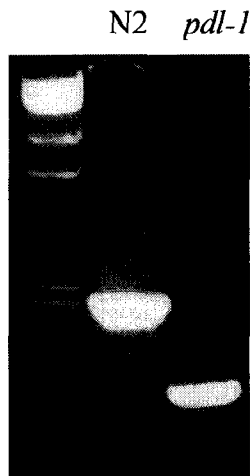
Figure 3.11   PCR to confirm the *pdl-1(gk157)* deletion. PCR was performed on DNA prepared from wild-type (N2) and *pdl-1* worms using the primers MMA17 and C27JSF1.

I then used Southern analysis to confirm that *pdl-1* worms do not have any extra copies of *pdl-1*. I used three restriction enzymes, two of which flank the deletion and one of which is removed by the deletion. The Southern blot confirms that there are no duplications of *pdl-1* in the genome of *pdl-1(gk157)* animals (Figure 3.12). The deletion obtained by the knockout consortium represents a true knockout of *pdl-1*.

70

A

probe

EcoR1   EcoR1   HindIII
BglII   BglII
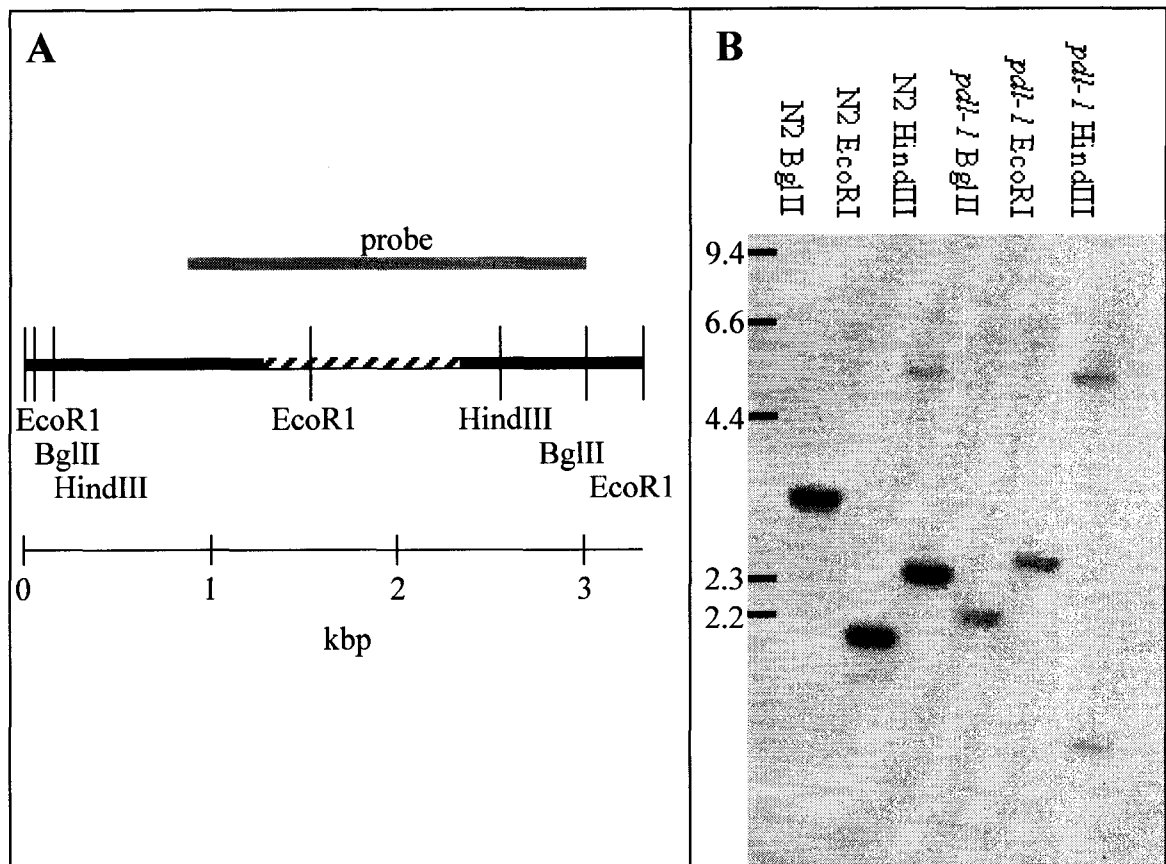HindIII   EcoR1

0   1   2   3

kbp

B

N2 BglII   N2 EcoRI   N2 HindIII   pdl-1 BglII   pdl-1 EcoRI   pdl-1 HindIII

9.4 —
6.6 —
4.4 —
2.3 —
2.2 —

Figure 3.12   Southern Blot of N2 and *pdl-1(gk157)* worms probed with a 2.1 kbp fragment of *pdl-1* genomic sequence. (A) Diagram of the probe used for this blot. The grey line at the top of the figure shows the genomic segment used to make the probe. The hatched line shows the location of the *pdl-1(gk157)* deletion. (B) Southern blot probed with *pdl-1* sequence. Genomic DNA from either N2 or *pdl-1(gk157)* worms was digested with BglII, EcoRI, or HindIII as indicated.

3.5 Phenotypic characterization of *pdl-1(gk157)*

Since *pdl-1* is expressed throughout the nervous system of the worm, one would expect a *pdl-1* mutant to exhibit defects in nervous system structure, development, or function. Therefore I focused my phenotypic characterization of *pdl-1* in these areas. However, I have also looked for gross abnormalities such as embryonic lethality, morphological defects, or developmental arrest.

3.5.1 Morphology, Mating, Mechanosensation and Motility

pdl-1 worms do not exhibit any embryonic lethality, developmental arrest, or gross morphological abnormality at 15, 20, or 25°C. Their brood size appears normal and they

71

do not appear to have any egg laying defects. Male *pdl-1* worms behave normally and mate as successfully as wild-type males. *pdl-1* motility is normal and they are responsive to anterior and posterior touch suggesting that their mechanosensory and motor systems function properly.

3.5.2 Sensory Systems

C. elegans has two groups of sensory neurons, the amphids in the head and the phasmids in the tail. These neurons are open to the environment and will normally take up fluorescent dye from the environment. I soaked *pdl-1(gk157)*, *unc-119(e2498)*, and N2 worms in a FITC solution to determine their dye filling abilities. As shown previously, *unc-119* animals have a dye filling defect whereby none of the amphids take up dye (Maduro, 1998). Conversely, N2 and *pdl-1* animals show robust dye filling in all 6 pairs of amphids (Figure 3.14).
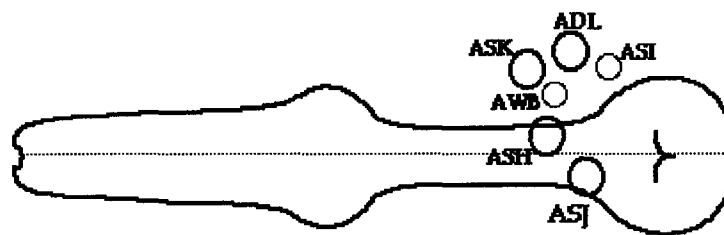
Figure 3.13   Amphid neurons. Circles show positions of amphid neuron cell bodies. Each circle represents one of a bilaterally symmetric pair of neurons. Figure from http://info.med.yale.edu/mbb/koelle/protocols/protocol_dye_filling_sens.html.
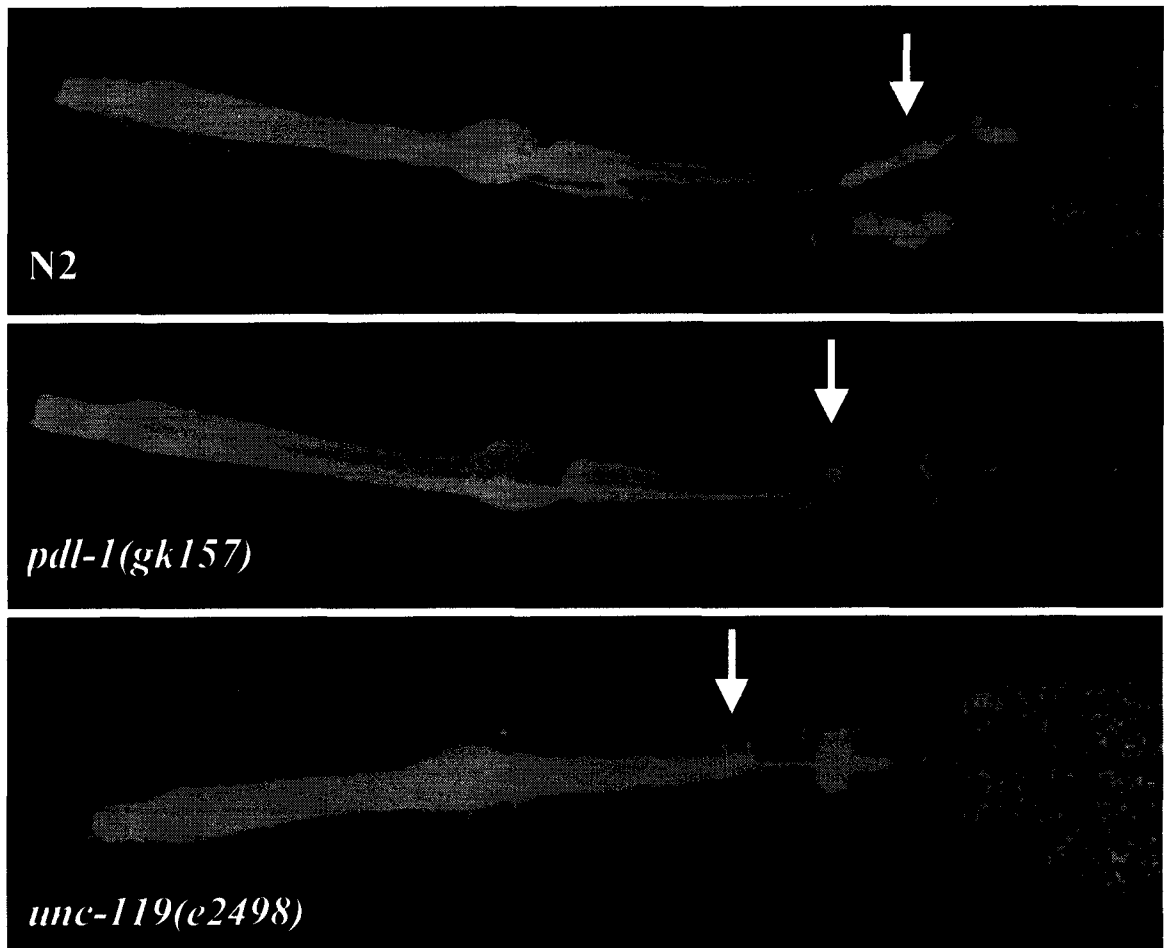
Figure 3.14 Dye filling in amphid neurons of wild-type, *pdl-1*, and *unc-119* worms (anterior to the left). The arrow indicates the middle of the cluster of amphid cell bodies. The lumen of the pharynx fluoresces as a result of worms ingesting the dye solution.

Another way to test sensory ability is to determine the animal's ability to enter dauer. Upon crowding or starvation, wild type *C. elegans* enter an alternative larval state known as dauer (Cassada and Russell, 1975). Mutants with defects in their sensory neurons fail to enter dauer as they are unable to detect dauer pheromone (Albert *et al.*, 1981; Golden and Riddle, 1982). I allowed plates of *pdl-1* animals to starve and found that they do form dauer larvae. When *pdl-1* dauer larvae are placed back onto food they recover and continue to develop normally, indicating that they are able to detect the presence of *E. coli*.

Finally, I looked at the ability of *pdl-1* animals to chemotax. *C. elegans* are responsive to a number of chemical stimuli including a variety of volatile and water soluble compounds

73

(reviewed by Bargmann and Mori, 1997). Since there are different neurons involved in detecting the two types of chemicals (Bargmann *et el.*, 1993) I tested *pdl-1* worms for response to butanol, isoamyl alcohol, ammonium acetate, copper sulfate, and SDS.

I used traditional chemotaxis assay plates to test N2 and *pdl-1* worms' response to butanol (10^{-2}) and isoamyl alcohol (10^{-1}). Both were strongly attracted to the alcohols: N2 animals showed a chemotaxis index of 1.0 for both butanol (n=13) and isoamyl alcohol (n=21) while *pdl-1* animals showed a chemotaxis index of 1.0 for butanol (n=125) and 0.95 for isoamyl alcohol (n=40).

I used two assays to test for *pdl-1* animals' response to water soluble molecules. To test for chemoattraction I set up quadrant plates where opposite quadrants contained agar with ammonium acetate (75mM) and the remaining quadrants contained agar without any attractant. In this assay, worms are plated on the attractant quadrants and left to crawl for 45 minutes. If they are responsive to the chemoattractant, they will stay on the attractant quadrants rather than disperse over the plate. In this assay, 1.4% of N2 animals left the attractant quadrants (n=142) while no *pdl-1* animals left the attractant quadrants (n=125).

To test for response to repellant molecules I used the soluble compound aversion assay as described by Wicks *et al.* (2000). Briefly, worms are placed onto plates that have an attractive volatile odorant surrounded by a semicircle of water soluble repellant. The worms are plated outside the semicircle and assayed to see if they will cross the repellant "barrier" to get at the attractant (10^{-1} isoamyl alcohol). I tested two repellants, 150 mM $CuSO_4$ and 2% SDS. Both N2 and *pdl-1* worms were sensitive to the repellants as summarized in Table 3.1.

	150 mM CuSO$_4$	2% SDS
N2	0.02 (n=102)	0.02 (n=92)
pdl-1	0.02 (n=52)	0 (n=80)

**Table 3.1**   Aversion Index for N2 and *pdl-1* worms to water soluble substances.

Aversion Index = # of worms that cross the aversive substance barrier
total number of worms plated

74

The results from the chemotaxis assays demonstrate that *pdl-1* worms do not have defects in their chemotactic response to either volatile or water soluble compounds. They are responsive to both attractive and aversive substances in a manner indistinguishable from wild-type.

3.5.3 Nervous System Structure

To look at the nervous system of *pdl-1* worms, I crossed three nervous system markers into a *pdl-1* background; $P_{F25B3.3}$::GFP (pan-neuronal), P*unc-129*::GFP (DA/DB motor neurons) and P*daf-7*::GFP (ASI neurons). All three reporters have been examined in *unc-119(ed3)* animals and have been used to highlight a number of nervous system defects such as ventral cord defasciculation, supernumerary axon branching, axon guidance defects, and nerve cell body displacement. (Wayne Materi, personal communication). I wanted to determine whether there are similar, perhaps milder, defects in *pdl-1*.

All three nervous system markers reveal that the structure of the nervous system in *pdl-1* animals is wild-type. The nervous system is well organized showing an orderly array of cell bodies and processes (Figure 3.15). Since it is difficult to visualize individual cells or processes with the F25B3.3::GFP marker, I also looked at GFP reporters which highlight only a subset of neurons. P*unc-129*::GFP is expressed in DA/DB motor neurons and is useful for looking at axon branching, cell body placement, and ventral cord fasciculation. As shown in Figure 3.16 *pdl-1* worms appear normal on all three counts.

75
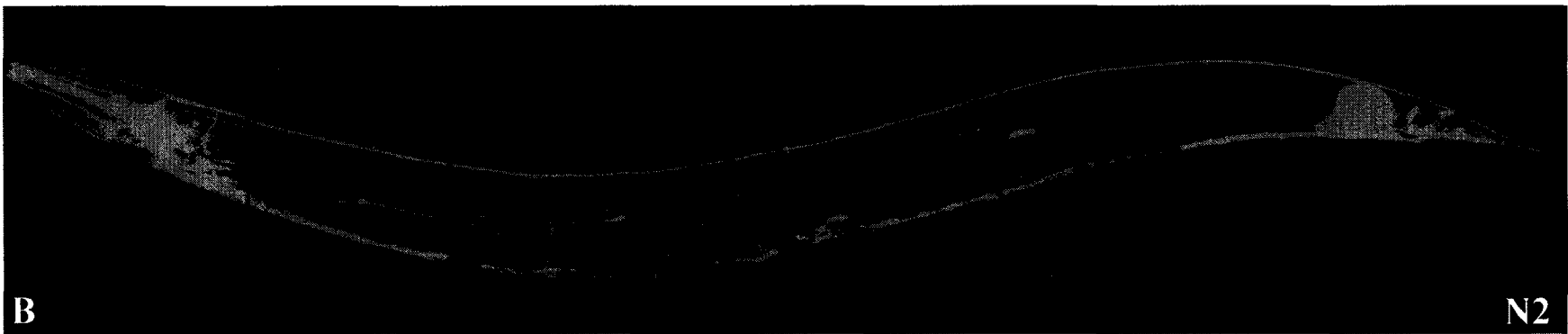
Figure 3.15   Overall nervous system structure in a *pdl-1(gk157)* animal. Both animals are expressing an integrated $P_{F25B3.3}$::GFP construct which is expressed pan-neuronally. Micrographs show the left side of the worm with the anterior to the left. (A) *pdl-1 (gk157)* adult hermaphrodite (B) wild-type hermaphrodite.
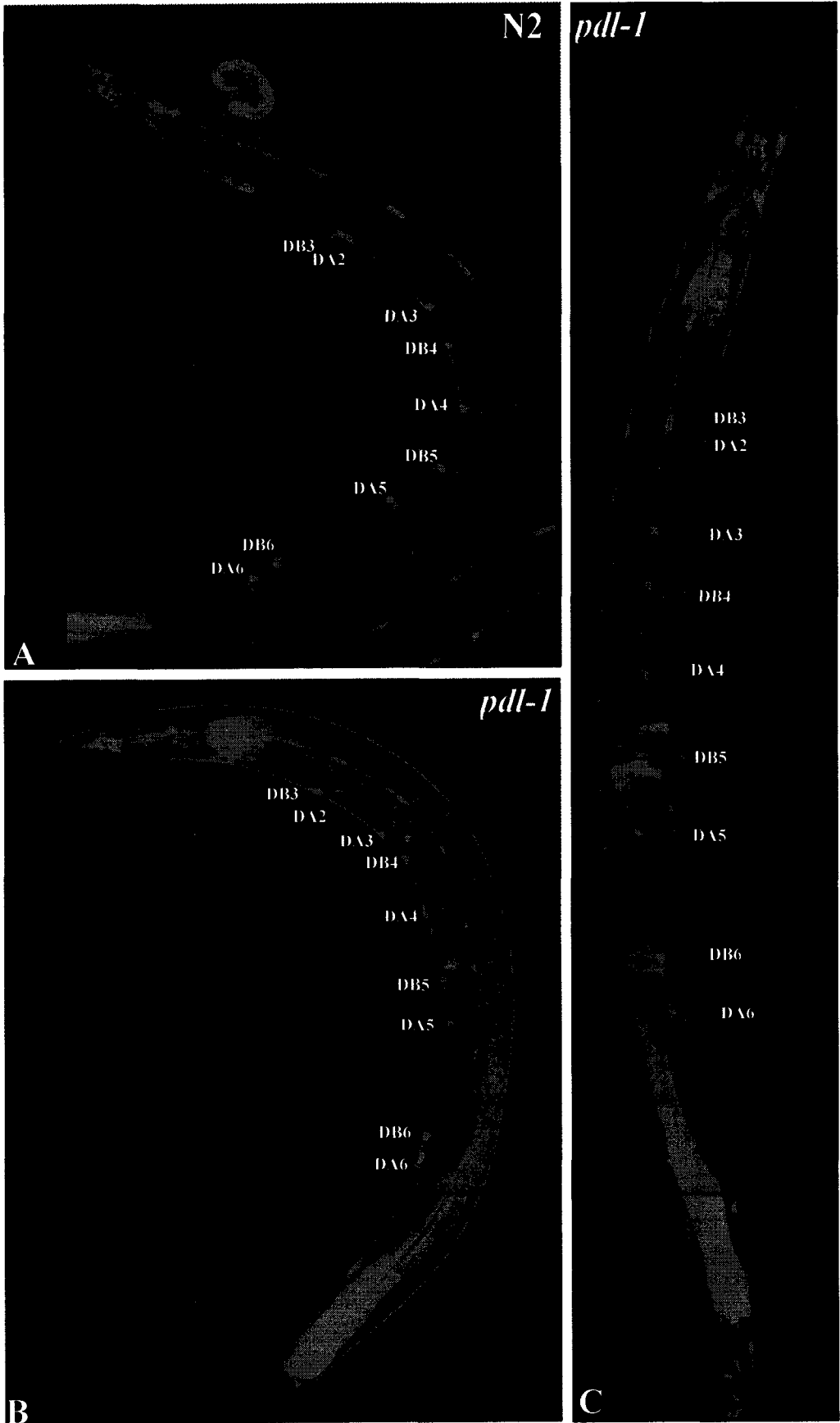
N2

pdl-1

DB3
D A2

D A3

DB4

D A4

DB5

D A5

DB6
D A6

A

pdl-1

DB3
D A2
D A3
DB4

D A4

DB5

D A5

DB6
D A6

B

DB3
D A2

D A3

DB4

D A4

DB5

D A5

DB6

D A6

C

Figure legend is on the following page

77

Figure 3.16   P*unc-129*::GFP in N2 and *pdl-1*. Cells along the ventral nerve cord are labelled to aid comparison. (A) and (B) The anterior of the animal is in the upper left corner. Comparison of N2 and *pdl-1* shows that the DA/DB motor neurons are present in the correct locations and in the correct number in the *pdl-1* mutant. Commissures do not show branching defects and processes extend at the appropriate locations. (C) A ventral view of a *pdl-1* animal (anterior at the top) shows tight fasciculation of the ventral cord, proper location of cell bodies and extension of commissures to the appropriate side of the animal.

P*daf-7*::GFP is expressed in the two ASI neurons in the head. These send processes into the nerve ring and are highly irregular in *unc-119* animals (Wayne Materi, personal communication). These neurons appear normal in *pdl-1* indicating appropriate entry of ASI processes into the nerve ring. (Figure 3.17).
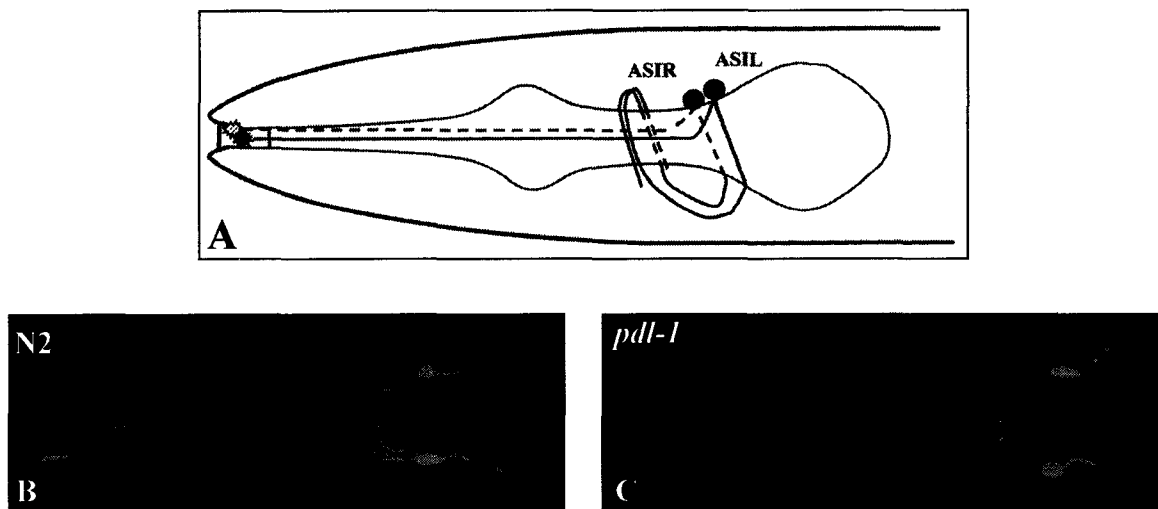
Figure 3.17   P*daf-7*::GFP in *pdl-1(gk157)* and N2 animals. (A) Diagram of the ASI neurons. This diagram shows the left side of the animal with the anterior to the left. Figure modified from White *et al.*, 1986. (B) and (C) Comparison of the ASI amphid neurons does not show any structural differences between *pdl-1* and N2 animals. Worms are viewed from a ventral perspective with the anterior to the left.

3.5.4 Neurotransmission

Although the behaviour of *pdl-1* animals appears normal, I wanted to test some aspect of neurotransmission in these animals. To do this, I treated them with levamisole, an acetylcholine receptor agonist that causes wild-type worms to hypercontract. *pdl-1* worms contract normally when treated with levamisole.

78

3.5.5 pdl-1; unc-119 Double Mutant

Since the *pdl-1* deletion mutant has no obvious phenotype, I wanted to determine whether there is functional overlap between *pdl-1* and any other genes. Since *unc-119* is the only sequence homologue of *pdl-1*, I crossed *pdl-1(gk157)* into an *unc-119(ed3)* background. Both *unc-119(ed3)* and *pdl-1(gk157)* are predicted to be null alleles (Maduro, 1998; this work) so these animals should be completely lacking function for both genes. Despite this, the double mutant appears phenotypically indistinguishable from *unc-119*.

To confirm this qualitative observation, I crossed an integrated P*unc-129*::GFP reporter into the double mutant. I used this to look qualitatively at ventral cord defasciculation and quantitatively at DA5 cell body displacement to the anterior of the vulva. DA5 is a motor neuron that normally resides along the ventral cord just to the posterior of the vulva. In *unc-119* animals, this cell body is frequently displaced to the anterior of the vulva. I wanted to see if the incidence of DA5 displacement is higher in the double mutant. Neither ventral cord defasciculation (data not shown) nor DA5 displacement were more pronounced in the *pdl-1*; *unc-119* double mutant (Figure 3.18).

79
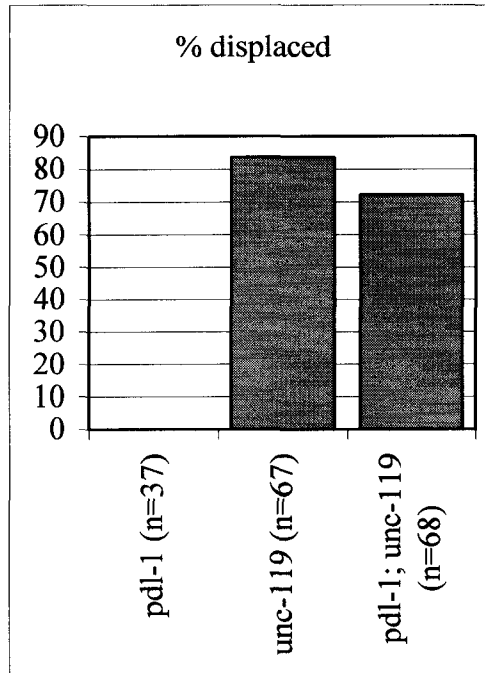
Figure 3.18   DA5 motor neuron displacement in *pdl-1(gk157)* and *unc-119(ed3)* animals. The DA5 cell body is normally located posterior to the vulva. In *unc-119* animals this cell is variably displaced to the anterior.

3.6 Yeast 2-hybrid assay

3.6.1 Screen

A yeast 2-hybrid screen using the full-length PDL-1 protein identified 66 potential interactors. Of these, eight did not show reproducible interaction with PDL-1 and one interacted promiscuously with the unrelated bait proteins Rad7 and Snf1. Rad7 is a yeast protein involved in DNA repair and Snf1 is a yeast serine/threonine kinase. Neither is expected to act similarly to PDL-1. Proteins that interact with the unrelated baits are presumed false positives as they do not show specificity for PDL-1. Prey that did not show reproducible interaction with PDL-1 or that showed promiscuous interaction with unrelated baits were not followed any further.

The remaining prey constructs were isolated and sequenced. Of the 58 plasmids sequenced, only eight were in-frame constructs in the correct orientation. Of the false positives (either out of frame or in reverse orientation), several were isolated multiple

times. Roughly half of the false positives had a synthetic prenylation signal (CAAX box) at their carboxyl terminus. The mammalian homologue of PDL-1, PDEδ has been shown to interact with the prenylated ends of the catalytic subunits of rod cGMP phosphodiesterase (Florio *et al.*, 1996; Cook *et al.*, 2000). While not conclusive, the prevalence of the prenylation signal in the yeast 2-hybrid positives suggests that PDL-1 also has an affinity for prenyl groups. A comparison of the peptides encoded by the false positives does not reveal any clear sequence similarity between them (data not shown). A list of false positives is shown in Table 3.2.

False Positive Identity	Number of Isolates	Why False?	CAAX box?
C31H2.2	8	reverse orientation	yes
C32D5.10	1	out of frame	yes
E04A4.8	1	reverse orientation	n/d
F22F4.2	2	out of frame	no
F27C1.8	7	out of frame	yes
F49H12.6	1	out of frame	yes
F56D12.5	3	reverse orientation	yes
T25G3.3	1	out of frame	no
W09C5.1	15	stop in 5' UTR	no*
Y105C5A.16	1	out of frame	yes
ZK829.4	2	out of frame	yes
ZK863.7	7	out of frame	no

Table 3.2 False positives identified in yeast 2-hybrid screen with PDL-1 bait. The column on the right indicates whether the peptide encoded by the prey contains a CAAX prenylation signal. *Although the W09C5.1 constructs do not contain a CAAX box, they end with CCNII which could be a target for double geranylgeranylation.

Of the eight prey constructs that were in frame, five correspond to unique sequences while the remaining three are clones of *let-2*. To test the validity of these interactions, I transformed the prey plasmids back into PDL-1 bait yeast and looked for growth. Curiously, the *let-2* constructs would grow if plated directly on quadruple knockout medium (SC-TRP-LEU-HIS-ADE) but would not grow if the transformations were first plated on SC-TRP-LEU (selects for the presence of both bait and prey plasmids) and then patched onto quadruple knockout medium. As the interaction between PDL-1 and LET-2 was not robust, I removed *let-2* from further consideration. The remaining five positives showed robust interaction in both assays. A list of positives is shown in Table 3.3.

81

Positive Name	Identity/Function	Number of Isolates	Interacts with Snf1?	Interacts with Rad7?	CAAX box?	Interacts with hsPDEδ?
C02F5.7	similar to yeast GRR1 (glucose induced repressor)	1	no	no	yes	yes
C49G7.3	unknown, worm specific	1	no	yes	yes	yes
let-2	alpha-2 type IV collagen	3	no	yes	no	n/d
W05B5.1a	unknown	1	no	weak	yes	no
Y113G7A.3	Sec23, vesicle transport	1	no	yes	no	no
Y55F3AM.9	unknown	1	no	no	yes	no

Table 3.3 PDL-1 interactors identified by yeast 2-hybrid screen.

3.6.2 Domain Analysis

I wanted to determine which regions of PDL-1 are required for interaction with the various prey constructs. There are no known domains in PDL-1 and the entire protein (with the exception of the N-terminal 10-20 amino acids) is very well conserved (Figure 1.4). As a result, it is difficult to determine distinct regions of the protein that might be required for function. I divided the protein roughly into quarters and tested the various domains for interaction with the yeast 2-hybrid positives. The results of this domain analysis are summarized in Table 3.4.
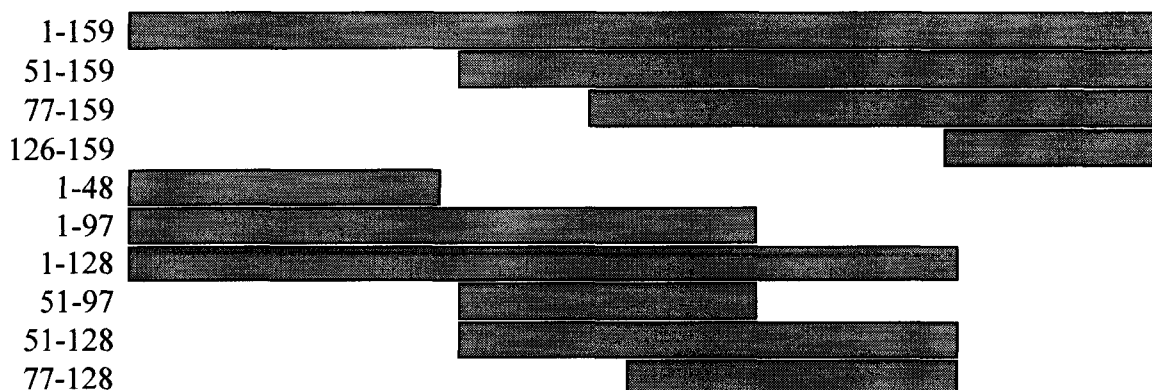


```
1-159
51-159
77-159
126-159
1-48
1-97
1-128
51-97
51-128
77-128
```

Figure 3.19 Regions of PDL-1 used for domain analysis.

PDL-1 amino acids:	C02F5.7	C49G7.3	W05B5.1a	Y55F3AM.9	Y113G7A.3
1-159	+	+	+	+	+
51-159	+/-	+	-	-	+
77-159	-	-	-	-	+
126-159	-	-	-	-	+
1-48	-	-	-	-	-
1-97	-	-	-	-	+
1-128	-	+	-	-	+
51-97	-	+	-	-	+
51-128	-	+	-	-	+
77-128	-	+/-	+	+	+

Table 3.4   Yeast 2-hybrid domain analysis results. + indicates growth, +/- indicates weak growth, and – indicates absence of growth on SC-TRP-LEU-HIS-ADE medium.

3.6.3 Vector Swapping and Testing For Interaction with hsPDEδ

Finally, I tried to confirm the validity of the yeast 2-hybrid interactions by swapping the bait and prey vectors. If these are genuine interactions, they will likely be maintained if PDL-1 is fused to the Gal4 activation domain and the positives are fused to the Gal4 binding domain. In fact, only W05B5.1a and Y113G7A.3 maintain their interaction with PDL-1 once the vectors are swapped.

I also tested the positives for interaction with human PDEδ. Since PDL-1 and hsPDEδ are highly conserved (85% similarity) and PDL-1 has been shown to interact with human rod cGMP phosphodiesterase indistinguishably from hsPDEδ (Li and Baehr, 1998), it seems reasonable to expect that proteins that interact with PDL-1 might also interact with hsPDEδ. Of the five positives identified by the yeast 2-hybrid screen only C02F5.7 and C49G7.3 interact with hsPDEδ.

3.6.4 Directed Yeast 2-Hybrid with evl-20 and Arl-2

Human PDEδ and UNC-119 have been shown to interact with Arl2 (Renault et al., 2001; Van Valkenburgh et al., 2001; Hanzal-Bayer et al., 2002; Kobayashi et al., 2003). I wanted to determine whether these interactions are maintained in other species. evl-20 is the closest sequence homologue of Arl2 in the worm genome. As well, evl-20 worms

have been rescued by transgenic expression of Arl2 (Antoshechkin and Han, 2002), suggesting that *evl-20* and Arl2 are functionally conserved. If this is true, then the binding partners of Arl2 may also be conserved between worm and human.

I tested this hypothesis using directed yeast 2-hybrid between Gal4 binding domain fusions of hsArl2(Q70L), hsArl2, and ceEVL-20(Q70L) and Gal4 activation domain fusions of cePDL-1, ceUNC-119, hsUNC-119, drPDEδ, and hsPDEδ. Arl2(Q70L) and EVL-20(Q70L) are mutant protein forms that are thought to be constitutively GTP-bound and therefore constitutively active. Specifically, the Q70L mutation should be deficient in GTP hydrolysis based on its analogy to the Ras Q61L mutation, which has been shown to lack GTPase activity (Temeles *et al.*, 1985; Frech *et al.*, 1994).

It has been reported that hsPDEδ will only interact with the activated form of Arl2 while hsUnc119 will interact with either activated or wild-type Arl2 (Van Valkenburgh *et al.*, 2001; Hanzal-Bayer *et al.*, 2002). In my 2-hybrid assay, the only combinations that grew well were drPDEδ, hsPDEδ, and cePDL-1 with hsArl2(Q70L). hsUNC-119 showed a weak interaction with hsArl2(Q70L) that was visible as poor growth after several days at room temperature. None of the other combinations grew (Table 3.5).

The previously published reports used HIS and LacZ as reporters to indicate protein interaction. I have used both HIS and ADE as selectable markers. It is possible that ADE provides more stringent selection that eliminates all but the strongest of interactions. So, I tested the yeast for LacZ expression to determine if there were weaker interactions that I was missing by assaying only for growth. This turned out to be the case as all 15 combinations were positive for LacZ (Table 3.5). The strains that had grown on selective medium showed stronger β-galactosidase staining than those which had not, but all combinations showed some degree of staining. This indicates that there is at least weak interaction between all of the protein pairs tested.

	drPDEδ	hsPDEδ	PDL-1	hsUNC-119	ceUNC-119
hsArl2	+	+	+	+	+
hsArl2(Q70L)	+++	+	+++	++	++
ceEVL-20	+	+	+	+	+

Table 3.5 Directed yeast 2-hybrid LacZ staining results. +++ indicates development of blue within 15 minutes, ++ indicates development of blue within 30 minutes and + indicates development of blue within 3 hours. Shading indicates combinations which grow on quadruple knockout plates. Dark shading indicates robust growth while light shading indicates weak growth.

3.6.5 Characterizing the Yeast 2-hybrid Positives in C. elegans

All of the positives identified in my yeast 2-hybrid screen correspond to predicted loci that have not been characterized in *C. elegans*. Since *pdl-1* is expressed throughout the nervous system, I wanted to determine which, if any, of the 2-hybrid positives are neurally expressed. The GFP fusions showed a range of expression varying from highly specific to very widespread (Figure 3.20). C49G7.3 has the tightest regulation showing expression solely in pharyngeal neurons. C02F5.7 shows clear expression in the nerve ring, along the ventral cord, and in various other tissues. W05B5.1a shows expression in various neurons in the head and along the ventral cord, pharyngeal muscles, and other tissues. Y55F3AM.9 shows expression in pharyngeal and body wall muscles, some neurons, and in hypodermal seam cells. Finally, Y113G7A.3 expression appears more or less ubiquitous. All of the yeast 2-hybrid positives show some degree of neural expression and hence, all of them could potentially interact with PDL-1 *in vivo*.

Figure 3.20 Expression patterns of positives identified in a yeast 2-hybrid screen with PDL-1. Reporter constructs are transcriptional fusions in which GFP is expressed under control of the upstream region for each predicted gene. The anterior of the worm is to the left in all micrographs. (A) C02F5.7::GFP expression pattern. Arrows indicate nerves in the nerve ring (nr), tail ganglia (tg), and ventral nerve cord (vnc). (B) C49G7.3::GFP expression pattern. GFP fluorescence is seen only in pharyngeal neurons. (C) W05B5.1a::GFP expression pattern. Arrows indicate cell bodies in the nerve ring, the ventral cord, and the tail ganglia. (D) Y55F3AM.9::GFP expression pattern. Closed arrow indicates a few cell bodies in the nerve ring. Expression is predominantly in non-neural tissues such as the pharyngeal muscles (pm), body wall muscles (bwm), and hypodermal seam cells (sc) as indicated by the open arrows. (E) Y113G7A.3::GFP expression pattern. GFP fluorescence appears to be more or less ubiquitous.

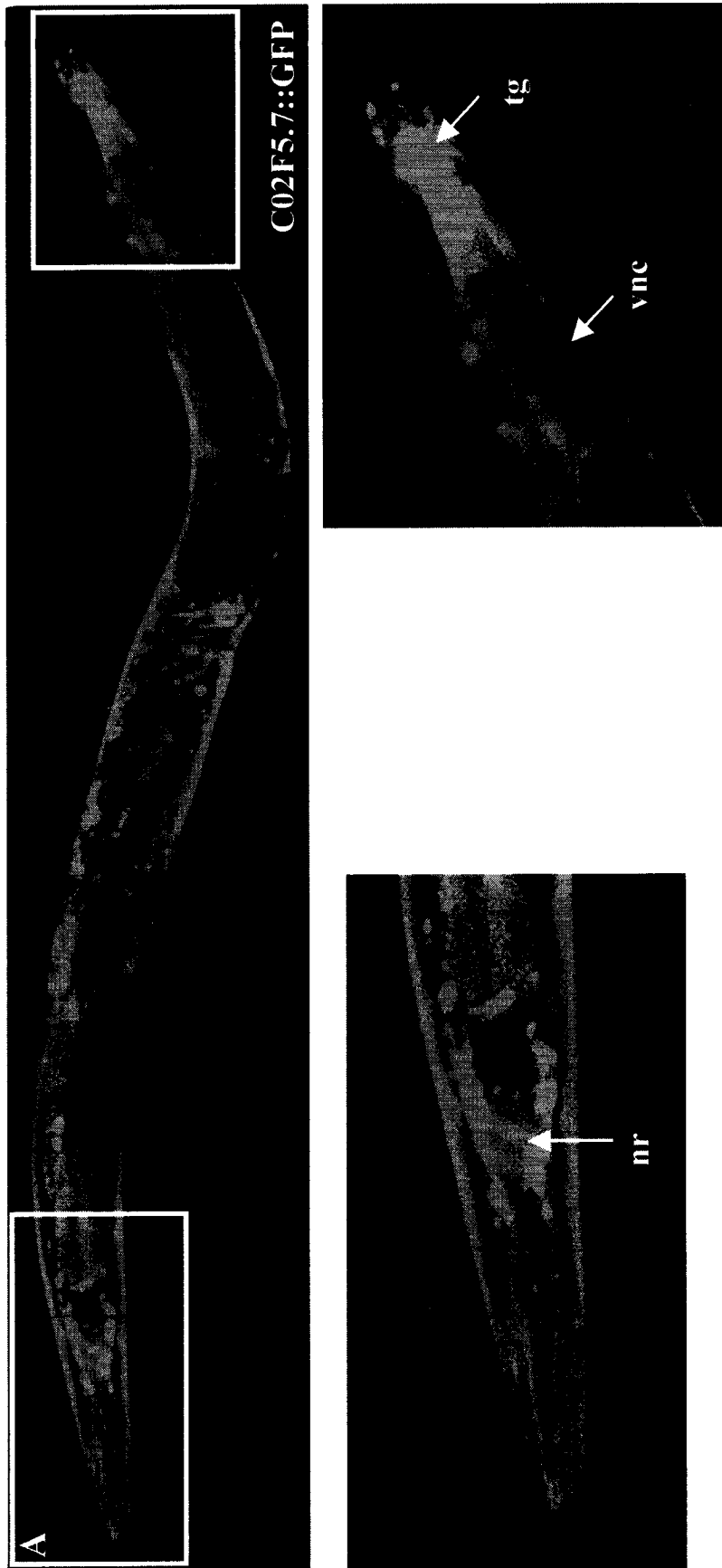*Figure is on the following pages.*

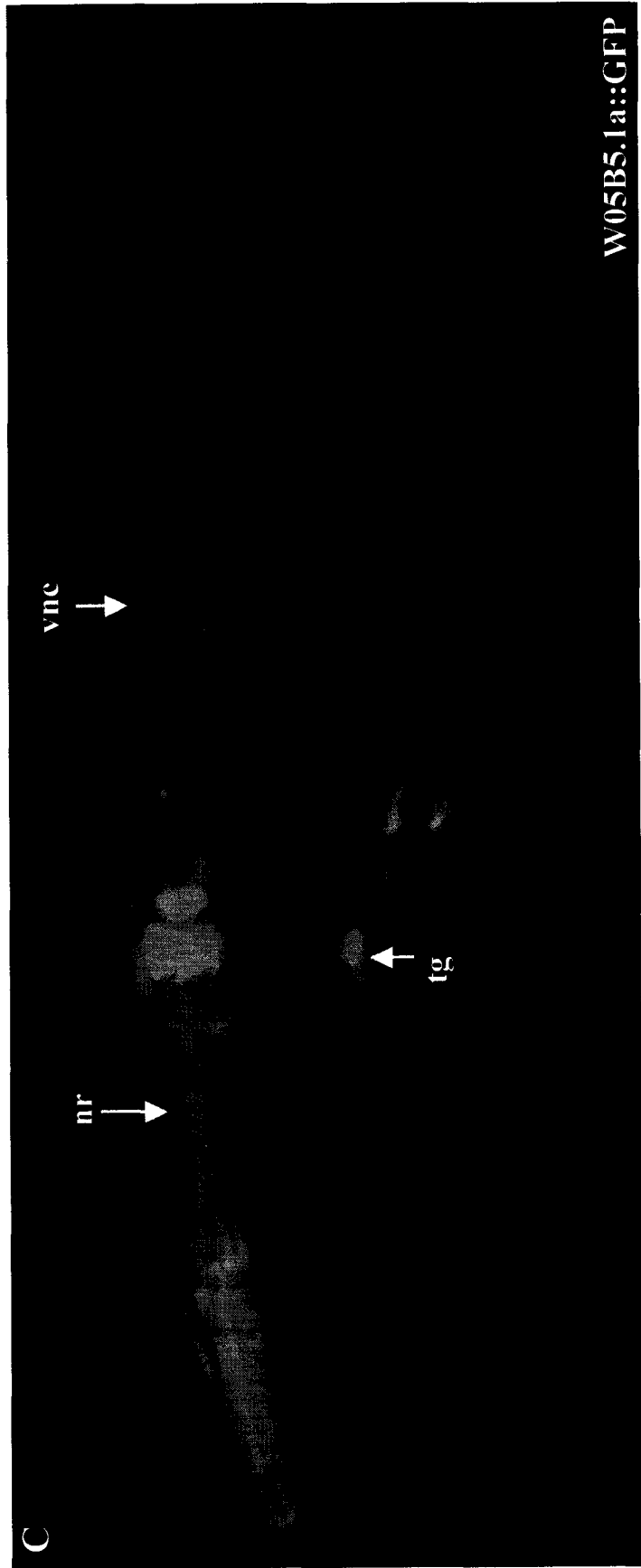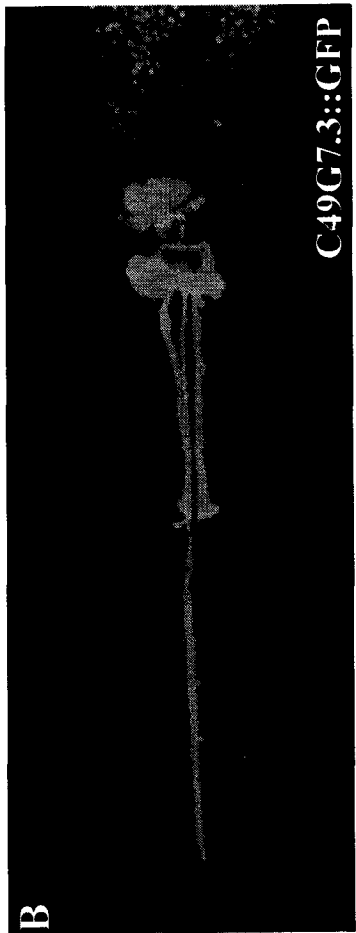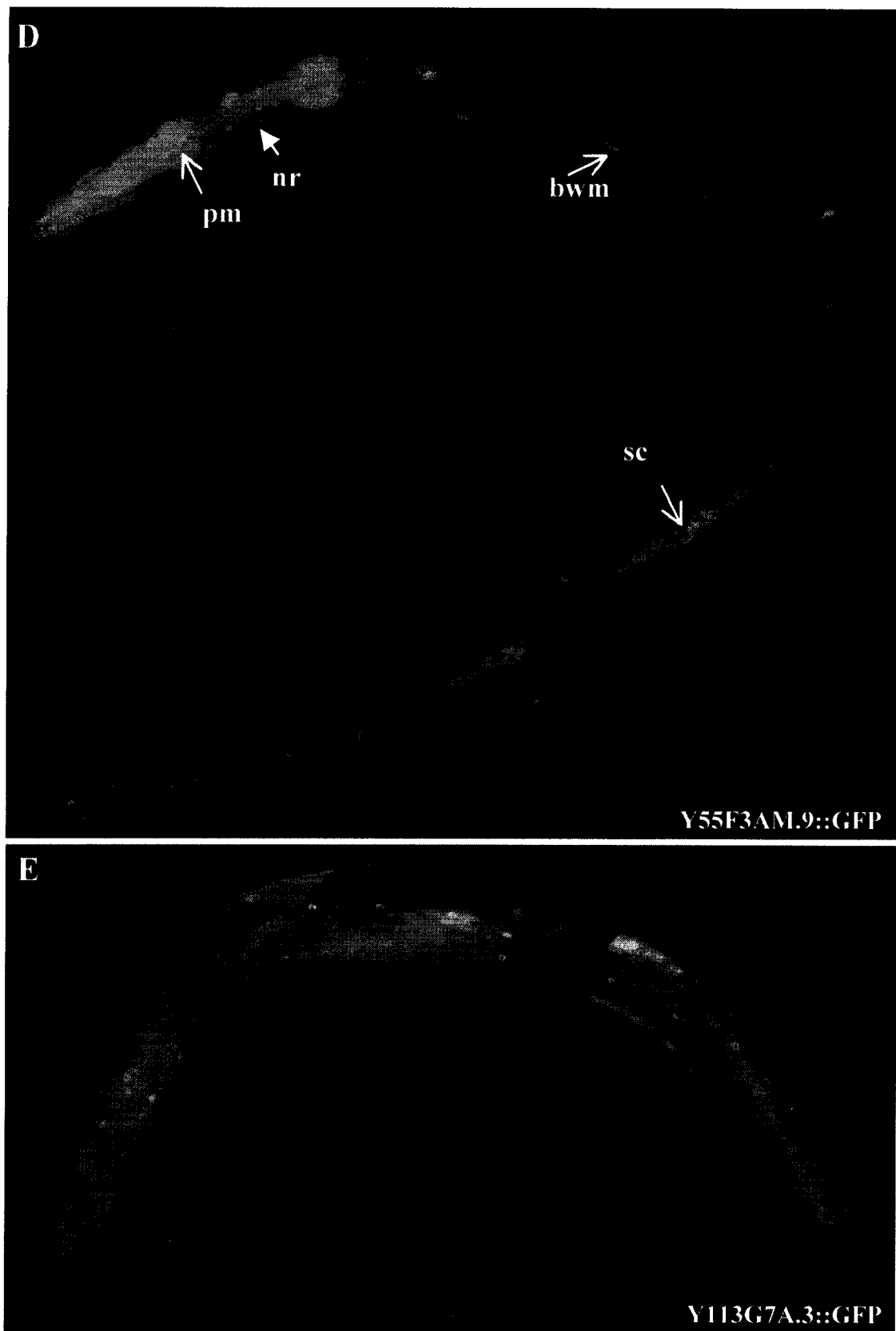*Figure 3.20 (Continued on following pages)*

86

B C49G7.3::GFP

C W05B5.1a::GFP

vnc →

nr →

tg ←

Figure 3.20 (Continued)

87

D

pm
nr
bwm

sc

Y55F3AM.9::GFP

E

Y113G7A.3::GFP

Figure 3.20 (Conclusion)

88

Finally, I wanted to see if there was any discernable phenotype for the yeast 2-hybrid positives. As there are no mutations available in any of them, I used RNAi to try to knock down their expression. I tried RNAi both through feeding and injection of dsRNA. Of the five positives, only Y113G7A.3 (*C. elegans* Sec23) showed a phenotype. Worms fed with bacteria expressing double stranded Y113G7A.3 RNA quickly become sterile. On average, adult worms manage to lay 5-6 embryos before egg production ceases and the few progeny that are produced die as embryos or young larvae. This embryonic lethality has been proposed to result from a failure in cuticle synthesis (Roberts *et al.*, 2003).

The wild-type RNAi phenotype observed for C02F5.7, Y55F3AM.9, and Y113G7A.3 agrees with results from a genome-wide feeding RNAi screen recently published by Kamath *et al.* (2003). RNAi targeted against W05B5.1 has also been reported to produce a wild-type phenotype when worms are soaked in double stranded RNA (Maeda *et al.*, 2001). These reports agree with my results from injecting worms with dsRNA, suggesting that either the wild-type RNAi phenotype is genuine or these genes are poor targets for RNAi. There are no published reports of RNAi against C49G7.3.

3.7 Antibody Production and Purification

I have produced antibodies against PDL-1 peptides and full-length PDL-1. Peptide antibodies were raised against two peptides C27R7E18 (RHQDSKLSEKAE) and C27K79K92 (KIEKFRLEQRVYLK) coupled to keyhole limpet hemocyanin while the holoprotein antibody was raised against insoluble His_6::PDL-1.

Dot blots using sera from 9B1, 9B3, 9B6, and 9B8 show that all four rabbits mounted an immune response against their respective KLH conjugated peptides (Figure 3.21). However, in a western against recombinant His_6::PDL-1, the protein is only recognized by the antiserum from rabbit 9B3 (Figure 3.22). The discrepancy between the dot blot and the western suggests that 9B3 is the only rabbit that mounted an immune response against the coupled peptide; the remaining rabbits mounted immune responses against the carrier protein KLH. The holoprotein antisera were tested for immunoreactivity against

89

recombinant GST::PDL-1 instead of His_6::PDL-1 to eliminate reactivity against the His_6 tag and its linker. Both 9AG1 and 9AG4 sera react strongly against GST::PDL-1 as shown in Figure 3.23. All antisera were tested for immunoreactivity against N2 lysate, but no band could be identified as PDL-1 (data not shown).

| 9B1 preimmune | 9B1 bleed 2 | 9B3 preimmune | 9B3 bleed 2 | 9B6 preimmune | 9B6 bleed 2 | 9B8 preimmune | 9B8 bleed 2 |

Spotted with 1 μg peptide
C27R7E18 conjugated to KLH

Spotted with 1 μg peptide
C27K79K92 conjugated to KLH
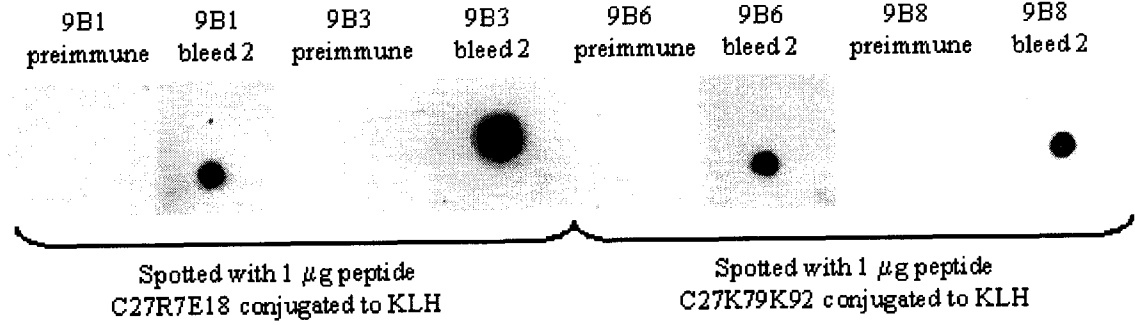
Figure 3.21 Dot blot to test immunoreactivity of anti-peptide sera. All sera were used at a dilution of 1/500.

←—His6::PDL-1—→
~24 K

A

B

Figure 3.22 Testing peptide antisera for reaction with PDL-1. (A) Peptide antisera tested for immunoreactivity against recombinant His6::PDL-1. All sera were used at a dilution of 1/500. (B) Testing titer of 9B3 immunoserum against His6::PDL-1. Serum was used at a dilution of 1/1000-1/5000 as indicated.

90

Lane labels (left to right): 1/1000 9AG4 pre-immune | 1/1000 9AG4 bleed 3 | 1/10,000 9AG4 bleed 3 | 1/5000 9AG4 bleed 3 | 1/2500 9AG4 bleed 3 | 1/1000 9AG1 pre-immune | 1/2500 9AG1 bleed 2 | 1/10,000 9AG1 bleed 2

M_R x1000
220
97
66
46
30
21.5
14.3
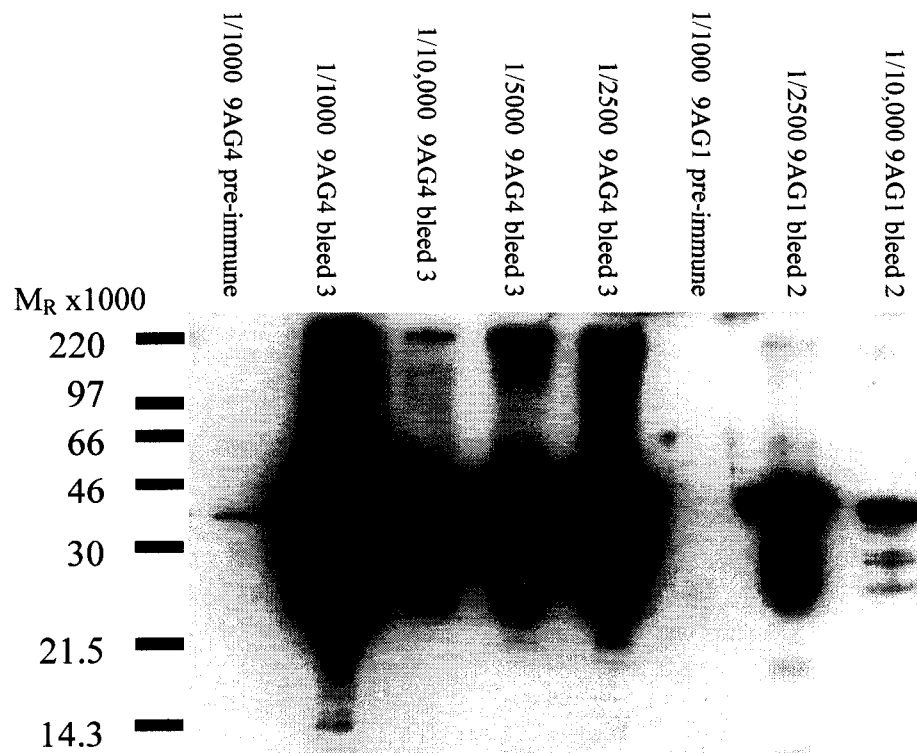
Figure 3.23   Testing holoprotein antisera for reaction with PDL-1. Antisera 9AG4 and 9AG1 were tested for immunoreactivity with lysate produced from *E. coli* expressing recombinant GST::PDL-1. Sera were used at dilutions of 1/1000 – 1/10,000 as indicated.

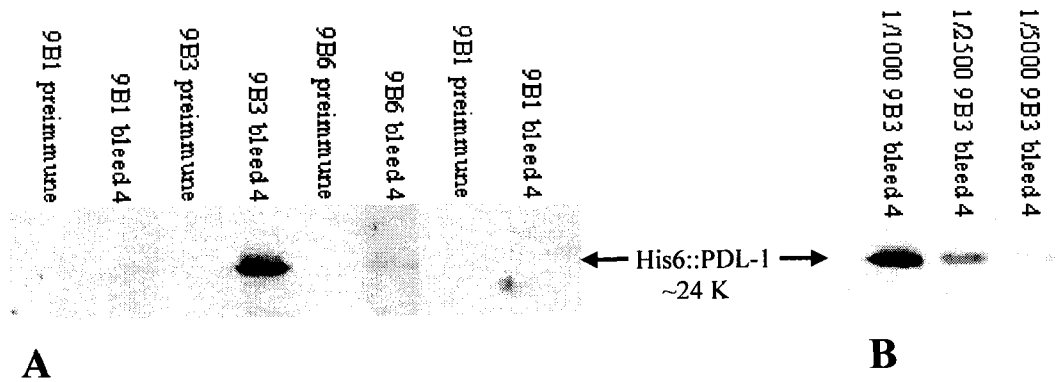Since the antiserum from 9AG4 showed the highest titer and reactivity against recombinant PDL-1, I purified this antibody on a GST::PDL-1 affinity column. The purified antibody reacts strongly against recombinant PDL-1 but does not detect a band in worm lysate (data not shown). This may be due to poor lysate quality or a failure of the antibody to recognize the native PDL-1 protein. To rule out these possibilities, I overexpressed PDL-1 in *C. elegans* under control of a heat shock promoter. I prepared lysate from heat shocked worms and ran the lysate on a western. The purified 9AG4 antibody detects a band of the appropriate size in these worms, suggesting that my inability to detect PDL-1 is likely due to low abundance of this protein in *C. elegans*.

91
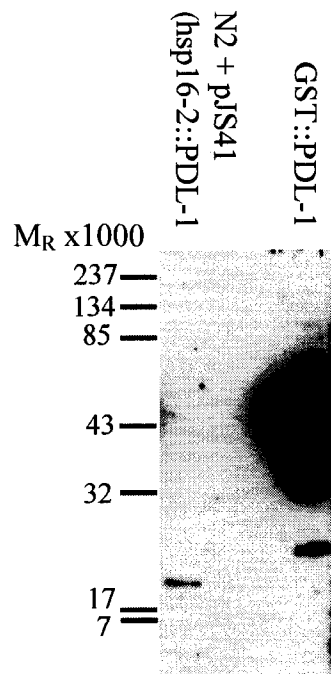
Figure 3.24   Western analysis of worms expressing *pdl-1* cDNA under control of a heat shock promoter. A lane with recombinant GST::PDL-1 was included as a positive control. Primary antibody was a 1/500 dilution of affinity purified 9AG4.

Knowing that the purified 9AG4 antibody is able to detect PDL-1 on a western blot I have tried immunostaining with this antibody in *C. elegans*. Unfortunately I have been unable to visualize any staining in my attempts.

Part 2: Zebrafish

3.8 Identifying PDEδ in zebrafish

I used TBLASTN to search the zebrafish EST and genomic databases for PDEδ sequence. I identified the genomic sequence for exons 2-5 in the WGS traces database and this sequence has subsequently been made available in the HTGS database as well. The EST database contains one EST (accession number AI722600) that appears to correspond to PDEδ. I designed nested primers and attempted to amplify this sequence from zebrafish cDNA. Despite repeated attempts, I was never able to amplify a PCR product using these primers. My lack of success raised suspicions that there may be something wrong with the EST sequence provided in the database. This suspicion was

92

heightened by the fact that there is no sequence in the genomic database that corresponds to the EST. Finally, phylogenetic analysis (Figure 3.25) shows that the EST sequence is more closely related to invertebrates than it is to mammals or rainbow trout. I suspect that the EST is a result of parasite contamination and does not reflect a genuine zebrafish PDEδ sequence. There are currently no ESTs in the zebrafish database that correspond to the genomic sequence of zebrafish PDEδ.
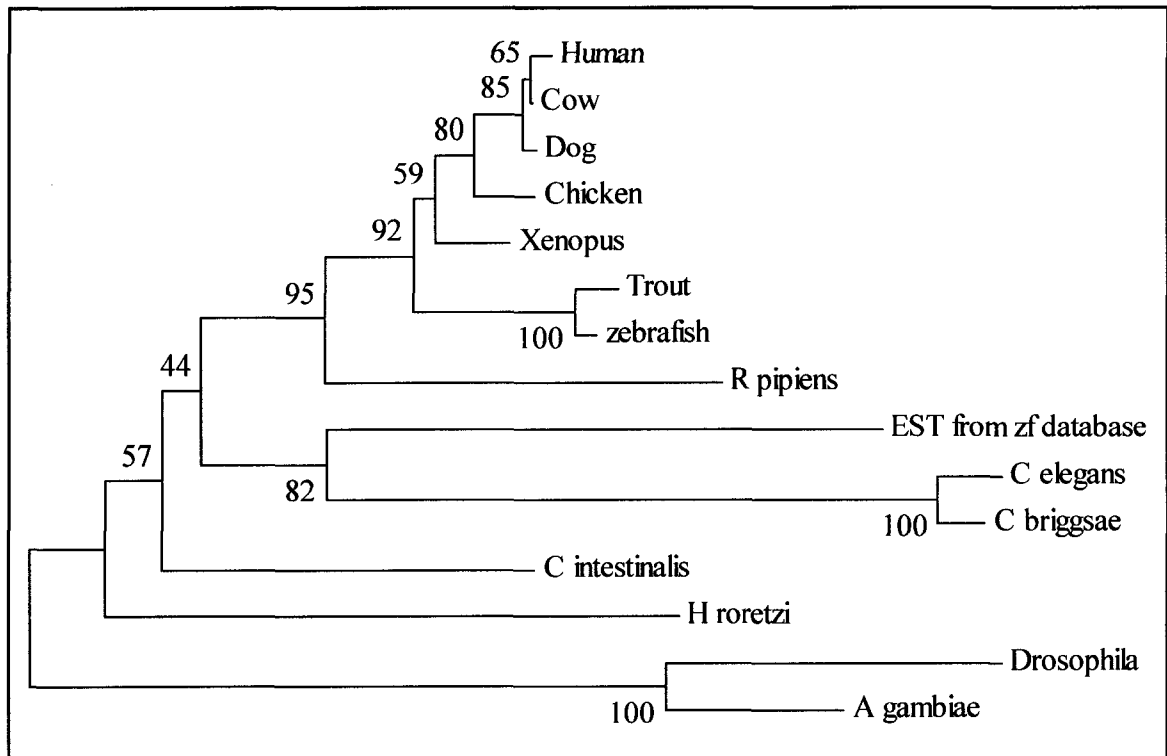
Figure 3.25   Phylogenetic tree constructed using predicted PDEδ protein sequences from different species. The translated cDNA sequence from the zebrafish database (accession number AI722600) is designated "EST from zf database". Tree was drawn using the MEGA 2.1 program, available at **www.megasoftware.net**, using the neighbour joining method with Poisson correction. Numbers indicate bootstrap values after 1000 replications.

Since I had no useful EST information, I used the genomic sequence of PDEδ to design primers against exons 2 and 5. I used these primers to amplify an RT-PCR product from 72 hpf cDNA as well as an adult cDNA library. I had no difficulties amplifying cDNA sequence using these primers. Unfortunately, I still lacked sequence for exon 1. Through further database searches I was able to find the peptide encoded by exon 1 of pufferfish (*Fugu subripes*) PDEδ. I used this peptide sequence to search the zebrafish genomic

93

database and was able to find the exon 1 sequence that I had been lacking. This had been difficult to find as it is a small 51 bp exon followed by a 9.4 kb intron. Fortunately the peptide sequence is identical to that of *Fugu*. The genomic structure of zebrafish PDEδ is diagrammed in Figure 3.26.
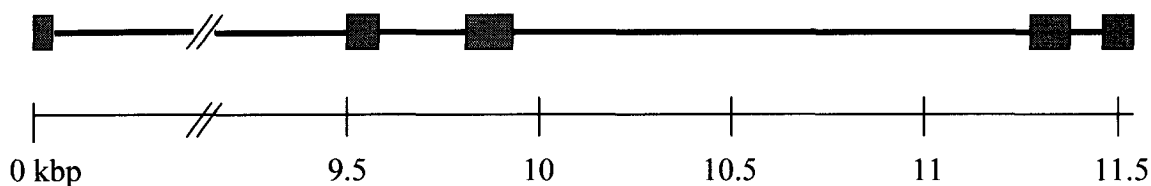
Figure 3.26   Genomic structure of zebrafish PDEδ. Shaded boxes indicate exons while lines represent introns. All exons and introns are drawn to scale except for intron 1.

Using the expanded genomic sequence, I designed primers against the presumptive UTRs and amplified the entire coding region of PDEδ from cDNA. I cloned this PCR product into pGEMT and sequenced a number of clones to look for error-free constructs. In so doing, I discovered that there are two transcripts that differ by four point changes. One agrees with the genomic prediction and my previous cDNA clone while the other three have four base changes in common. I translated the "new" cDNA *in silico* and discovered that three of the point mutations are silent while the fourth results in a F92Y amino acid change. These point changes are unlikely to represent reverse transcriptase or Taq induced errors as the same point changes were present in several independent clones. I therefore wondered whether these differences reflect polymorphism or a duplication of PDEδ in the zebrafish genome. The sequence of the cDNA is shown in Figure 3.27 and a translation of the cDNA sequence is shown in Figure 3.28.

94

ttccatctgctgaagctgaacatcaaggaaaaagATGTCTTCGGACGAAGACAGAGCGAAGGAGA
TTCTGAAGGGGTTTAAACTAAACTGGATGAATCTTCGAGATGCTGAGACAGG
GAAGGTTCTCTGGCAGGGGAC(C/T)GAAGACCTCTCTCTTCCTGGGGTAGAAC
A(T/C)GAAGCTCGAGTTCCTAAGAAGATCCTCAAATGTAAAGCTGTCTCCAGA
GAGCTGAATTTCTCTTCAGTAGAAAAACTGGAAAAATTC(C/A)GACTGGAGCA
GAAAGTTT(T/A)CTTTAAAGGCCAGTGCCTAGAAGAGTGGTTTTTTGAGTTTG
GCTTTGTGATTCCTAATTCAACAAACACATGGCAGTCTTTGATAGAAGCCGCA
CCAGAGTCACAGATGATGCCTGCAAATGTCTTAACTGGTAATGTTGTTATAGA
GACCAAGTTTTTTGATGACGACCTTCATGTCAGCACATCCCGGGTACGACTCT
TCTATGTCTGAgacatggtacctttcttcctctttttttttctttttttttttttttttttttactgtcactccggaggatggacccatcacta
caagagaggagatgctcgtcatattgagtatttcttctaagatgctgtaaaaacggcatgaaagggattatttcaataaaacccagtt
ttgacacaaacggtcacaccagttttatggcagaaaaagacttgtacataagagctctcatgctcatgactacctggttgtgtaaaa
tacctgtttgtatatgttcttttttcttcttctataattcaatcctgcaatgtacactgcttccttttcagctctttttaaaaggttttctcccagtc
tgtggtcattcatggtctttttttttttagttaaactgtaagataggctgtgttttaaaaataaatgatgtaattaattaaaaaaaaaaaaaaaaa
aaaaaaaaaaaa

Figure 3.27   Known sequence of zebrafish PDEδ cDNA. This does not include the complete 5' UTR. The coding region is indicated in upper case with polymorphisms shown in brackets. The polymorphism which causes the F92Y amino acid change is underlined.

Figure 3.28   Translation of zebrafish PDEδ cDNA and comparison to *C. elegans* PDL-1. Black shading indicates amino acid identity while grey shading indicates similarity.

To determine whether the base changes in the cDNA sequence result from polymorphism, I amplified exons 2-5 of PDEδ from genomic DNA. I sequenced three clones and found that they differed by approximately 2% at the nucleotide level. Significantly, the introns were very well conserved suggesting that the changes are due to polymorphism within the genome rather than duplication and subsequent divergence of the gene. Additionally, there is no evidence for a second PDEδ in any of the zebrafish genomic databases. To confirm that there is only one copy of PDEδ in the zebrafish genome, I used PDEδ cDNA to probe a zebrafish genomic Southern blot at low stringency. NotI and PvuII, which are not predicted to cut within the genomic sequence

95

of exons 2-5 show a single band suggesting that there is only one copy of PDEδ (Figure 3.29).
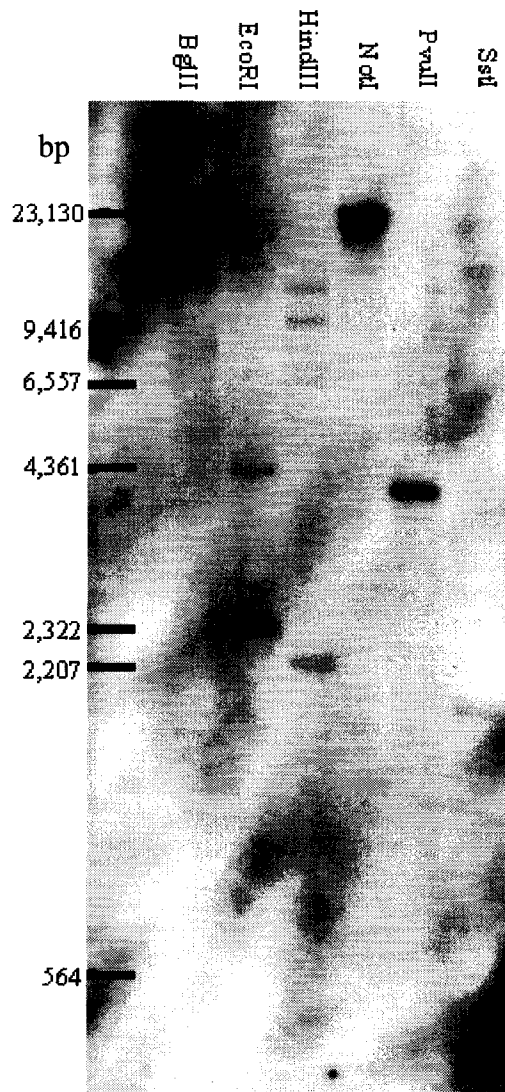

Figure 3.29   Low stringency Southern to determine copy number of PDEδ in zebrafish. The blot was probed with full-length drPDEδ cDNA. Note that NotI and PvuII show a single band, suggesting that there is a single copy of PDEδ in the zebrafish genome.

3.9 Expression of PDEδ in zebrafish

3.9.1 Transcript Analysis

I wanted to determine the PDEδ transcript size and expression profile using northern analysis. Unfortunately, the loading of the lanes was very uneven making most of the lanes uninformative. However, the blot does provide a transcript size as there is a single transcript of approximately 1.15 kb in the oocyte and adult lanes, both of which were grossly overloaded (Figure 3.30). Obviously this blot is not useful for determining the expression profile due to the uneven loading and the seemingly low abundance of the transcript. I would have repeated this experiment but this blot suggests that northern analysis is likely not sensitive enough to reliably detect PDEδ at different developmental stages.
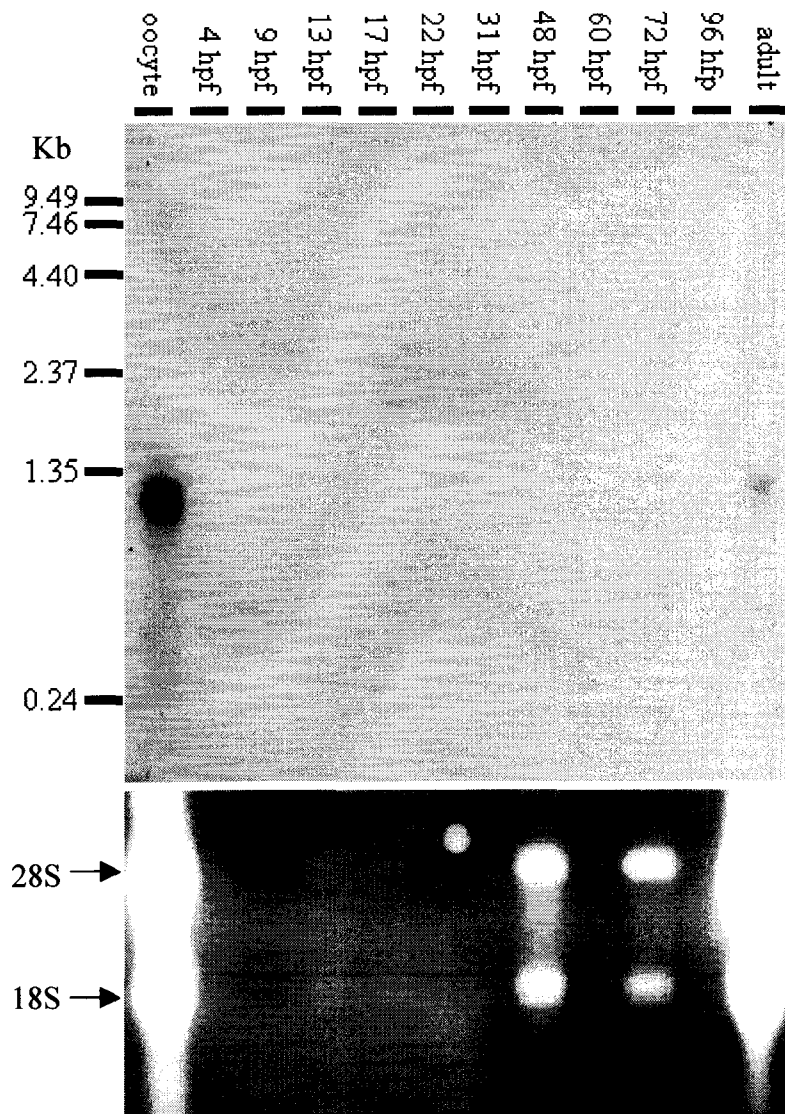
97

Figure 3.30 Zebrafish developmental northern blot probed with PDEδ cDNA. Lanes were loaded with total RNA from a variety of developmental stages as indicated.

To address this problem, I performed RT-PCR on cDNA from embryos of various stages using PDEδ specific primers. This technique is more sensitive than northern analysis and shows that there is transcript present in all stages tested (oocyte, 6, 12, 24, 36, 72, and 100 hpf) (Figure 3.31). I have also successfully amplified PDEδ from adult cDNA (data not shown) suggesting that PDEδ is expressed at many if not all developmental stages.
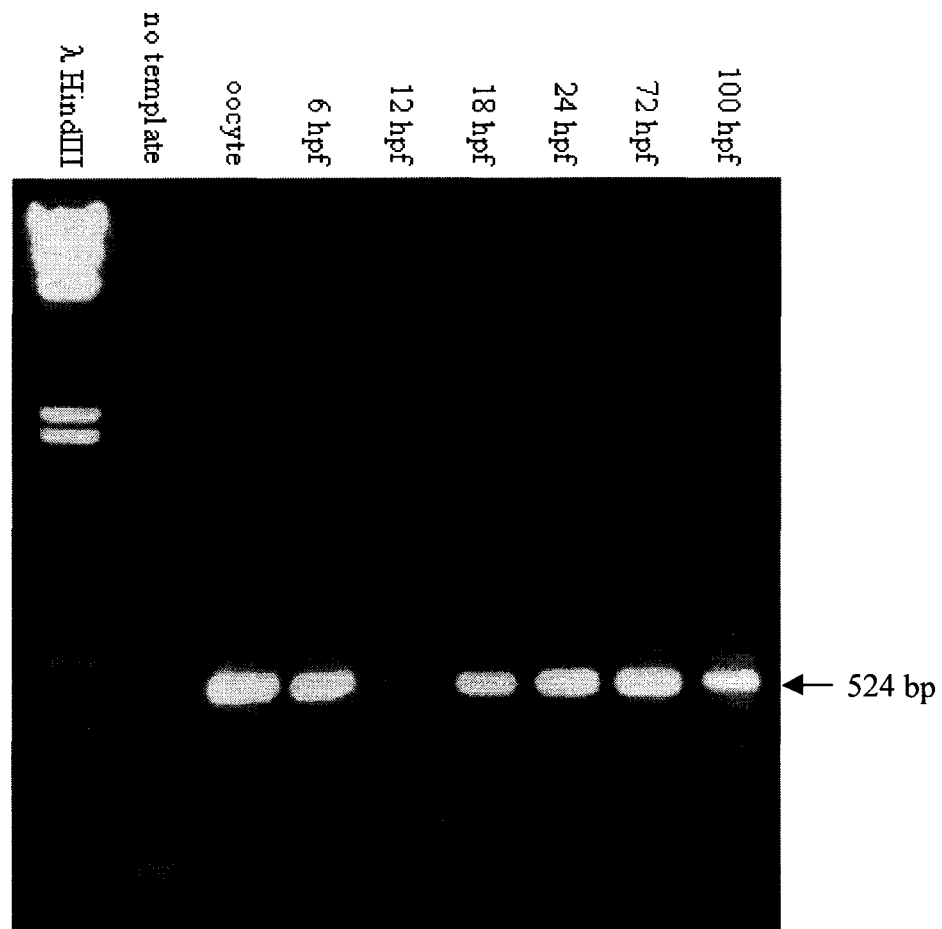
98

Figure 3.31 RT-PCR to determine the developmental expression profile of PDEδ in zebrafish embryos. cDNA was prepared from a variety of stages as indicated.

3.9.2 Protein Expression

I also wanted to determine whether the PDEδ protein is produced. Given the conservation between *C. elegans* PDL-1 and zebrafish PDEδ, it seemed reasonable to suspect that the polyclonal antibody I raised against PDL-1 would cross-react with the zebrafish protein. I used purified anti-PDL-1 to probe a embryonic zebrafish developmental western. A band of the appropriate size is present in 2-4 and 36-72 hpf embryo lysates while lysates from 6-31 hpf show either a low abundance or absence of the protein (Figure 3.32).
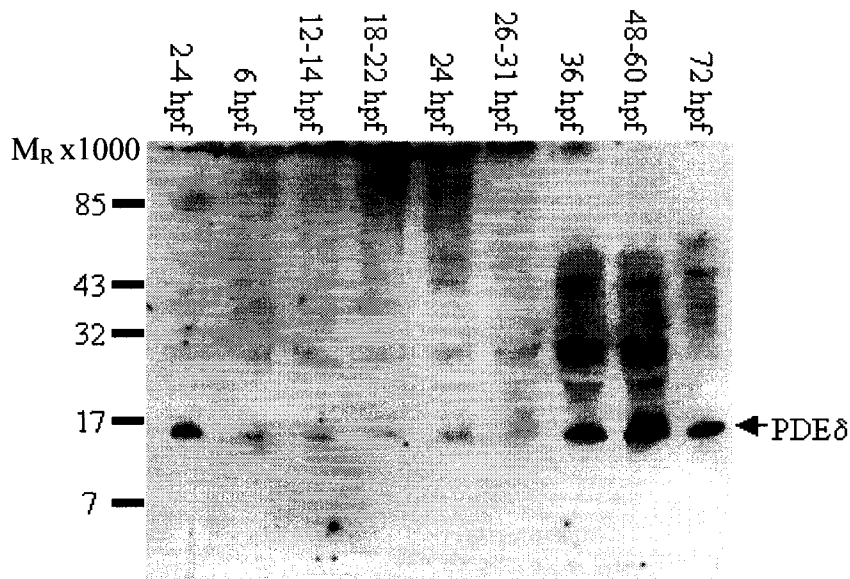
Figure 3.32   Developmental western on zebrafish embryo lysate. The blot was probed with polyclonal antibody raised against worm PDL-1. Arrow indicates the expected size of zebrafish PDEδ. The film is shown after overnight exposure resulting in high background, especially in the 36 and 48-60 hpf lanes.

3.9.3 In situ Staining

Finally, I wanted to determine the expression pattern of PDEδ in zebrafish embryos. I did this by *in situ* staining using the PDEδ 3'UTR as a probe. The staining pattern does not highlight any particular structures. Rather, there appears to be low-level staining throughout the embryo (Figure 3.33). A control *in situ* with UNC-45 shows robust staining in the heart and somites, showing that the weak staining for PDEδ does not reflect a failure to permeabilize or prepare the embryos correctly.
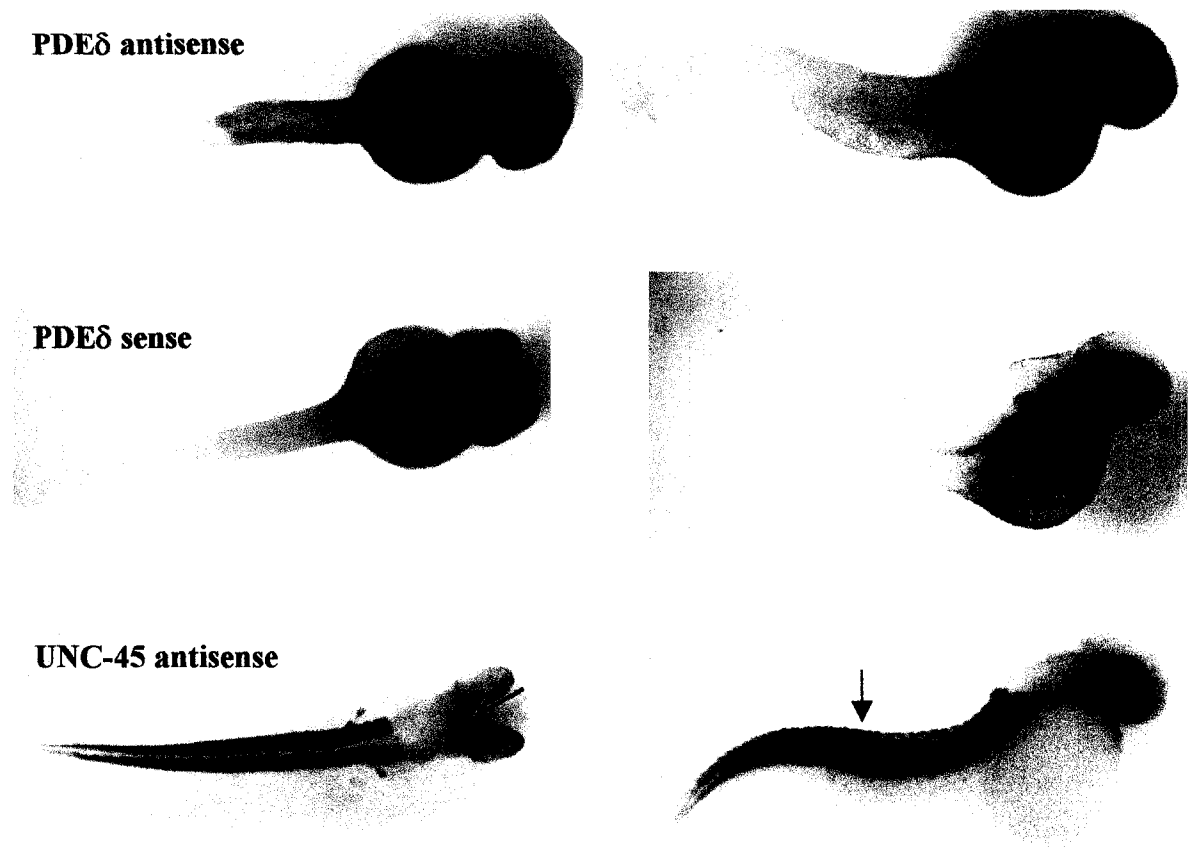
100

Figure 3.33 *In situ* staining on 48 hpf *nacre* embryos. The *nacre* mutation suppresses body pigmentation but does not affect pigmentation in the eyes. Both PDEδ probes were developed overnight while the UNC-45 probe was developed for 30 minutes. (A) Embryos probed with a PDEδ antisense probe. Staining appears to be ubiquitous. (B) Control embryos probed with a PDEδ sense probe to show background level of staining. (C) Positive control embryos probed with UNC-45 antisense probe. Staining is visible in the heart and somites (open and closed arrows respectively).

3.9.4 Immunostaining

I have tried staining zebrafish embryos with the polyclonal antibody raised against full-length PDL-1. The purified antibody cross-reacts with a band of the appropriate size on a zebrafish western blot (Figure 3.31), suggesting that it could be used for immunostaining in fish. I have tried different fixation techniques (paraformaldehyde and trichloroacetic acid) as well as different visualization techniques (fluorescence and DAB staining) but have been unable to identify a staining pattern (Figure 3.34). It is possible that there is low-level ubiquitous staining but that is almost impossible to distinguish from non-specific background.
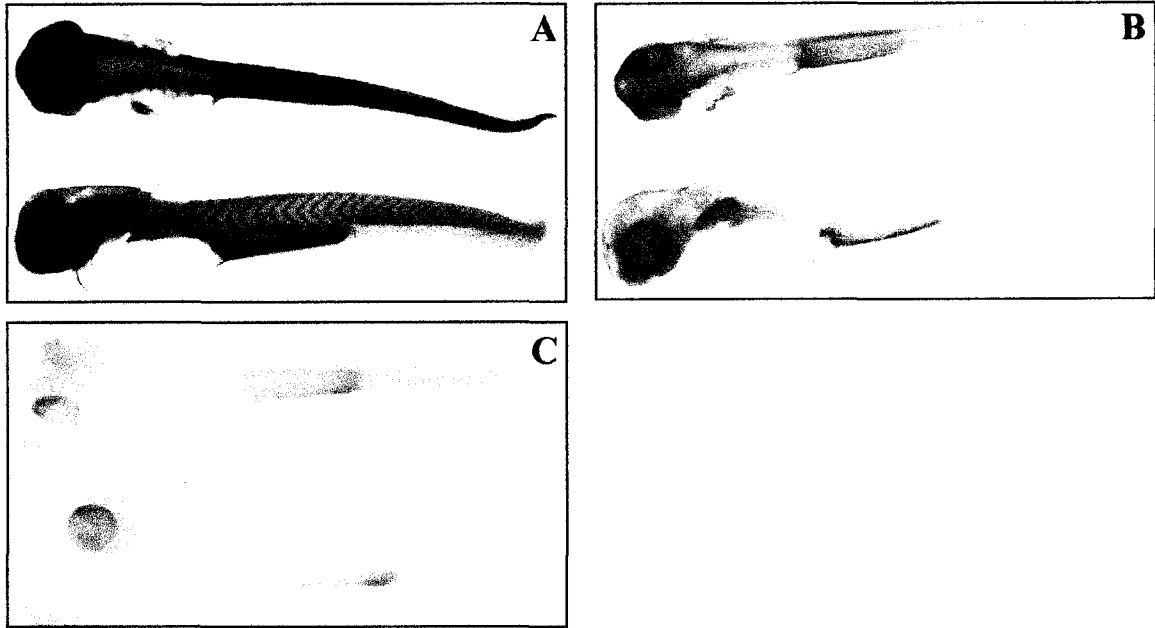
101

Figure 3.34 Immunostaining on 48 hpf wild-type embryos. Embryos were treated with PTU to suppress pigmentation. (A) Embryo stained with anti-FAK (focal adhesion kinase). Staining is visible at somite boundaries. (B) Embryo stained with anti-PDL-1. (C) Embryo stained without any primary antibody. All images were collected using the same exposure settings.

3.10 Phenocopy by morpholino injection

In order to determine the knockdown phenotype of PDEδ in the zebrafish, I ordered morpholino antisense oligonucleotides directed against the start codon ("zfdelta real ATG") and the exon 2 splice donor ("zfdelta ex2don") (Figure 3.35). Morpholinos have been shown to knock down expression of zebrafish genes required early in development (Nasevicius and Ekker, 2000). Start-site directed morpholinos inhibit translation initiation while splice-site directed morpholinos prevent splicing at the targeted location. Both techniques have been shown to phenocopy known mutations (Nasevicius and Ekker, 2000; Draper *et al.*, 2001).
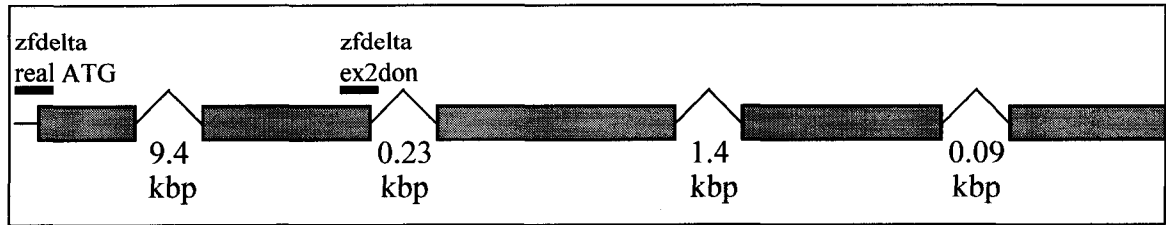
102

Figure 3.35   Location of anti-PDEδ morpholino oligonucleotides "zfdelta real ATG" and "zfdelta ex2don" relative to the genomic sequence of PDEδ. Exons are drawn to scale but introns are not. Approximate intron sizes are provided in kbp.

I have injected embryos with both the ATG and exon 2 splice donor morpholinos at a concentration of 1 and 5 mg/ml (approximately 2.5-25 ng of morpholino administered per embryo). Neither oligo resulted in an observable phenotype in embryos up to 48 hours after injection. I wanted to know whether the technique was working so I isolated RNA from 20 embryos injected with "zfdelta ex2don" and tested for inclusion of intron 2 by RT-PCR. Intron 2 contains an in-frame stop codon and the incorrectly spliced transcript should result in truncation of PDEδ.

The RT-PCR results show that "zfdelta ex2don" is able to disrupt splicing but the inhibition is incomplete. Since small PCR products tend to outcompete larger ones, it is difficult to compare the two bands to determine what fraction of transcripts are incorrectly spliced. However, it is possible to get a conservative estimate of the morpholino efficiency in this way. Based on the PCR results, roughly 30-35% of transcripts are affected by the morpholino (Figure 3.36). I performed RT-PCR on embryos injected with "zfdelta real ATG" and a morpholino designed against the "invertebrate EST" in the zebrafish database. As the EST does not appear to exist in zebrafish, this is effectively a random sequence morpholino that can be used as a negative control for both morpholino toxicity and defects caused by the injection process. These controls confirm that the process of morpholino injection does not cause incorrect splicing of the transcript and that this effect is a specific result of the "zfdelta ex2don" injection.

103

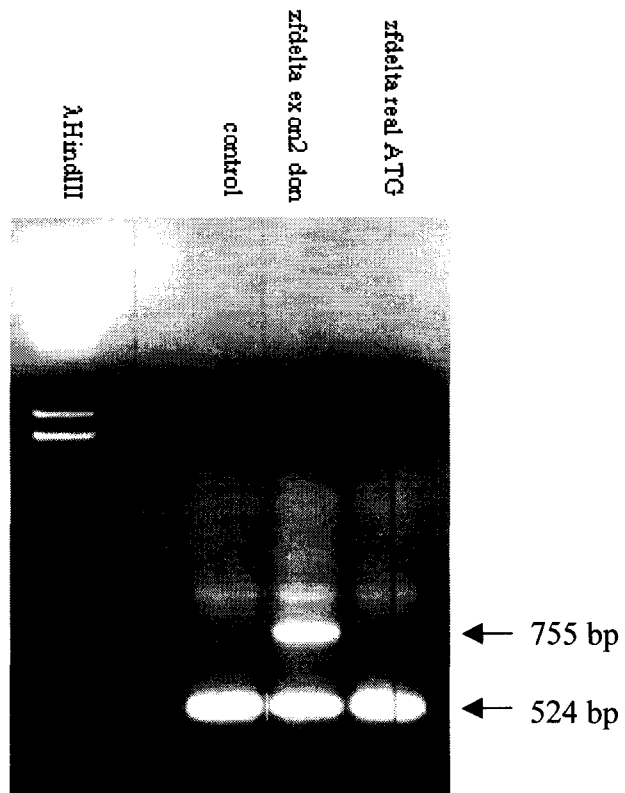**Figure 3.36** RT-PCR on cDNA prepared from embryos injected with antisense morpholino oligonucleotides. Morpholinos were injected at a concentration of 1 mg/ml. The control lane is RT-PCR on cDNA prepared from embryos injected with "zfdelta" morpholino (effectively a random sequence morpholino). The 524 bp band represents the expected size of the PDEδ cDNA while the 755 bp band includes intron 2.

104

Discussion

4.1 Conservation of PDEδ

Using cDNA and genomic sequences, it is possible to predict the PDEδ amino acid sequence in a wide variety of metazoans. Prediction is assisted by the fact that PDEδ is very highly conserved across species, showing strong divergence only in its amino-terminal 7-19 amino acids. The remaining 140 amino acids show 75% similarity across all species for which PDEδ sequence is available. With the exception of the amino terminus, the sequence similarity is distributed more or less evenly over the length of the protein.
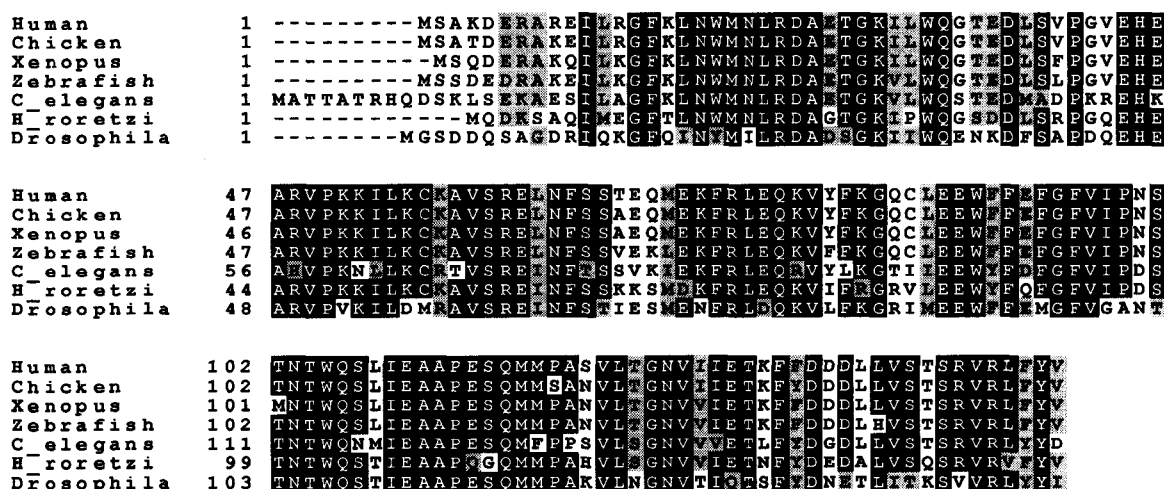
Figure 4.1 Comparison of PDEδ proteins across phyla. Black shading indicates amino acid identity while grey shading indicates similarity. 85% of sequences must agree for shading to apply.

The conservation of PDEδ indicates that there has been selective pressure for the maintenance of PDEδ function throughout evolution. Despite this, loss of PDL-1 function in *C. elegans* has no visible effect. While this was initially surprising, robustness against mutation is now known to be a common occurrence (discussed below).

4.2 No-phenotype mutations

There are many cases where gene knockout results in no apparent phenotype. This phenomenon is best documented in the yeast *Saccharomyces cerevisiae*. Systematic gene

105

knockout has been used to create precise deletions of nearly every gene in the *S. cerevisiae* genome. In total, 5,916 open reading frames (ORFs) have been deleted and roughly 60% of these knockouts have no known phenotype (Giaver *et al.*, 2002). A recent study in *S. cerevisiae* compared the effect of knockouts in 1,147 duplicate genes (those with a clear paralogue in the genome) and 1,275 singleton genes (Gu *et al.*, 2003). Deletions in duplicate genes were less likely to be lethal (12.4% versus 29.0% for singletons) and more likely to have little or no fitness effect (64.3% versus 39.5%), suggesting that there is functional overlap between paralogues. However, the proportion of singleton deletions with little or no effect is remarkably high. Assuming that there are no "useless" genes, this robustness against mutation suggests that there is functional redundancy within the genome which is not revealed by sequence similarity. Alternatively, these deletions have fitness effects which are not detrimental under the growth conditions used in these experiments. More likely, a combination of these two factors is responsible for the apparent lack of phenotype exhibited by many singleton deletions.

4.3 Theories of molecular evolution

The neutral theory of evolution, as proposed by Kimura (1968, 1983), suggests that most sequence divergence is driven by mutation and genetic drift rather than by positive selection. In cases where selection applies, it is thought to be predominantly negative selection against deleterious mutations. A modified version of this theory, termed the nearly neutral theory, has also been proposed (Ohta 1973, 1992). This theory suggests that mutations which are only slightly deleterious (nearly neutral) may still be subject to purifying selection within a population. Slightly deleterious mutations would be selected against in a large population but may become established in small populations. Mutations that strongly reduce fitness are lost through negative selection regardless of population size. These theories predict that highly conserved amino acids represent positions where neutral mutations are not possible.

With respect to PDL-1/PDEδ, the neutral and nearly neutral theories of evolution would suggest that most of the amino acids in this protein cannot be changed without some deleterious effect. The negative effects of mutation may be minor at the level of the

106

individual but even slight defects could prevent these mutations from becoming established within a population.

4.4 The relationship between protein conservation and dispensability

It has been predicted that proteins that are essential for survival will evolve more slowly than those that are dispensable (Wilson *et al.*, 1977). Therefore one would expect a highly conserved protein to be important for the fitness of an organism. However there is some debate as to the relationship between protein dispensability and the rate of protein evolution. A study of mouse knockouts of 64 essential genes and 74 nonessential genes showed that the rate of nonsynonymous nucleotide substitution does not correlate with the severity of its knockout phenotype as long as immune system genes are not used in the analysis (Hurst and Smith, 1999). Hurst and Smith (1999) also looked at tissue-specific differences in the rate of protein evolution. They report that neuronal genes show a significantly lower rate of change than genes expressed in other tissues, but the relative rate of evolution between essential and nonessential genes is the same for all tissues.

Independent studies in bacteria and yeast have shown a significant correlation between protein dispensability and evolution rate. Jordan *et al.* (2002) examined protein dispensability in three bacterial species: *Escherichia coli, Helicobacter pylori,* and *Neiseria meningitidis.* In all three species, the rate of nonsynonymous nucleotide substitutions is significantly higher for nonessential genes than for essential genes, indicating that essential genes are more highly conserved. Hirsch and Fraser (2001) looked at 119 non-essential gene deletions in *S. cerevisiae* that show effects ranging from no effect to an intermediate effect on growth rate and compared them to 168 essential gene deletions. The rate of evolution was determined by comparing the yeast genes to their closest *C. elegans* orthologues. This study suggests that proteins that have a discernable effect on the growth rate of yeast evolve more slowly than those that do not. However, an initial comparison of essential and non-essential proteins showed no difference in the rate of evolution. When this analysis was repeated comparing essential proteins to non-essential proteins with low fitness effects, then the essential proteins were

107

found to evolve significantly more slowly. Therefore essential and nonessential proteins with intermediate fitness effects appear to be under similar selective pressure while proteins with mild fitness effects are able to evolve more quickly.

The discrepancy between the results from mouse, bacteria, and yeast prompted Yang *et al.* (2003) to re-evaluate the relationship between protein dispensability and evolution rate. They looked at fitness effects of knockouts in *S. cerevisiae*, using orthologous sequences from a second yeast, *Candida albicans*, to determine the rate of evolution. They looked at a total of 1,864 open reading frames, which they divided into singletons and duplicate genes. Their analysis shows a weak relationship between the fitness effects of gene deletion and the rate of protein evolution. Surprisingly, this relationship is limited to duplicate genes. Duplicate genes with intermediate or strong fitness effects show fewer nonsynonymous nucleotide substitutions than those with mild fitness effects but singleton genes show no correlation between protein dispensability and evolution rate.

There is ongoing debate as to whether dispensable genes evolve more rapidly than genes that have clear fitness effects (Pal *et al.*, 2003; Hirsch and Fraser, 2003). Unfortunately, these studies have all used different organisms, experimental conditions, and criteria. In studying knockout mice, Hurst and Smith (1999) classified knockouts as either essential, those required for viability and fertility, or non-essential. They did not look at a range of fitness effects nor did they have a large sample size (n=138). Jordan *et al.* (2002) analyzed a large number of genes from *E. coli* (n=1886) but inferred some phenotypes from proposed gene function rather than from knockout studies. Finally, Hirsch and Fraser (2001) and Yang *et al.* (2003) looked at *S. cerevisiae* knockouts, but they had significantly different sample sizes (n=287 vs. n=2422) and used different outgroups to determine evolution rates. Because of these differences, it is difficult to say whether the results from these studies can reasonably be compared to one another. However, if there were a strong relationship between the dispensability of a protein and its sequence conservation then one would expect that relationship to be revealed despite changes in methodology.

108

The lack of strong evidence for conservation reflecting protein importance suggests that we do not have a firm grasp on the mechanism(s) of molecular evolution. Assuming that there is negative selection against deleterious changes within a protein, we must carefully consider the way in which we look at protein conservation. Sequence comparisons may be insufficient or misleading. As long as mutations do not adversely affect protein structure or function, there should be no negative selection against them. Proteins with fewer/shorter critical domains or those with greater conformational flexibility ('flexible proteins') should be better able to accommodate amino acid changes than proteins which are made up of many/large critical domains or those that have limited conformational flexibility. Both types of proteins could be essential but the 'flexible proteins' would evolve more quickly at the amino acid level.

If this hypothesis is correct, then PDL-1/PDEδ must have structural requirements that oppose changes in the protein sequence. It is possible that amino acid changes in PDL-1/ PDEδ cause dominant lethal effects. That would help to explain the high degree of sequence conservation exhibited by this protein. It does not explain why PDL-1/PDEδ has been maintained throughout evolution, despite the fact that *pdl-1* knockout worms do not appear to have a phenotype. Maintenance of PDL-1/PDEδ likely results from weak selection against loss-of-function mutants. Alternatively, there may be redundancy within the genome that masks the *pdl-1* mutant phenotype.

A similar example is provided by the H-Ras, N-Ras, and K-Ras signalling genes in mice. Ras was first identified as an oncogene in the rat sarcoma virus and dominant alleles of *ras* were subsequently found to be associated with a variety of human tumours. Mouse knockouts of H-*ras* and N-*ras*, either alone or in combination, have no observable phenotype (Umanoff *et al.*, 1995; Esteban *et al.*, 2001). K-*ras* knockout mice are embryonic lethal (Johnson *et al.*, 1997; Koera *et al.*, 1997). Ras is very highly conserved within mouse (79% identity) and between other model organisms such as *C. elegans* (76% identity). While H-Ras and N-Ras appear to be dispensable, they have a very low rate of evolution, likely due to the fact that most *ras* alleles are dominant lethal. As well, H-*ras* and N-*ras* loss-of-function defects are masked by the presence of K-Ras. A similar

109

situation could apply to PDL-1, only we have yet to determine what its redundant partner(s) might be.

4.5 Nonhomologous redundancy in *C. elegans*

Genetic redundancy is commonly found in eukaryotes. Mutations in redundant genes often do not give rise to a phenotype if genes are knocked out individually but can lead to visible defects when these mutations are combined. Often redundancy arises through gene duplication where two or more closely related genes are present in the genome. These genes may be fully or partially redundant depending on how they have diverged since duplication. For example, *C. elegans* has three *rac*-like genes (*ced-10*, *mig-2*, and *rac-2*) which act redundantly in axon guidance and outgrowth (Lundquist *et al.*, 2001). These proteins are highly conserved yet individual loss-of-function mutations in any of the three genes have little effect. Inactivating more than one of them gives rise to axon outgrowth defects. Such redundancy between paralogues is relatively easy to uncover through targeted knockout as the *C. elegans* genome has been fully sequenced.

Another possibility is that of nonhomologous redundancy. In this case, redundant proteins have similar functions but do not resemble one another at the sequence level. Relatively few examples of nonhomologous redundancy have been identified in *C. elegans*. The best-known example is the synthetic-multivulval (SynMuv) genes (Ferguson and Horvitz, 1989; for review see Fay and Han, 2000). These genes influence vulval cell fate determination in *C. elegans*. There are two separate pathways that prevent epidermal cell precursors from adopting a vulval cell fate. Loss of function in either pathway is insufficient to produce a multivulva phenotype. However, mutants that lack function in both pathways have ectopic vulva formation.

Other examples of nonhomologous redundancy in *C. elegans* include; *mec-8* and *unc-52* (Lundquist *et al.*, 1996); and *fzr-1* and *lin-35* (Fay *et al.*, 2002). MEC-8 is a splicing factor that allows for alternate splicing of certain mRNAs. UNC-52 is an essential component of the extracellular matrix. Certain alleles of *unc-52* are viable in the presence of MEC-8 because exon skipping allows stop codons in exons 17 and 18 to be removed from the transcript (Lundquist *et al.*, 1996). In the absence of MEC-8, these

110

exons are retained and a truncated form of UNC-52 is produced. In the case of *fzr-1* and *lin-35*, the genes are thought to cooperate to control cell proliferation (Fay *et al.*, 2002). Loss of either gene results in a mild phenotype while loss of both genes acts synthetically to cause hyperproliferation of cells. FZR-1 and LIN-35 are thought to co-regulate cyclin levels during G1. In the absence of both FZR-1 and LIN-35, cyclin levels rise and cells precociously overcome G1 arrest.

These examples highlight several mechanisms whereby mutations in nonhomologous genes can lead to synthetic phenotypes. Unrelated genes can be required in converging pathways, as seen for the SynMuv genes; proteins involved in transcript processing may allow for the viability of certain mutant alleles, as seen for *mec-8* and *unc-52*; or nonhomologous proteins may perform similar functions.

4.6 Why doesn't *pdl-1(gk157)* have a phenotype?

There are several possible explanations for this observation:

1.   *Caenorhabditis* has lost the requirement for PDL-1 function but the loss was recent enough that the protein has not had time to diverge.

2.   *C. elegans pdl-1* mutants have a subtle phenotype that was not revealed by the set of assays that I applied.

3.   *C. elegans pdl-1* mutants have a phenotype that is not visible under laboratory conditions.

4.   There is redundancy in the genome that renders harmless the loss of *pdl-1* alone.

4.6.1 Conservation of PDL-1 in Caenorhabditis

A possible explanation for the lack of phenotype observed in *pdl-1* worms is that *pdl-1* is not required in *C. elegans*. Given the conservation of PDEδ across phyla, the requirement for PDL-1 would need to have been lost quite recently for this to be true. A comparison of PDL-1 between the two closely related *Caenorhabditis* species, *elegans* and *briggsae,* suggests that this is probably not the case. Of the eight amino acid

111

differences, five are similar amino acid substitutions. The remaining three are within the N-terminal 11 amino acids, which is the least conserved region of the protein. The pattern of amino acid substitutions suggests that the amino terminus is free to diverge but the remainder of the protein is under selective pressure in *Caenorhabditis*.

```
C_elegans      1  MATTATRHQDSKLSEKAESILAGFKLNWMNLRDAETGKVLWQSTEDMADP
C_briggsae     1  MTTTATRHPDPKMSEKAESILAGFKLNWMNLRDAETGKVLWQSTEDMADP

C_elegans     51  KREHKAHVPKNLLKCRTVSREINFTSSVKIEKFRLEQRVYLKGTIIEEWK
C_briggsae    51  KREHKAHVPKNLLKCRTVSREINFTSSVKIEKFRLEQRVYLKGTIIEEWK

C_elegans    101  FDFGFVIPDSTNTWQNMIEAAPESQMFPPSVLSGNVVVETLFYDGDLLVS
C_briggsae   101  FDFGFVIPDSTNTWQNMIEAAPESQMFPPSXLSGNVVVETLFYDGDLLVS

C_elegans    151  TSRVRLYYD
C_briggsae   151  TSRVRLYYD
```

Figure 4.2   Comparison of PDL-1 between two *Caenorhabditis* species. Black shading indicates identity while grey shading indicates similarity.

This selective pressure is further evidenced by the number of synonymous base pair substitutions. Of the 153 codons that encode conserved amino acids, 57 have synonymous base pair changes. This shows that there has been divergence at the nucleotide level but most of the base pair changes are synonymous. This suggests that there is pressure for maintenance of PDL-1 protein function in *Caenorhabditis* and that the *pdl-1* gene has not become vestigial.

4.6.2 pdl-1 (gk157) May Have a Subtle Phenotype

It is possible that *pdl-1* mutants have a subtle phenotype that was not addressed by the assays I performed. Given the nervous system expression of *pdl-1*::GFP reporter constructs, it seemed reasonable to expect a *pdl-1* deletion to give rise to nervous system defects. However, it is possible that the GFP expression pattern is misleading. There could be a regulatory element missing from the GFP fusion that would lead to either expansion or restriction of native *pdl-1* expression. If *pdl-1* is normally expressed outside the nervous system, then it is possible that *pdl-1* worms show subtle defects in those tissues. Alternatively, *pdl-1* expression might normally be restricted to a subset of

112

neurons. In that case, there may be specific defects in a particular subset of neurons other than the DA/DB motor neurons and the ASI amphid neurons.

Another possibility is that *pdl-1* mutants have a subtle nervous system defect that does not affect nervous system structure. It has been shown that overexpression of PDEδ in mammalian cell culture leads to an overall decrease in the rate of phototransduction (Cook *et al.*, 2001). If PDL-1 has a similar regulatory effect, then it is possible that the kinetics of sensory transduction are altered in a *pdl-1* mutant. Chemotaxis, thermotaxis, and social feeding in *C. elegans* all rely on cGMP signalling (Komatsu *et al.*, 1996; Coates and de Bono, 2002). If PDL-1 interacts with a *C. elegans* cGMP phosphodiesterase in a manner similar to mammalian PDEδ, then *pdl-1* worms may have a minor alteration in their response to environmental stimuli even though they are fully capable of stimulus response. Such a defect would lead to subtle changes in *pdl-1* worms' behaviour and would be very difficult to detect at a phenotypic level. Alternatively, *pdl-1* worms may have subtle memory or learning defects. Without knowing exactly what to look for, it is very difficult to assay for slight changes in *C. elegans* behaviour.

4.6.3 C. elegans in the Lab and in the Wild

C. elegans are commonly found living in soil where they subsist on a diet of bacteria. Isolates of *C. elegans* have been collected from various locations in North America, Europe, and Australia (Fitch and Thomas, 1997). Clearly, the conditions encountered by *C. elegans* in the wild are different from those experienced by their domesticated counterparts. Lab-raised *C. elegans* live in a very stable environment with an abundant and monospecific food supply.

These conditions are ideal for raising large numbers of worms and for maintaining worms with motility or morphological defects. In fact, lab conditions are designed to be as non-selective as possible. Clearly these conditions do not reflect the natural environment of *C. elegans*. Feral *C. elegans* are likely to encounter a variety of environmental influences including temperature fluctuations, predators, droughts, floods, and food shortages. Even

113

when food is abundant, they are likely to encounter a variety of bacteria species that are not present in the lab.

In order to survive and reproduce, *C. elegans* must be able to withstand adverse conditions and respond to their environment appropriately to increase their chances of survival. It is possible that *pdl-1* worms have a behavioural defect that reduces their success. For example, they may be unable to distinguish toxic bacteria from nutritious bacteria. An example of such a defect is shown by the *C. elegans tol-1(nr2033)* mutant. These worms show normal chemotaxis to water soluble and volatile compounds. However, they fail to avoid the toxic bacterium *Serratia marcenscens* (Pujol *et al.*, 2001).

Alternatively, *pdl-1* worms may have a defect in their dispersal response. It is likely that *C. elegans* in the wild spend much of their time as dauer larvae as they probably do not have a constant food supply. *C. elegans* have a set of dauer-specific behaviours that includes crawling upwards, standing on their tails, and waving their heads (Riddle, 1988). These behaviours have been proposed to aid in the dispersal of dauer larvae by allowing them to stick to passing insects. Another dauer-specific behaviour is to seek out novel temperatures whereas adult worms prefer to maintain themselves along isothermal lines (Hedgecock and Russell, 1975). *pdl-1* dauer larvae may have less robust dispersal behaviour than wild-type worms. Although this would be difficult to observe in the laboratory, it would reduce the survival of *pdl-1* mutants in the wild.

I have described two types of behavioural defects that would be detrimental in the wild but innocuous in a laboratory setting. Other defects, such as a failure to sense or avoid predators, are also possible. Behavioural abnormalities seem likely candidates for a *pdl-1* mutant defect as *pdl-1* is expressed throughout the nervous system of the worm. As well, mammalian PDEδ has been shown to influence phototransduction (Cook *et al.*, 2001), indicating that this protein can affect at least one sensory pathway. While *C. elegans* lack photoreceptors, they have highly developed senses of taste and olfaction; it is possible that PDL-1 modulates these processes. The soil ecosystem is highly complex and a failure of *pdl*-1 mutants to navigate that environment successfully may explain the conservation of PDL-1 in *C. elegans*.

114

4.6.4 Redundancy of pdl-1?

A final possibility is that *pdl-1* worms are genuinely wild-type. This does not necessarily mean that PDL-1 is dispensable. There may be redundancy in the *C. elegans* genome that accounts for the lack of phenotype observed in the *pdl-1(gk157)* mutant.

Based on sequence similarity, a possible candidate for redundancy is *unc-119*. However, the nervous system defects characteristic of *unc-119* are not worsened in an *unc-119; pdl-1* double mutant. It is possible that the *unc-119* null phenotype is so severe that it cannot be made worse by loss of *pdl-1*. However there are two lines of evidence that suggest that this is not the case. First, a *pdl-1* mutant heterozygous for *unc-119(ed3)* has a wild-type phenotype. In this case, there is a partial loss of *unc-119* function which could be exacerbated by loss of *pdl-1* but this is not observed. Second, a screen for synthetic lethal mutations has been performed in an *unc-119* null mutant background and several synthetic lethal mutations have been identified (Kathy Bueble, personal communication). This shows that the *unc-119* phenotype can be made worse. Few of the synthetic lethal mutations show any phenotype in the absence of the *unc-119* mutation indicating that the lethality is directly related to loss of *unc-119* function. All of these mutations complement *pdl-1* (Kathy Bueble, personal communication).

As *unc-119* is the only recognizable paralogue of *pdl-1* in the *C. elegans* genome, it is difficult to predict what other genes might have overlapping function. One candidate is *rhi-1*, the *C. elegans* homologue of RhoGDI. Since PDEδ behaves similarly to RhoGDI and has a similar crystal structure, it is possible that there might be functional overlap between these two proteins. Unfortunately RNAi against *rhi-1* yields a wild-type phenotype in both N2 and *pdl-1* worms. It is difficult to say whether the apparent lack of phenotype is genuine or whether *rhi-1* is targeted ineffectively by RNAi. As there are no known mutations in *rhi-1*, it is not yet possible to make a *pdl-1; rhi-1* double mutant.

Without further study, it is impossible to say whether there are genes that share functional redundancy with *pdl-1*. One way to address this would be to perform a screen for mutations that show a synthetic phenotype with *pdl-1*. This could be done using *pdl-1(gk157)* worms carrying a rescuing copy of *pdl-1* on a transgenic array. These worms

115

would be mutagenized and the F2 generation screened for a visible phenotype or lethality corresponding with transgene loss.

If *pdl-1* has a redundant function, it may also be possible to identify dominant alleles of *pdl-1* that have a phenotype. Any dominant alleles of *pdl-1* are unlikely to yield an uncoordinated phenotype as no uncoordinated animals were identified in the F1 screen for *pdl-1* mutations. This suggests that dominant alleles of *pdl-1* could hypothetically be sterile or lethal. Unfortunately, it is impossible to maintain dominant lethal mutations unless they are conditional. It is also difficult to screen for conditional alleles that are specific to a particular locus unless you know exactly what phenotype to look for. It may be possible to create dominant lethal alleles of *pdl-1* using *in vitro* mutagenesis but it would be difficult to establish and maintain transgenic lines. The easiest approach would be to drive a mutant copy of *pdl-1* behind a heat shock promoter to determine whether conditional ectopic expression has deleterious effects.

4.7 Searching for a phenotype in zebrafish

Since the *C. elegans pdl-1* knockout is apparently without phenotype, I turned my attention to a second model system, the zebrafish. I had hoped to use morpholino knockdown to produce a PDEδ phenocopy in fish embryos. As the zebrafish is a more complex organism, I reasoned that it might be easier to produce a phenotype in this system. Unfortunately, I was unable to produce a phenotype by morpholino injection. It seems likely that the morpholinos are unable to thoroughly knock down the wild-type protein levels. RT-PCR on cDNA isolated from embryos injected with a splice-site directed morpholino shows that there is still properly spliced transcript present. This could represent perdurance of maternal transcript or inefficient targeting of nascent transcript.

Another alternative is that zygotic PDEδ is not required during the time when morpholinos are effective. Morpholino knockdown is most effective for the first 48 hours of development (Nascevicius and Ekker, 2000). Western analysis shows that PDEδ protein is maternally provided. Protein levels seem low between 6-31 hpf then high again at 36 hpf and later. It is possible that the increase in protein at 36 hpf represents the

116

onset of zygotic PDEδ production. If this is true, then the maternally provided protein could be sufficient to allow embryos to develop normally to that point. By 36 hpf, morpholinos have lost some of their efficacy. The combined contributions of maternal PDEδ transcript and protein may make it impossible to effectively target PDEδ by morpholino injection.

4.8 Phenotype summary

Despite considerable effort to determine the PDEδ knockout or knockdown phenotype in *C. elegans* and *D. rerio*, I have been unable to discern a phenotype in either species. In the case of zebrafish, it is likely that the morpholino antisense knockdown is simply ineffective at eliminating wild-type PDEδ protein. It is possible that a mutation in PDEδ would produce a phenotype. Unfortunately, there is no easy way to target specific genes in zebrafish and we are not equipped to do a mutagenic screen in fish. Even if we were set up for large scale mutagenesis, it is impossible to know what phenotype to screen for.

In the case of *C. elegans*, it is clear that we have a *pdl-1* knockout. The deletion removes a sizeable portion of the promoter along with exons 1 and 2. Even if transcription and translation were able to occur, the remaining exons encode only the carboxyl terminal 60 amino acids of the 159 amino acid protein. Given the high degree of conservation observed throughout the length of the protein, it seems highly unlikely that the carboxyl 60 amino acids would be sufficient for function. Another possibility is that the UV-TMP mutagenesis used to create the deletion also created a duplication of *pdl-1*. However, Southern analysis clearly indicates that there is only one cross-reacting *pdl-1* sequence in the genome and that it contains the deletion. Therefore, *pdl-1(gk157)* animals carry only a null allele of *pdl-1*. Despite this, they do not appear to have a phenotype. Whether this is due to genetic redundancy or phenotypic subtlety remains to be determined.

Finally, I have searched the human and *Drosophila* databases for mutations that map to the vicinity of PDEδ. Human PDEδ (aka PDE6D) maps to chromosome 2q36-q37. The only disorders that map to this region have been ascribed to other loci. In *Drosophila*, PDEδ (aka CG9296) maps to chromosome 2L 29E3. The nearest P-element insertion is

117

700 bp upstream of the start codon. This insertion disrupts a neighbouring gene that encodes the *Drosophila* homologue of synbindin. The lethality associated with this P-element insertion is most likely due to disruption of the synbindin gene rather than disruption of PDEδ regulation. Therefore, the only known PDEδ mutation is that in *C. elegans* and it is not known whether PDEδ loss of function can produce a visible phenotype in any other species.

4.9 Expression of PDL-1/PDEδ

Reporter constructs show that *pdl-1* is expressed throughout the nervous system in *C. elegans*. Zebrafish *in situs* suggest that PDEδ is expressed ubiquitously at low level in developing embryos. Zebrafish PDEδ is maternally provided at both the transcript and protein levels while *C. elegans pdl-1* comes on early in embryogenesis. Both are expressed throughout life. These expression patterns do not provide us with much information about the role of PDEδ. However, they do suggest that PDEδ plays a nervous system specific role in *C. elegans* while perhaps playing a more general role in zebrafish. The maternal contribution of PDEδ in zebrafish suggests that it is involved in early embryo development. PDL-1 does not appear to be required for nervous system development in *C. elegans* unless there is redundancy built into the system. It is possible that PDL-1 is required for some as yet undetermined aspect of nervous system function.

Interestingly, the expression patterns of *pdl-1* and PDEδ are reminiscent of their respective paralogues *unc-119* and UNC119/UNC119b. Both *pdl-1* and *unc-119* are expressed pan-neuronally in *C. elegans* while PDEδ and UNC119/UNC119b are expressed ubiquitously in early zebrafish embryos (Manning, 1999). While zebrafish UNC119 and UNC119b are ubiquitously transcribed, immunostaining shows more specific localization in a variety of tissues including nerves, muscle, and retina (Angela Manning, personal communication). It is possible that PDEδ protein is more specifically localized than its transcript distribution would suggest. Indeed, this appears to be the case in *C. elegans* as the transcriptional GFP reporter shows wider expression than translational reporters. Unfortunately I have been unable to determine the PDL-1 or

118

PDEδ protein localization using polyclonal αPDL-1. While this antibody works on western blots, it does not appear to work for immunostaining.

It is interesting that UNC119 and PDEδ show such similar patterns of expression in *C. elegans* and zebrafish. Although these proteins do not appear to have overlapping roles, as evidenced by the phenotype of a *pdl-1*; *unc-119* double mutant, they may be involved in similar processes in the different organisms. One way to look at these processes is through the study of protein interactions.

4.10 Protein interactions

Several protein partners have been identified for mammalian PDEδ. By and large, these protein interactions are thought to occur through PDEδ binding the prenylated carboxyl termini of its interacting partners. One effect of this binding is to release the prenylated protein from the membrane in a similar manner to RhoGDI. One exception is the PDEδ interaction with Arl2. PDEδ binds and activates Arl2, but the PDEδ lipid binding pocket remains empty (Hanzal-Bayer *et al.*, 2002). It is possible that PDEδ acts as a bridge between activated Arl2 and a variety of prenylated small GTPases.

I wanted to identify PDL-1 protein partners in *C. elegans* to help us understand the function of PDL-1 and to determine whether PDL-1 acts similarly to PDEδ. I approached this by doing a yeast 2-hybrid screen of a *C. elegans* cDNA library. I identified five predicted proteins that interact with PDL-1 and pulled out a number of other clones that were either backwards or out of frame. The yeast 2-hybrid results suggest that prenylation plays a role in PDL-1 interactions as more than 75% of the interacting peptides have a prenylation signal at their carboxyl terminus. Of the in-frame positives, four have a CAAX box. Unfortunately, the positives identified in my screen are largely uncharacterized and do not shed much light on the role of PDL-1.

Three of the predicted proteins (C49G7.3, W05B5.1a and Y55F3AM.9) are of completely unknown function. C02F5.7 shows similarity to the yeast GRR1 which is part of a ubiquitin ligase complex (Li and Johnston, 1997). C02F5.7 may play a role in targeting proteins for degradation although this gene has not been studied in *C. elegans*

119

and RNAi against C02F5.7 does not produce a phenotype. The only 2-hybrid positive that has any ascribed function is Y113G7A.3. This is the *C. elegans* homologue of Sec23, a component of the COPII coat which is required for transport of vesicles from the ER to Golgi (Barlowe *et al.*, 1994). RNAi against Y113G7A.3 causes sterility in the injected parent and embryonic lethality in the few offspring that are produced. These defects are thought to result from defective protein secretion (Roberts *et al.*, 2003). Of the five interactors identified, only Y113G7A.3 lacks a prenylation signal.

In an attempt to determine which yeast 2-hybrid positives could possibly interact with PDL-1 *in vivo*, I looked at their expression patterns using GFP reporter constructs. All of the reporter constructs showed some degree of nervous system expression indicating that any or all of them may interact with PDL-1. C02F5.7 has the broadest nervous system expression although it may not be completely pan-neural. It is also expressed in body-wall muscles and the intestine. As this gene is predicted to be part of a ubiquitin ligase complex, it likely plays a general role in protein degradation and its broad expression is not surprising. C49G7.3 shows GFP expression limited to the pharyngeal nervous system. These 20 neurons act together to regulate the rhythm and timing of pharyngeal muscle activity, although they are not essential for pharyngeal pumping (Avery and Horvitz, 1989; Avery, 1993). Given its expression throughout the pharyngeal nervous system, C49G7.3 likely influences pharyngeal function and feeding. Both W05B5.1a and Y55F3AM.9 are widely expressed, including expression in some neurons. The function of these proteins is unknown but their expression pattern suggests that they might play a housekeeping role. Finally, Y113G7A.3 is expressed ubiquitously. As this protein is required for exocytic vesicle transport and protein secretion, it too plays a housekeeping role in many, if not all, tissues.

My attempts to determine the regions of PDL-1 required for interaction with the various 2-hybrid positives were inconclusive. Amino acids 77-128 in isolation were sufficient to interact with every positive except for C02F5.7. However, larger portions of the protein that included these amino acids often failed to interact. It is possible that truncated forms of the protein misfold, thereby confusing the results. Y113G7A.3 was the most promiscuous interactor as it interacted with every construct except for amino acids 1-48.

120

This could reflect multiple binding sites on the PDL-1 protein or it could suggest that the Y113G7A.3 interaction is non-specific despite the fact that Y113G7A.3 does not autoactivate nor does it interact with the control protein Snf1.

In an attempt to determine the validity of the 2-hybrid interactions, I swapped the bait and prey vectors to see if the interactions were maintained. Only W05B5.1a and Y113G7A.3 interacted with PDL-1 once the vectors were swapped. However, C02F5.7 and C49G7.3 are the only positives that show an interaction with human PDEδ. As PDL-1 is thought to be functionally conserved with PDEδ (Li and Baerh, 1998) one might expect their protein interactions to be maintained.

Given the conflicting evidence from the yeast 2-hybrid assays, it is difficult to draw any conclusions about the protein partners of PDL-1. Y113G7A.3 seems to have the most robust interaction although it does not interact with hsPDEδ. All five 2-hybrid positives show some degree of expression in the nervous system so all of them could theoretically encounter PDL-1 in the worm. Only Y113G7A.3 has a proposed function.

Since my yeast 2-hybrid screen results were inconclusive, I decided to try directed yeast 2-hybrid with Arl2. This protein has been shown to interact with mammalian PDEδ and its *C. elegans* homologue, EVL-20, has been shown to regulate cytoskeletal dynamics (Antoshechkin and Han, 2002). Furthermore, mammalian Arl2 has been shown to interact with UNC119 (Van Valkenburgh *et al.*, 2001). I wanted to determine whether these interactions are conserved in *C. elegans*. This would lend credence to the idea that these proteins are playing analogous roles in the different systems and that our study of *C. elegans* is more broadly applicable.

Both PDL-1 and UNC-119 show weak interaction with EVL-20(Q70L). The interaction is not sufficient for growth on selective medium but is sufficient for a weakly positive β-galactosidase assay. Both PDL-1 and UNC-119 show stronger interaction with human Arl2(Q70L). This suggests that EVL-20 may not interact with PDL-1 in *C. elegans* or that the interaction is not as robust as in mammals. Although the amino acids which interact with PDEδ are conserved between Arl2 and EVL-20, there may be

121

conformational differences between the two proteins that subtly alter their positions. Alternatively, *C. elegans* EVL-20 may not fold correctly in yeast. Further *in vivo* study is required before the validity of these interactions can be determined.

The strong interaction of PDL-1 with hsArl2(Q70L) confirms that the behaviour of PDL-1 is similar to that of hsPDEδ. Additionally zebrafish PDEδ interacts strongly with hsArl2(Q70L) suggesting functional conservation of this protein throughout a variety of species.

4.11 Conclusions

PDEδ is very highly conserved at the sequence level and there is evidence for functional conservation in the interactions between *C. elegans* PDL-1 and the human proteins PDE and Arl2(Q70L) (Li and Baehr, 1998; this work). As nematodes and mammals separated very early in evolution, there must be considerable selection for the maintenance of PDEδ function. Despite this, the *C. elegans pdl-1* knockout has no apparent defect. It is possible that *pdl-1* worms have some behavioural defect that would threaten their survival in the wild but I have so far been unable to identify such a deficiency. Another possibility is that there is redundancy within the system. I have tested for synergy with *unc-119*, which is the only recognizable sequence homologue of *pdl-1*, but there does not appear to be any functional overlap between these two genes. There may be a functional homologue for *pdl-1* but such a gene has yet to be identified.

My yeast 2-hybrid results suggest that PDL-1 behaves similarly to PDEδ in that it can interact with a number of prenylated proteins. As well, PDL-1 and drPDEδ interact with human Arl2 in the yeast 2-hybrid system, suggesting that they can substitute for hsPDEδ. This implies functional conservation of these proteins and their interacting domains. I had hoped to use *C. elegans* as a genetic model to better understand this function but the apparent absence of a phenotype has made that difficult.

Based on the information currently available, it would appear the PDEδ plays a regulatory role through its interaction with signalling molecules. Whether it does this by removing membrane associated proteins from the membrane environment or through

122

activation of GTP binding proteins such as the Arls is unclear. The function of PDEδ may vary depending on the cellular environment. As *pdl-1* loss of function does not have severe consequences in *C. elegans*, it seems likely that PDEδ interaction acts as a fine-tuning mechanism for signalling. In the case of phototransduction, PDEδ overexpression slows the overall rate of signalling but the effect is mild (Cook *et al.*, 2001). Loss of PDEδ may have an equally mild effect.

Of course, it is difficult to align mild effects with the high degree of conservation exhibited by PDEδ. Conventional wisdom would suggest that PDEδ must play a critical role to be so well conserved. It could be that loss of PDEδ negatively affects behaviour in such a way that would be detrimental in the wild. Clearly, PDEδ is not required for fertility or proper morphology so there must be some other way in which it affects organism survival. Either there is redundancy in the system, or PDEδ acts more subtly than we had anticipated based on its conservation.

4.12 Future directions

My involvement with *pdl-1* has come to conclusion. However, there are questions remaining. First and foremost, is there anything in the *C. elegans* genome that is functionally redundant with *pdl-1*? This question must be addressed for the conservation of this protein to make sense. If there is non-homologous redundancy, then identifying these genes will enhance our understanding of the role of PDL-1. The easiest way to do this would be to perform a screen for mutations that show a synthetic phenotype with *pdl-1*. Secondly, it would be helpful to use co-immunoprecipitation or pulldown to identify further protein partners of PDL-1 and clarify whether PDL-1 plays a similar role to that of hsPDEδ.

It is difficult to say whether we should continue working with zebrafish PDEδ. Without genetic analysis, the study of zebrafish PDEδ is likely to parallel the work being done in mammals. We could study protein interactions using yeast 2-hybrid or pulldowns. This would be useful for confirming the mammalian results but would be unlikely to provide further insights into PDEδ function. It would be worthwhile to raise an antibody against

123

zebrafish PDEδ. While the *C. elegans* antibody recognizes zebrafish PDEδ on a western blot, it does not appear to work for immunostaining. The only vertebrate immunolocalization of PDEδ was performed in retinal tissue but northern analysis of mammalian tissues shows that PDEδ is ubiquitously expressed. Similar ubiquitous expression is evident for PDEδ in zebrafish embryos as shown by *in situ* hybridization. Immunostaining in zebrafish is likely to expand our knowledge of PDEδ localization in a variety of tissues and perhaps provide some insight as to its function.

124

References

Ackley, B.D., Crew, J.R., Elamaa, H., Pihlajaniemi, T., Kuo, C.J., and Kramer, J.M. (2001). The NC1/endostatin domain of *Caenorhabditis elegans* type XVIII collagen affects cell migration and axon guidance. *Journal of Cell Biology*. **152**: 1219-1232.

Albert, P.S., Brown, S.J., and Riddle, D.L. (1981). Sensory control of dauer larva formation in *Caenorhabditis elegans*. **198**: 435-451.

Anderegg, R.J., Betz, R., Carr, S.A., Crabb, J.W., and Duntzell, W. (1988). Structure of *Saccharomyces cerevisiae* mating hormone a-Factor. *Journal of Biological Chemistry*. **263**: 18236-18240.

Antoshechkin, I., and Han, M. (2002). The *C. elegans evl-20* gene is a homolog of the small GTPase ARL2 and regulates cytoskeleton dynamics during cytokinesis and morphogenesis. *Developmental Cell*. **2**: 579-591.

Avery, L. (1993). Motor neuron M3 controls pharyngeal muscle relaxation timing in *Caenorhabditis elegans*. *Journal of Experimental Biology*. **175**: 283-97.

Avery, L. and Horvitz, H.R. (1989). Pharyngeal pumping continues after laser killing of the pharyngeal nervous system of *C. elegans*. *Neuron*. **3**: 473-85.

Bargmann C.I., Hartwieg E., Horvitz H.R. (1993). Odorant-selective genes and neurons mediate olfaction in *C. elegans*. *Cell*. **74**: 515-27.

Bargmann, C.I. and Mori, I. (1997). Chemotaxis and thermotaxis. *C. elegans* II (Riddle, Blumenthal, Meyer & Priess, editors). pp 717-737. Cold Spring Harbor Laboratory Press, Cold Spring Harbor Laboratory, NY.

Barlowe, C., Orci, L., Yeung, T., Hosobuchi, M., Hamamoto, S., Salama, N., Rexach, M.F., Ravazzola, M., Amherdt, M., and Schekman, R. (1994). COPII: a membrane coat formed by Sec proteins that drive vesicle budding from the endoplasmic reticulum. *Cell*. **77**: 895-907.

Bartolini, F., Bhamidipati, A., Thomas, S., Schwann, U., Lewis, S.A., and Cowan, N.J. (2002). Functional overlap between retinitis pigmentosa 2 protein and the tubulin-specific chaperone cofactor C. *Journal of Biological Chemistry*. **277**: 14629-14634.

Bhamidipati, A., Lewis, S.A., and Cowan, N.J. (2000). ADP ribosylation factor-like protein 2 (Arl2) regulates the interaction of tubulin-folding cofactor D with native tubulin. *Journal of Cell Biology*. **149**: 1087-1096.

Brenner, S. (1974). The genetics of *Caenorhabditis elegans*. *Genetics*. **77**: 71-94.

Cassada, R.C. and Russell, R.L. (1975). The dauerlarva, a post-embryonic developmental variant of the nematode *Caenorhabditis elegans*. *Developmental Biology*. **46**: 326-42.

Cen, O., Gorska, M.M., Stafford, S.J., Sur, S., and Alam, R. (2003). Identification of UNC119 as a novel activator of SRC-type tyrosine kinases. *Journal of Biological Chemistry*. **10**: 8837-8845.

Chan, S.S., Zheng, H., Su, M.W., Wilk, R., Killeen, M.T., Hedgecock, E.M., and Culotti, J.G. (1996). UNC-40, a *C. elegans* homolog of DCC (Deleted in Colorectal Cancer), is required in motile cells responding to UNC-6 netrin cues. *Cell*. **87**: 187-95.

Chavrier, P. and Goud, B. (1999). The role of ARF and Rab GTPases in membrane transport. *Current Opinion in Cell Biology*. **11**: 466-475.

Church, G.M. and Gilbert, W. (1984). Genomic sequencing. *Proceedings of the National Academy of Science*. **81**: 1991-1995.

Coates, J.C. and de Bono M. (2002). Antagonistic pathways in neurons exposed to body fluid regulate social feeding in *Caenorhabditis elegans*. *Nature*. **419**: 925-9.

Colavita, A., Krishna, S., Zheng, H., Padgett, R.W., and Culotti, J.G. (1998). Pioneer Axon Guidance by UNC-129, a *C. elegans* TGF-β. *Science*. **281**: 706-709.

Cook, T.A., Ghomashchi, F., Gelb, M.H., Florio, S.K., and Beavo, J.A. (2000). Binding of the delta subunit to rod phosphodiesterase catalytic subunits requires methylated, prenylated C-termini of the catalytic subunits. *Biochemistry*. **39**: 13516-13523.

Cook, T.A., Ghomashchi, F., Gelb, M.H., Florio, S.K., and Beavo, J.A. (2001). The δ subunit of type 6 phosphodiesterase reduces light-induced cGMP hydrolysis in rod outer segments. *Journal of Biochemistry*. **276**: 5248-5255.

Denhardt, D.T. (1966). A membrane-filter technique for the detection of complementary DNA. *Biochemical and Biophysical Research Communications*. **23**: 641-646.

Denholm, C. (2003). Characterization of the UNC-119 family in mammals. M.Sc. Thesis. University of Alberta.

Dickson, B.J. (2001). Rho GTPases in growth cone guidance. *Current Opinion in Neurobiology*. **11**: 103-110.

Dickson, B.J. (2002). Molecular mechanisms of axon guidance. *Science*. **298**: 1959-1964.

Draper, B.W., Morcos, P.A., and Kimmel, C.B. (2001). Inhibition of Zebrafish *fgf8* Pre-mRNA Splicing With Morpholino Oligos: A Quantifiable Method for Gene Knockdown. *Genesis*. **30**: 154-156.

Esteban, L.M., Vicario-Abejon, C., Fernandez-Salguero, P., Fernandez-Medarde, A., Swaminathan, N., Yienger, K., Lopez, E., Malumbres, M., McKay, R., Ward, J.M., Pellicer, A., and Santos, E. (2001). Target genomic disruption of H-*ras* and N-*ras*, Individually or in combination, reveals the dispensability of both loci for mouse growth and development. *Molecular and Cellular Biology*. **21**: 1444-1452.

Farnesworth, C.C., Wolda, S.L., Gelb, M.H., and Glomset, J.A. (1989). Human lamin B contains a farnesylated cysteine residue. *Journal of Biological Chemistry*. **34**: 20422-20429.

Fay, D.S., and Han, M. (2000). The synthetic multivulva genes of *C. elegans*: Functional redundancy, Ras-antagonism, and cell fate determination. *Genesis*. **26**: 279-284.

Fay, D.S., Keenan, S., and Han, M. (2002). *fzr-1* and *lin-35*/Rb function redundantly to control cell proliferation in *C. elegans* as revealed by a nonbiased synthetic screen. *Genes and Development*. **16**: 503-517.

Fenton, R.G., Kung, H., Longo, D.L., and Smith, M.R. (1992). Regulation of intracellular actin polymerization by prenylated cellular proteins. *Journal of Cell Biology*. **117**: 347-356.

Ferguson, E.L., and Horvitz, H.R. (1989). The multivulva phenotype of certain *Caenorhabditis elegans* mutants results from defects in two functionally redundant pathways. *Genetics*. **123**: 109-121.

Fire, A., Xu, S., Montgomery, M.K., Kostas, S.A., Driver, S.E., Mello, C.C. (1998). Potent and specific genetic interference by double-stranded RNA in *Caenorhabditis elegans*. *Nature*. **391**: 806-811.

Fitch, D.H.A., and Thomas, W.K. (1997). Evolution. C. elegans II (Riddle, Blumenthal, Meyer & Priess, editors). pp 815-850. Cold Spring Harbor Laboratory Press, Cold Spring Harbor Laboratory, NY.

Florio, S.K., Prusti, R.K., and Beavo, J.A. (1996). Solubilization of membrane-bound rod phosphodiesterase by the rod phosphodiesterase recombinant δ subunit. *Journal of Biological Chemistry*. **271**: 24036-24047.

Frech, M., Darden, T.A., Pedersen, L.G., Foley, C.K., Charifson, P.S., Anderson, M.W., and Wittinghofer, A. (1994). Role of glutamine-61 in the hydrolysis of GTP by p21H-ras: an experimental and theoretical study. *Biochemistry*. **33**: 3237-44.

Fukomoto, Y., Kaibuchi, K., Hori, Y., Fujioka, H., Araki, S., Ueda, T., Kikuchi, A., and Takai, Y. (1990). Molecular cloning and characterization of a novel type of regulatory protein (GDI) for the rho proteins, ras p21-like small GTP-binding proteins. *Oncogene*. **5**: 1321-1328.

Giaever, G., Chu, A.M., Ni, L., Connelly, C., Riles, L., Veronneau, S., Dow, S., Lucau-Danila, A., Anderson, K., Andre, B., Arkin, A.P., Astromof, A., Bakkoury, M.E., Bangham, R., Benito, R., Brachat, S., Campanaro, S., Curtiss, M., Davis, K., Deutschbauer, A., Entian, K., Flaherty, P., Foury, F., Garfinkel, D.J., Gerstein, M., Gotte, D., Guldener, U., Hegemann, J.H., Hempel, S., Herman, Z., Jaramillo, D.F., Kelly, D.E., Kelly, S.L., Kotter, P., LaBonte, D., Lamb, D.C., Lan, N., Liang, H., Liao, H., Liu, L., Luo, C., Lussier, M., Mao, R., Menard, P., Ooi, S.L., Revuelta, J.L., Roberts, C.J., Rose, M., Ross-Macdonald, P., Scherens, B., Schimmack, G., Shafer,

127

B., Shoemaker, D.D., Sookhai-Mahadeo, S., Storms, R.K., Strathern, J.N., Valle, G., Voet, M., Volckaert, G., Wang, C., Ward, T., Wilhelmy, J., Winzeler, E.A., Yang, Y., Yen, G., Youngman, E., Yu, K., Bussey, H., Boeke, J.D., Snyder, M., Phillippsen, P., Davis, R.W., and Johnstone, M. (2002). Functional profiling of the *Saccharomyces cerevisiae* genome. *Nature*. **418**: 387-391.

Gillespie, P.G., Prusti, R.K., Apel, E.D., and Beavo, J.A. (1989). A soluble form of bovine rod photoreceptor phosphodiesterase has a novel 15-kDa subunit. *Journal of Biological Chemistry*. **264**: 12187-12193.

Golden, J.W. and Riddle, D.L. (1982). A pheromone influences larval development in the nematode Caenorhabditis elegans. *Science*. **218**: 578-80.

Grayson, C., Bartolini, F., Chapple, J.P., Willison, K.R., Bhamidipati, A., Lewis, S.A., Luthert, P.J., Hardcastle, A.J., Cowan, N.J., and Cheetham, M.E. (2002). Localization in the human retina of the X-linked retinitis pigmentosa protein RP2, its homologue cofactor C and the RP2 interacting protein Arl3. *Human Molecular Genetics*. **11**: 3065-3074.

Gu, Z., Steinmetz, L.M., Gu, X., Scharfe, C., Davis, R.W., and Li, W. (2003). Role of duplicate genes in genetic robustness against null mutations. *Nature*. **421**: 63-66.

Guo, S. and Kemphues, K.J. (1996). A non-muscle myosin required for embryonic polarity in Caenorhabditis elegans. *Nature*. **382**: 455-458.

Hamelin, M., Zhou, Y., Su, M.W., Scott, I.M., and Culotti J.G. (1993). Expression of the UNC-5 guidance receptor in the touch neurons of *C. elegans* steers their axons dorsally. *Nature*. **364**: 327-30.

Hanzal-Bayer, M., Renault, L., Roversi, P., Wittinghofer, A. and Hillig, R.C. (2002). The complex of Arl2-GTP and PDE delta: from structure to function. *EMBO Journal*. **21**: 2095-2106.

Hao JC, Yu TW, Fujisawa K, Culotti JG, Gengyo-Ando K, Mitani S, Moulder G, Barstead R, Tessier-Lavigne M, Bargmann CI. (2001). *C. elegans* slit acts in midline, dorsal-ventral, and anterior-posterior guidance via the SAX-3/Robo receptor. *Neuron*. **32**: 25-38.

Hedgecock, E.M. and Russell, R.L. (1975). Normal and mutant thermotaxis in the nematode *Caenorhabditis elegans*. *Proceedings of the National Academy of Science*. **72**: 4061-4065.

Hedgecock, E.M., Culotti, J.G., and Hall, D.H. (1990). The *unc-5*, *unc-6*, and *unc-40* genes guide circumferential migrations of pioneer axons and mesodermal cells on the epidermis in *C. elegans*. *Neuron*. **4**: 61-85.

Hedgecock, E.M., Culotti, J.G., Thomson, J.N., and Perkins, L.A. (1985). Axonal guidance mutants of Caenorhabditis elegans identified by filling sensory neurons with fluorescein dyes. *Developmental Biology.* **111**: 158-70.

Higashide, T., McLaren, M.J., and Inana, G. (1998). Localization of HRG4, a photoreceptor protein homologous to *Unc-119*, in ribbon synapse. *Investigative Opthamology & Visual Science.* **39**: 690-698.

Higashide, T., Murakami, A., McLaren, M.J., and Inana, G. (1996). Cloning of the cDNA for a novel photoreceptor protein. *Journal of Biological Chemistry.* **271**: 1797-1804.

Hirsch, A.E., and Fraser, H.B. (2003). Rate of evolution and gene dispensability. *Nature.* **421**: 497-498.

Hirsh, A.E., and Fraser, H.B. (2001). Protein dispensability and rate of evolution. *Nature.* **411**: 1046-1049.

Hong, D-H., Pawlyk, B.S., Shang, J., Sandberg, M.A., Berson, E.L., and Li, T. (2000). A retinitis pigmentosa GTPase regulator (RPGR)-deficient mouse model for X-linked retinitis pigmentosa (RP3). *Proceedings of the National Academy of Science.* **97**: 3649-3654.

Hong, D-H., Yue, G., Adamian, M., and Li, T. (2001). Retinitis pigmentosa GTPase regulator (RPGR)-interacting protein is stably associated with the photoreceptor ciliary axoneme and anchors RPGR to the connecting cilium. *Journal of Biological Chemistry.* **276**: 12091-12099.

Hurst, L.D. and Smith, N.G.C. (1999). Do essential genes evolve slowly? *Current Biology.* **9**: 747-750.

Isomura, M., Kikuchi, A., Ohga, N., and Takai, Y. (1991). Regulation of binding of rhoB p20 to membranes by its specific regulatory protein, GDP dissociation inhibitor. *Oncogene.* **6**: 119-124.

James, P., Halladay, J. & Craig, E. A. (1996). Genomic libraries and a host strain designed for highly efficient two- hybrid selection in yeast. *Genetics.* **144**: 1425-1436.

Johnson, L., Greenbaum, D., Cichowski, K., Mercer, K., Murphy, E., Schmitt, E., Bronson, R.T., Umanoff, H., Edelmann, W., Kucherlapati, R., and Jacks, T. (1997). K-*ras* is an essential gene in the mouse with partial functional overlap with N-*ras*. *Genes and Development.* **11**: 2468-2481.

Jordan, I.K., Rogozin, I.B., Wolf, Y.I., and Koonin, E.V. (2002). Essential genes are more evolutionarily conserved than are nonessential genes in bacteria. *Genome Research.* **12**: 962-968.

Kahn, R.A., Kernll, F.G., Clark, J., Gelmann, E.P., and Rulka, C. (1991). Human ADP-ribosylation factors. *Journal of Biological Chemistry.* **266**: 2606-2614.

Kamath, R.S., Fraser, A.G., Dong, Y., Poulin, G., Durbin, R., Gotta, M., Kanapink, A., Le Bot, N., Moreno, S., Sohrmann, M., Welchman, D.P., Zipperlin, P., and Ahringer, A. (2003). Systemic functional analysis of the *Caenorhabditis elegans* genome using RNAi. *Nature.* **421**: 231-237.

Kamath, R.S., Martinez-Campos, M., Zipperlen, P., Fraser, A.G., and Ahringer, J. (2000). Effectiveness of specific RNA-mediated interference through ingested double-stranded RNA in *Caenorhabditis elegans. Genome Biology.* **2**: research0002.1-0002.10.

Keep, N.H., Barnes, M., Barsukov, I., Badii, R., Lian, L-Y., Segal, A.W., Moody, P.C.E., and Roberts, G. (1997). A modulator of the rho family G proteins, rhoGDI, binds these G proteins via an immunoglobulin-like domain and a flexible N-terminal arm. *Structure.* **5**: 623-633.

Kim, S., and Wadsworth, W.G. (2000). Positioning of longitudinal nerves in *C. elegans* by nidogen. *Science.* **288**: 150-4.

Kimura, M. (1968). Evolutionary rate at the molecular level. *Nature.* **217**: 624-626.

Kimura, M., (1983). *The Neutral Theory of Molecular Evolution.* Cambridge University Press, Cambridge, UK.

Knobel, K.M., Davis, W.S., Jorgensen, E.M., and Bastiani, M.J. (2001). UNC-119 suppresses axon branching in *C. elegans. Development.* **128**: 4079-4092.

Kobayashi, A., Higashide, T., Hamasaki, D., Kubota, S., Sakuma, H., An, W., Fujimaki, T., McLaren, M.J., Weleber, R.G., and Inana, G. (2000). HRG4 (UNC119) mutation found in cone-rod dystrophy causes retinal degeneration in a transgenic model. *Investigative Opthamology & Visual Science.* **41**: 3268-3277.

Kobayashi, A., Kubota, S., Mori, N., McLaren, M.J., and Inana, G. (2003). Photoreceptor synaptic protein HRG4 (UNC119) interacts with ARL2 via a putative conserved domain. *FEBS Letters.* **534**: 26-32.

Koera, K., Nakamura, K., Nakao, K., Miyoshi, J., Toyoshima, K., Hatta, T., Otani, H., Aiba, A., and Katsuki, M. (1997). K-*ras* is essential for the development of the mouse embryo. *Oncogene.* **15**: 1151-1159.

Komatsu, H., Mori, I., Rhee, J.S., Akaike, N., and Ohshima, Y. (1996). Mutations in a cyclic nucleotide-gated channel lead to abnormal thermosensation and chemosensation in *C. elegans. Neuron.* **17**: 707-18.

130

Kramer, R.H. and Molokanova, E. (2001). Modulation of cyclic-nucleotide-gated channels and regulation of vertebrate phototransduction. *Journal of Experimental Biology*. **204**: 2921-2931.

Lai, R.K., Perez-Sala, D., Canada, F.J., and Rando, R.R. (1990). The gamma subunit of transducin is farnesylated. *Proceedings of the National Academy of Science*. **87**: 7673-7.

Leonard, D., Hart, M.J., Platko, J.V., Eva, A., Henzel, W., Evans, T., and Cerione, R.A. (1992). The identification and characterization of a GDP-dissociation inhibitor (GDI) for the CDC42Hs protein. *Journal of Biological Chemistry*. **267**: 22860-8.

Li, F.N., and Johnstone, M. (1997). Grr1 of *Saccharomyces cerevisiae* is connected to the ubiquitin proteolysis machinery through Skp1:coupling glucose sensing to gene expression and the cell cycle. *EMBO Journal*. **16**: 5629-5638.

Li, N. and Baehr, W. (1998). Expression and characterization of human PDEdelta and its *Caenorhabditis elegans* ortholog Cedelta. *FEBS Letters*. **440**: 454-457.

Linari, M., Hanzal-Bayer, M., and Becker, J. (1999). The delta subunit of rod specific cyclic cGMP phosphodiesterase, PDEδ, interacts with the Arf-like protein Arl3 in a GTP specific manner. *FEBS Letters*. **458**: 55-59.

Linari, M., Ueffing, M., Manson, F., Wright, A., Meitinger, T., and Becker, J. (1999). The retinitis pigmentosa GTPase regulator, RPGR, interacts with the delta subunit of rod cyclic GMP phosphodiesterase. *Proceedings of the National Academy of Science*. **96**: 1315-1320.

Longenecker, K., Read, P., Derewenda, U., Dauter, Z., Liu, X., Garrard, S., Walker, L., Somlyo, A.V., Nakamoto, R.K., Somlyo, A.P., and Derewenda, Z. (1999). How RhoGDI binds Rho. *Acta Crystallographica Section D: Biological Crystallography*. **D55**: 1503-1515.

Lorenz, B., Migliaccio, C., Lichtner, P., Meyer, C., Strom, T.M., D'Urso, M., Becker, J., Ciccodicola, A., and Meitinger, T. (1998). Cloning and gene structure of the rod cGMP phosphodiesterase delta subunit gene (PDED) in man and mouse. *European Journal of Human Genetics*. **6**: 283-290.

Lowe, S.L., Wong, S.H., and Hong, W. (1996). The mammalian ARF-like protein 1 (Arl1) is associated with the Golgi complex. *Journal of Cell Science*. **109**: 209-220.

Lu, L., Horstmann, H., Ng, C., and Hong, W. (2001). Regulation of Golgi structure and function by ARF-like protein 1 (Arl1). *Journal of Cell Science*. **114**: 4543-4555.

Lundquist EA, Herman RK, Shaw JE, and Bargmann CI. (1998). UNC-115, a conserved protein with predicted LIM and actin-binding domains, mediates axon guidance in *C. elegans*. *Neuron*. **21**: 385-92.

131

Lundquist, E.A., Herman, R.K., Rogalski, R.M., Mullen, G.P., Moerman, D.G., and Shaw, J.E. (1996). The *mec-8* gene of *C. elegans* encodes a protein with two RNA recognition motifs and regulates alternative splicing of *unc-52* transcripts. *Development.* **122**: 1601-1610.

Lundquist, E.A., Reddien, P.W., Hartweig, E., Horvitz, H.R., and Bargmann, C.I. (2001). Three *C. elegans* Rac proteins and several alternative Rac regulators control axon guidance, cell migration, and apoptotic cell phagocytosis. *Development.* **128**: 4475-4488.

Luo, L. (2002). Actin cytoskeleton regulation in neuronal morphogenesis and structural plasticity. *Annual Review of Cell and Developmental Biology.* **18**: 601-635.

Maduro, M. (1998). Characterization of the *unc-119* gene in *Caenorhabditis elegans.* Ph.D. Thesis. University of Alberta.

Maduro, M. and Pilgrim, D. (1995). Identification and cloning of *unc-119*, a gene expressed in the *Caenorhabditis elegans* nervous system. *Genetics.* **141**: 977-988.

Maduro, M.F., Gordon, M., Jacobs, R. and Pilgrim, D.B. (2000). The UNC-119 family of neural proteins is functionally conserved between humans, *Drosophila*, and *C. elegans. Journal of Neurogenetics.* **13**: 191-212.

Maeda, I., Kohara, Y., Yamamoto, M., and Sugimoto, A. (2001). Large-scale analysis of gene function in *Caenorhabditis elegans* by high-throughput RNAi. *Current Biology.* **11**: 171-176.

Manning, A. (1999). Characterization of *unc-119* homologues in the zebrafish *Danio rerio*. M.Sc. Thesis. University of Alberta.

Marzesco, A-M., Dunia, I., Pandjaitan, R., Recouvreur, M., Dauzonne, D., Benedetti, E.L., Lourvard, D., and Zahraoui, A. (2002). The small GTPase Rab13 regulates assembly of functional tight junctions in epithelial cells. *Molecular Biology of the Cell.* **13**: 1819-1831.

Marzesco, A-M., Galli, T., Louvard D., and Zahraoui, A. (1998). The rod cGMP phosphodiesterase δ subunit dissociates the small GTPase Rab13 from membranes. *Journal of Biological Chemistry.* **273**: 22340-22345.

Marzesco, A-M., Galli, T., Louvard, D. and Zahraoui, A. (2001). Properties of Rab13 interaction with rod cGMP phosphodiesterase δ subunit. *Methods in Enzymology.* **329**: 197-209.

McGinnis, J.F., Matsumoto, B., Whelan, J.P., and Cao, W. (2002). Cytoskeleton participation in subcellular trafficking of signal transduction proteins in rod photoreceptor cells. *Journal of Neuroscience Research.* **67**: 290-297.

Mello, C.C., Kramer, J.M., Stinchcomb, D., and Ambros, V. (1991). Efficient gene transfer in *C. elegans*: extrachromosomal maintenance and integration of transforming sequences. *EMBO Journal*. **10**: 3959-3970.

Mou, H., Grazio III, H.J., Cook, T.A., Beavo, J.A., and Cote, R.H. (1999). cGMP binding to noncatalytic sites on mammalian rod photoreceptor phosphodiesterase is regulated by binding of its γ and δ subunits. *Journal of Biological Chemistry*. **274**: 18813-18820.

Nancy, V., Callebaut, I., Marjou, A.E., and de Gunzburg, J. (2002). The δ subunit of retinal rod cGMP phosphodiesterase regulates the membrane association of Ras and Rap GTPases. *Journal of Biological Chemistry*. **277**: 15076-15084.

Nasevicius, A. and Ekker, S.C. (2000). Effective targeted gene 'knockdown' in zebrafish. *Nature Genetics*. **26**: 216-220.

Ohta, T. (1973). Slightly deleterious mutant substitutions in evolution. *Nature*. **246**: 96-98.

Ohta, T. (1992). The nearly neutral theory of molecular evolution. *Annual Review of Ecology and Systematics*. **23**: 263-286.

Pal, C., Papp, B., and Hurst, L.D. (2003). Rate of evolution and gene dispensability. *Nature*. **421**: 496-497.

Panic, B, Whyte, J.R.C., and Munro, S. (2003). The ARF-like GTPases Arl1p and Arl3p act in a pathway that interacts with vesicle-tethering factors at the golgi apparatus. *Current Biology*. **13**: 405-410.

Pujol, N., Link, E.M., Liu, L.X., Kurz,C.L., Alloing, G., Tan, M-W., Ray, K.P., Solari, R., Johnson, C.D., and Ewbank, J.J. (2001). A reverse genetic analysis of components of the Toll signaling pathway in *Caehorhabditis elegans*. *Current Biology*. **11**: 809-821.

Radcliffe, P.A., Vardy, L., and Toda, T. (2000). A conserved small GTP-binding protein Alp41 is essential for the cofactor-dependent biogenesis of microtubules in fission yeast. *FEBS Letters*. **468**: 84-88.

Ren, P., Lim, C.S., Johnsen, R., Albert, P.S., Pilgrim, D., and Riddle, D.L. (1996). Control of *C. elegans* larval development by neuronal expression of a TGF-beta homolog. *Science*. **274**: 1389-91.

Renault, L., Hanzal-Bayer, M., and Hillig, R.C. (2001). Coexpression, copurification, crystallization and preliminary X-ray analysis of a complex of ARL2-GTP and PDE delta. *Acta Crystallographica Section D: Biological Crystallography*. **57**: 1167-1170.

133

Riddle, D.L. (1988). The Dauer Larva. The Nematode *Caenorhabditis elegans* (Wood, editor). pp. 393-412. Cold Spring Harbor Laboratory Press, Cold Spring Harbor Laboratory, NY.

Roberts, B., Clucas, C., and Johnstone, I. (2003). Loss of SEC-23 in *Caenorhabditis elegans* causes defects in oogenesis, morphogenesis, and extracellular matrix secretion. *Molecular Biology of the Cell.* **14**: 4414-4426.

Roepman, R., Bernoud-Hubac, N., Schick, D.E., Maugeri, A., Berger, W., Ropers, H-H., Cremers, F.P.M., and Ferreira, P.A. (2000). The retinitis pigmentosa GTPase regulator (RPGR) interacts with novel transport-like proteins in the outer segments of rod photoreceptors. *Human Molecular Genetics.* **9**: 2095-2105.

Rosenwald, A.G., Rhodes, M.A., Van Valkenburgh, H.V., Palanivel, V., Chapman, G., Boman, A., Zhang, C., and Kahn, R. (2002). *ARL1* and membrane traffic in *Saccharomyces cerevisiae. Yeast.* **19**: 1039-1056.

Sheth, B., Fontaine, J-J., Ponza, E., McCallum, A., Page, A., Citi, S., Louvard, D., Zahraoui, and Fleming, T.P. (2000). Differentiation of the epithelial apical junctional complex during mouse preimplantation development: a role for rab13 in the early maturation of the tight junction. *Mechanisms of Development.* **97**: 93-104.

Simmer, F., Tijsterman, M., Parrish, S., Koushika, S.P., Nonet, M.L., Fire, A. Ahringer, J. and Plasterk, R.H. (2002). Loss of the putative RNA-directed RNA polymerase RRF-3 makes *C. elegans* hypersensitive to RNAi. *Current Biology.* **12**: 1317-1319.

Spang, A. (2002). ARF1 regulatory factors and COPI vesicle formation. *Current Opinion in Cell Biology.* **14**: 423-427.

Steven, R., Kubiseski, T.J., Zheng, H., Kulkarni, S., Mancillas, J., Morales, A.R., Hogue, C.W., Pawson, T., and Culotti, J. (1998). UNC-73 activates the Rac GTPase and is required for cell and growth cone migrations in *C. elegans. Cell.* **92**: 785-795.

Sulston, J. and Hodgkin, J. (1988). Methods. The Nematode *Caenorhabditis elegans* (Wood, editor). pp. 587-606. Cold Spring Harbor Laboratory Press, Cold Spring Harbor Laboratory, NY.

Swanson, D.A., Chang, J.T., Campochiaro, P.A., Zack, D.J., and Valle, D. (1998). Mammalian orthologues of *C. elegans unc-119* highly expressed in photoreceptors. *Investigative Opthamology & Visual Science.* **39**: 2085-2094.

Takai, Y., Sasaki, T., and Matozaki, T. (2001). Small GTP-binding proteins. *Physiological Reviews.* **81**: 153-208.

Tamkun, J.W., Kahn, R.A., Kissinger, M., Brizuela, B.J., Rulka, C., Scott, M.P., and Kennison, J.A. (1991). The arflike gene encodes an essential GTP-binding protein in *Drosophila. Proceedings of the National Academy of Science.* **88**: 3120-3124.

Temeles, G.L., Gibbs, J.B., D'Alonzo, J.S., Sigal, I.S., and Scoln, E.M. (1985). Yeast and mammalian *ras* proteins have conserved biochemical properties. *Nature*. **313**: 700-703.

Tian, G., Bhamidipati, A., Cowan, N.J., and Lewis, S.A. (1999). Tubulin folding cofactors as GTPase-activating proteins. *Journal of Biological Chemistry*. **274**: 24054-24058.

Timmons, L., Court, D.L, and Fire, A. (2001). Ingestion of bacterially expressed dsRNAs can produce specific and potent genetic interference in *Caenorhabditis elegans*. *Gene*. **263**: 103-112.

Umanoff, H., Edelmann, W., Pellicer, A., and Kucherlapati, R. (1995). The murine N-*ras* gene is not essential for growth and development. *Proceedings of the National Academy of Science*. **92**: 1709-1713.

Van Valkenburgh, H., Shern, J.F., Sharer, J.D., Zhu, X. and Kahn, R.A. (2001). ADP-ribosylation factors (ARFs) and ARF-like 1 (ARL1) have both specific and shared effectors: characterizing ARL1-binding proteins. *Journal of Biological Chemistry*. **276**: 22826-22837.

Venolia, L., Ao, W., Kim, S., Kim, C., and Pilgrim D. (1999). *unc-45* gene of *Caenorhabditis elegans* encodes a muscle-specific tetratricopeptide repeat-containing protein. *Cell Motility and the Cytoskeleton*. **42**: 163-77.

Wadsworth, W.G., Bhatt, H., and Hedgecock, E.M. (1996). Neuroglia and Pioneer Neurons Express UNC-6 to Provide Global and Local Netrin Cues for Guiding Migrations in *C. elegans*. *Neuron*. **16**: 35-46.

Wang, W., Zhang, Q., Acland, G.M., Mellersh, C., Ostrander, E.A., Ray, K., and Aguirre, G.D. (1999). Molecular characterization and mapping of canine cGMP-phosphodiesterase delta subunit (*PDE6D*). *Gene*. **236**: 325-332.

Westerfield, M. (2000). The zebrafish book. A guide for the laboratory use of zebrafish (*Danio rerio*). 4th ed., University of Oregon Press, Eugene.

White, J.G., Southgate, E., Thomson, J.N., and Brenner, S. (1986). The structure of the nervous sytem of the nematode *Caenorhabditis elegans*. *Philosophical Transactions of the Royal Society of London, Series B*. **314**: 1-340.

Wicks, S.R., de Vries, C.J., van Leunen, H.G.A.M., and Plasterk, R.H.A. (2000). CHE-3, a cytosolic dynein heavy chain, is required for sensory cilia structure and function in *Caenorhabditis elegans*. *Developmental Biology*. **221**: 295-307.

Wilson, A.C., Carlson, S.S., and White, T.J. (1977). Biochemical evolution. *Annual Review of Biochemistry*. **46**: 573-639.

135

Wood, W.B. (1988). Introduction to *C. elegans* Biology. The Nematode *Caenorhabditis elegans* (Wood, editor). pp. 1-16. Cold Spring Harbor Laboratory Press, Cold Spring Harbor Laboratory, NY.

Yan, D., Swain, P.K., Breuer, D., Tucker, R.M., Wu, W., Fujita, R., Rehemtulla, A., Burke, D., and Swaroop, A. (1998). Biochemical characterization and subcellular localization of the mouse retinitis pigmentosa GTPase regulator (mRPGR). *Journal of Biological Chemistry.* **273**: 19656-19633.

Yang, J., Gu, Z., and Li, W. (2003). Rate of protein evolution versus fitness effect of gene deletion. *Molecular Biology and Evolution.* **20**: 772-774.

Yarfitz, S. and Hurley, J.B. (1994). Transduction mechanisms of vertebrate and invertebrate photoreceptors. *Journal of Biological Chemistry.* **269**: 14329-14332.

Yu, T.W., Hao, J.C., Lim, W., Tessier-Lavigne, M., and Bargmann CI. (2002). Shared receptors in axon guidance: SAX-3/Robo signals via UNC-34/Enabled and a Netrin-independent UNC-40/DCC function. *Nature Neuroscience.* **5**: 1147-1154.

Yuan, X., Jin, M., Xu, X., Song, Y., Wu, C., Poo. M., and Duan, S. (2003). Signalling and crosstalk of Rho GTPases in mediating axon guidance. *Nature Cell Biology.* **5**: 38-45.

Zahraoui, A., Joberty, G., Arpin, M., Fontaine, J.J., Hellio, R., Tavitian, A., and Louvard, D. (1994). A small rab GTPase is distributed in cytoplasmic vesicles in non polarized cells but colocalizes with the tight junction marker ZO-1 in polarized epithelial cells. *Journal of Cell Biology.* **124**: 101-115.

Zallen, J.A., Yi, B.A., and Bargmann, C.I. (1998). The Conserved Immunoglobulin Superfamily Member SAX-3/Robo Directs Multiple Aspects of Axon Guidance in *C. elegans. Cell.* **92**: 217-227.

Zhang, F.L. and Casey, P.J. (1996). Protein prenylation: Molecular mechanisms and functional consequences. *Annual Review of Biochemistry.* **65**: 241-269.

Zhao, Y., Hong, D-H., Pawlyk, B., Yue, G., Adamian, M., Grynberg, M., Godzik, A., and Li, T. (2003). The retinitis pigmentosa GTPase regulator (RPGR)-interacting protein: subserving RPGR function and participating in disk morphogenesis. *Proceedings of the National Academy of Science.* **100**: 3965-3970.

Appendices

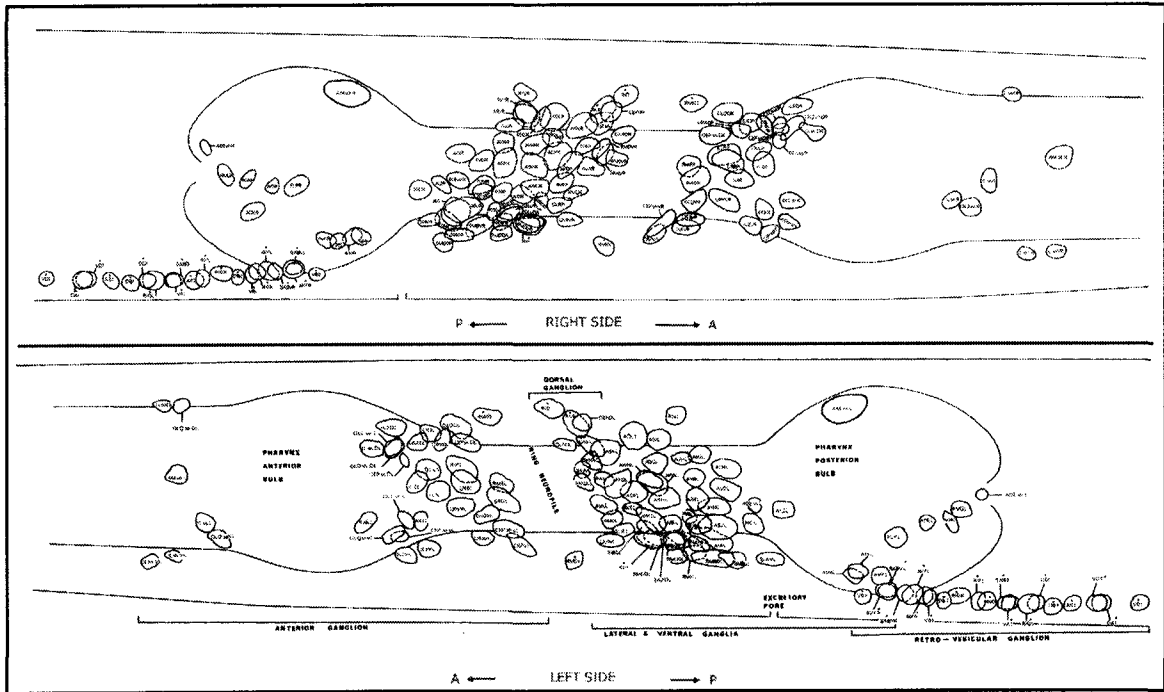## Appendix I Nervous system structure in *C. elegans*

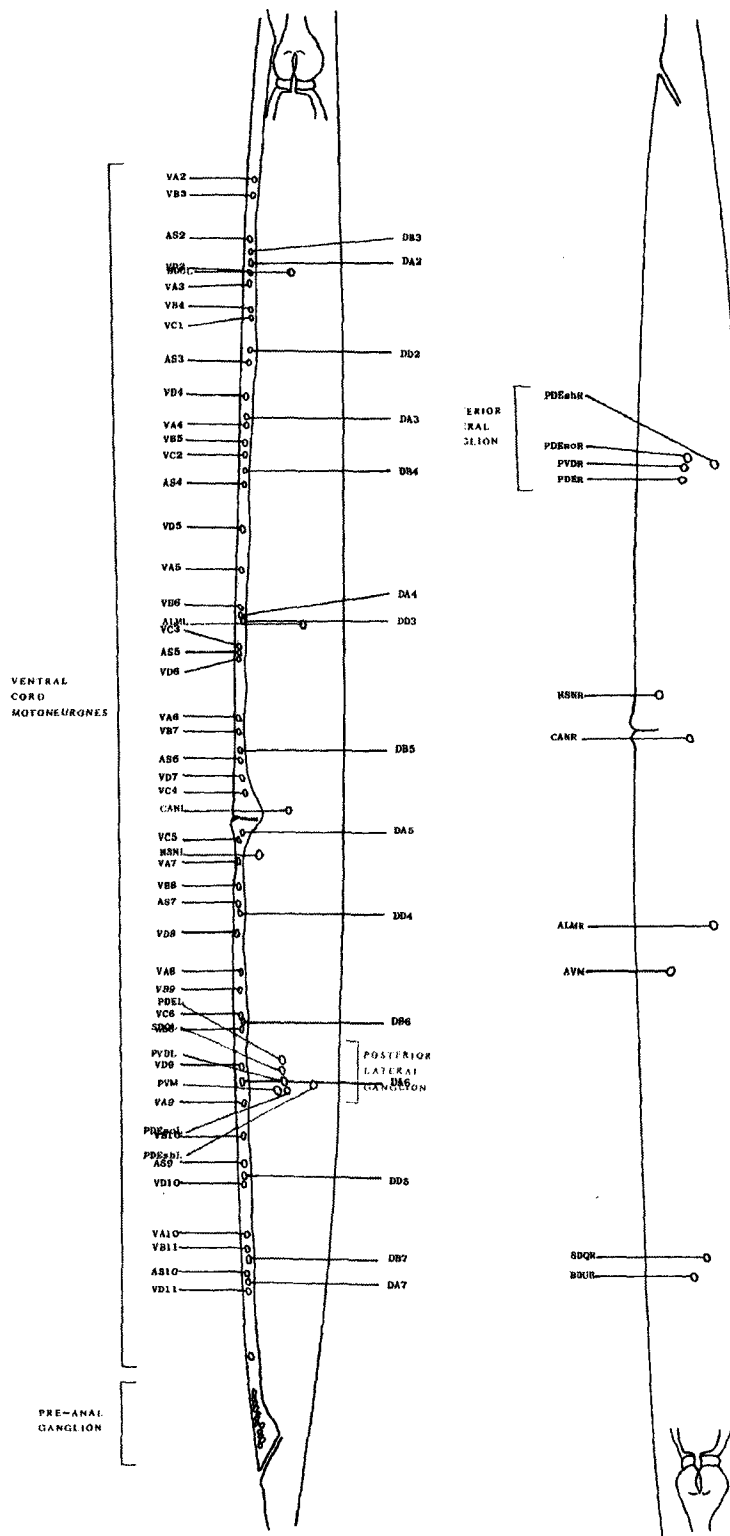**Figure I.1** Position of nerve cell bodies around the nerve ring. Figure from White *et al.*, 1986.

Figure I.2   Position of cell bodies in the ventral cord and along the body of an adult hermaphrodite. Figure adapted from White *et al.*, 1986.

138

Figure I.3   Axon processes in an adult hermaphrodite. Figure from White *et al.*, 1986.

139

Appendix II Strains and genotypes

C. elegans

Strains were provided by the *C. elegans* Genome Center (Minneapolis, MN) with the following exceptions: *mg366* and *mg367* were provided by Gary Ruvkun while VC282 was provided by the *C. elegans* Genome Knockout Consortium (Vancouver, B.C.).

CB2322	*unc-4(e2322ts)* II
CB4845	*unc-119(e2498)* III
DP265	edIs28 (P*pdl-1*::GFP); *him-8(e2489)* IV
DP288	*pdl-1(gk157)* II; *unc-119(ed3)* III
DP289	*pdl-1(gk157)* II; P*unc129*::GFP X
DP290	edEx134 (*pdl-1*::GFP)
DP291	*pdl-1(gk157)*; evIs111 (P$_{F25B3.3}$::GFP)
DP292	*pdl-1(gk157)* II; *unc-119(ed3)* III; evIs111 (P$_{F25B3.3}$::GFP)
DP293	*pdl-1(gk157)* II; edIs124 (P*daf-7*::GFP)
DP294	*pdl-1(gk157)* II; *unc-119(ed3)* III; P*unc-129*::GFP X
DP38	*unc-119(ed3)* III
mg366	uncloned mutation (shows RNAi sensitivity in nervous system)
mg367	uncloned mutation (shows RNAi sensitivity in nervous system)
ML335	*dpy-2(e489)* mcDf1 *unc-4(e120)*/mnC1 *dpy-10(e128) unc-52(e444)* II
N2	wild-type, Bristol isolate
NL2099	*rrf-3(pk1426)* II
VC282	*pdl-1(gk157)* II

<u>*E. coli*</u>

HT115 was provided by the *C. elegans* Genome Center (Minneapolis, MN) while BL21(DE3)pLysS was purchased from Stratagene.

140

HT115   F-, mcrA, mcrB, IN(rrnD-rrnE)1, rnc14::Tn10(DE3 lysogen:
                      lavUV5 promoter -T7 polymerase) (IPTG-inducible T7
                      polymerase) (RNAse III minus)

BL21(DE3) pLysS   F- dcm ompT hsdS(rB- mB-) gal λ (DE3) [pLysS Camr][a]

Danio rerio

Fish were provided by the Zebrafish International Resource Center (Eugene, OR).

nacre   *nac^{w2}*
AB   wild-type

Saccharomyces cerevisiae

PJ69-4A is described in James *et al.*, 1996.

PJ69-4A   trp1-901 leu2-3,112 ura3-52 his3-200 gal4(deleted) gal80(deleted)
             LYS2::GAL1-HIS3 GAL2-ADE2 met2::GAL7-lacZ

Appendix III   Primer sequences

Primer Name	Sequence (5'-3')
A1065	CCTACATCGTTGTCTGCTCCC
A1066	AAGTGGATCCCACGAGACACCGTACGAC
adapter primer (Gibco)	GGCCACGCGTCGACTAGTAC(T)$_{17}$
C02 PROM F1	AAAAAGCTTCTCGGAGCATTCTGGTCATC
C02 PROM R1	AAAGTCGACTGGTGAAAGCGTCGTAATC
C273RACE1	TACCGCTACTCGTCATCAAGA
C273RACE2	GAGAGCATTCTGGCTGGCTTC
C275RACE1	ACGACGACGTTTCCGCTGAGT
C27DOMF1	AAAAAGGATCCTGGCAGAGCACAGAAGACAT
C27DOMF2	AAAAAGGATCCTTGAAGGGAACCATCATTGAAGA
C27DOMF4	AAAGGATCCATGTTCCCACCATCTGTACT
C27DOMF5	AAAGGATCCAAAAGGGAACACAAAGCACAC
C27DOMR1	AAAAACTGCAGTTAGTCAGCCATGTCTTCTGTG
C27DOMR3	AAAAACTGCAGTTAAGGTGGGAACATTTGTGAT
C27DOMR4	AAACTGCAGTTATTCAATGATGGTTCCCTTCA
C27F11	GAAAACATTGTGCCAGAGACTG
C27JSF1	TCATCTCACCTCGTCTTGCCTCTTG
C27JSF2	TATCACCTAATCCCATCCTGCTCAA
C27JSR1	TGTTGTGTCCTTTGCTTCTCCTTCA
C27JSR2	CACACAGAGAAACGGAAACAAATGG
C49 PROM F1	AAAAAGCTCCACAGGCACTGGAGGATCAT
C49 PROM R1	AAAGTCGACTGGATCAGAAGCTGGGTAAA
Gal4AD	GTTTGGAATCACTACAGGGATG
Gal4BD	ATGCCTCTAACATTGAGA
LVSL1	GGTTTAATTACCCAAGTTTGAG
MMA17	ATAAAGACGGACTCGAGA
MMA18	TCCATCATAAAGAATAAAGTCT
SEQED3L	AAATTAAAGACGGTCGGCGCG
SEQED3U	ACCACCGAGGCGGAGCTTCTC
SP6	ATTTAGGTGACACTATAG
SP6 becomes T7	GCCAGCTTAATACGACTCACTATAGGATACTCAAGC
T3	ATTAACCCTCACTAAAG

142

Primer Name	Sequence (5'-3')
T7	AATACGACTCACTATAG
T7 big	CCAGTGAATTGTAATACGACTCACTAT
TermseqCD	TTGCGGGGTTTTTCAGTATCT
UAP (Gibco)	CTACTACTACTAGGCCACGCGTCGACTAGTAC
W05 PROM F1	AAACTGCAGCAATGGGGACACTCTCCTCAA
W05 PROM R1	AAAGGATCCGGGCGACGAGATGGCAACTGA
Y113 PROM F1	AAAGTCGACAGCTTCCCGTCGCAGAGATTC
Y113 PROM R1	AAAGGATCCATTGTTGCAGAATGGGCACATC
Y55 PROM F1	AACTGCAGTCACGGCGTTCGGGTCCTGGAAGAC
Y55 PROM R1	AATGGCCAGGCTTCAGGGGACTCTTCCGTTGAT
zfdelta real F1	TGCTGAGACAGGGAAGGTTCT
zfdelta real F2	TTCCATCTGCTGAAGCTGAAC
zfdelta real R1	GCTGACATGAAGGTCGTCATC
zfdelta real R2	GAGGAAGAAAGGTACCATGTC

143